Functional analysis of ENTH domain proteins

Dissertation

zur Erlangung des akademischen Grades

Doctor rerum naturalium

(Dr. rer. nat.)

in der Wissenschaftsdisziplin Molekulare Pflanzenphysiologie

eingereicht an der

Mathematisch-Naturwissenschaftlichen Fakultät

Institut für Biochemie und Biologie

der Universität Potsdam

von

Laura Tegtmeier (Heinze)

Unless otherwise indicated, this work is licensed under a Creative Commons License Attribution – NonCommercial – NoDerivatives 4.0 International.
This does not apply to quoted content and works based on other permissions.
To view a copy of this licence visit:
https://creativecommons.org/licenses/by-nc-nd/4.0

Betreuer: Prof. Dr. Markus Grebe
Dr. Michael Sauer

Gutachtende: Dr. Michael Sauer
Prof. Dr. Guido Grossmann
Dr. habil Barbara Korbei

Parts of this work were published in *Proc. Natl. Acad. Sci. USA* as the following article:
Heinze, L., Freimuth, N., Rößling, A.K., Hahnke, R., Riebschläger, S., Fröhlich, A., Sampathkumar, A., McFarlane, H. E. and Sauer, M. (2020). EPSIN1 and MTV1 define functionally overlapping but molecularly distinct *trans*-Golgi network subdomains in *Arabidopsis*. *Proc. Natl. Acad. Sci. USA* 117, 41, 25880–25889.

Published online on the
Publication Server of the University of Potsdam:
https://doi.org/10.25932/publishup-57004
https://nbn-resolving.org/urn:nbn:de:kobv:517-opus4-570049

Acknowledgment

I would like to say thank you to many people who have accompanied me over the past years.

First hand Dr. Michael Sauer who had the great idea of this project and gave me the opportunity to work with him. He offered me the chance to try out my own ideas and supported me in all matters. I am so happy and thankful for the opportunity to participate in many different conferences.

Many thanks to K. A. and Nina Freimuth. I will miss you. Both of you helped me so much with lab stuff, plant care and proofreading. I will never forget our insider jokes.

Special thanks go out to Ann-Kathrin Rößling, Sarah Riebschläger and Reni Hahnke who were very talented students and supported my work. I wish you all the best for your future career.

I would like to mention Prof. Dr. Markus Grebe with great gratitude. He supported me by critically discussing my results. Moreover, thank you very much for proofreading.

I say thank you to the people from AG Grebe.

I would like to say thank you to my family. They simply believed in me.

My life has changed enormously since I started my work and I am glad and thankful that Florian Tegtmeier is with me, still. Now as my fiance and the best father of our son. You supported me in every perspective to achieve this thesis. I am thankful. I love you.

Table of Contents

Abbreviation

(v/v)	Volume per volume
(w/v)	Weight per volume
°C	Degree Celsius
µ	mu
µl	Microliter
µM	Micromolar
A. thaliana	*Arabidopsis thaliana*
A. tumefaciens	*Agrobacterium tumefaciens*
ALP	ALKALINE PHOSPHATASE
Amp	Ampicillin
ANOVA	Analysis of variance
ANTH	AP180 N-terminal homology
AP	ADAPTOR PROTEIN
APS	Ammonium persulfate
ARA7	ARABIDOPSIS RAB GTPASE HOMOLOG7
ARF GAP	ADP ribosylation factor GTPase-activating protein
AS	Acetosyringone
a.u.	arbitrary units
bp	Base pairs
$Ca(NO_3)_2$	Calcium nitrate
$CaCl_2$	Calcium chloride
CCV	Clathrin-coated vesicles
cDNA	Complementary DNA
CDS	Coding sequence
CESA	CELLULOSE SYNTHASE
CFP	CYAN FLUORESCENT PROTEIN
CHC	CLATHRIN HEAVY CHAIN
CHX	Cycloheximide
CI	Confidence Interval
CLC	CLATHRIN LIGHT CHAIN
CLINT	Clathrin-interacting protein localized in the *trans*-Golgi region
cm	Centimeter
CME	Clathrin-mediated endocytosis
Col-0	Columbia-0 accession of *Arabidopsis thaliana*
COP I	COATOMER PROTEIN I
COP II	COATOMER PROTEIN II
ct	Cycle threshold
DAG	Days after germination
DiAna	Distance analysis
DNA	Desoxyribonucleic acid
dpi	Dots per inch
DPSS	Diode-pumped solid state
DTE	1,4-Dithioerythritol
E. coli	*Escherichia coli*
ECH	ECHIDNA
EDTA	Ethylenediaminetetraacetic acid

EE	Early endosome
EM	Electron microscopy
ENTH	Epsin N-terminal homology
ER	Endoplasmic reticulum
et al.	et alia (and others)
g	Gram
ga	Gravitational acceleration
g/l	Gram per liter
GaAsP	Gallium arsenide phosphide
GABA	γ-aminobutyric acid
GA-TGN	Golgi-associated TGN
GFP	GREEN FLUORESCENT PROTEIN
GFS4	GREENFLUORESCENT SEED4
GFS5	GREENFLUORESCENT SEED5
GFS6	GREENFLUORESCENT SEED6
Got1	GOLGI TRANSPORT 1
GST	GLUTATHIONE S-TRANSFERASE
GUS	β-GLUCURONIDASE
h	Hour
H_2O	Water
HAP13	HAPLESS13
Hyg	Hygromycin
IPTG	Isopropyl β- d-1-thiogalactopyranoside
$K_3Fe(CN)_6$	Potassium ferricyanide
$K_4Fe(CN)_6$	Potassium hexacyanoferrate(II)
Kan	Kanamycin
KCl	Potassium chloride
kDa	Kilo Dalton
KH_2PO_4	Dipotassium phosphate
l	Liter
LB	Lysogeny broth / Luria broth
M	Molar
mA	Milliampere
MES	2-(N-morpholino)ethanesulfonic acid
mg	Milligramm
$MgSO_4$	Magnesium sulfate
min	Minute
mKO	Monomeric Kusabira Orange
ml	Milliliter
mm	Millimeter
mM	Millimolar
MS	Murashige & Skoog
MTV1	MODIFIED TRANSPORT TO THE VACUOLE1
MTV4	MODIFIED TRANSPORT TO THE VACUOLE4
MVB	Multivesicular body
MWCO	Molecular weight cut-off
N	Asparagine
Na_2HPO_4	Dinatriumhydrogenphosphat

NaCl	Sodium chloride
nm	Nanometer
OD	Optical density
P	Proline
PAT10	PROTEIN AFFECTED TRAFFICKING10
PAT2	PROTEIN AFFECTED TRAFFICKING2
PAT3	PROTEIN AFFECTED TRAFFICKING3
PAT4	PROTEIN AFFECTED TRAFFICKING4
PBS	Phosphate-buffered saline
PCR	Polymerase chain reaction
pH	Pondus Hydrogenii
PIN1	PIN-FORMED1
PIN2	PIN-FORMED2
PIs	Phosphoinositides
PM	Plasma membrane
PtdIns	Phosphatidylinositol
PtdIns(3)P	Phosphatidylinositol-3-phosphate
PtdIns(3,4,5)P_3	Phosphatidylinositol-3,4,5-trisphosphate
PtdIns(4)P	Phosphatidylinositol-4-phosphate
PtdIns(4,5)P_2	Phosphatidylinositol-4,5-bisphosphate
PVC	Prevacuolar compartment
qPCR	Quantitative polymerase chain reaction
R	Arginine
RABA1g	RAB GTPASE HOMOLOG A1G
RabF2b	RAB GTPASE HOMOLOG F2B
RFP	RED FLUORESCENT PROTEIN
RNA	Ribonucleic acid
rpm	Rounds per minute
S	Serine
SD	Standard deviation
SDS	Sodium dodecyl sulfate
SNARE	Soluble N-ethylmaleimide-sensitive factor attachment protein receptors
SOB	Super optimal broth
Spec	Spectinomycin
SUC4	SUCROSE TRANSPORTER4
SYP32	SYNTAXIN OF PLANTS32
SYP61	SYNTAXIN OF PLANTS61
SYP42	SYNTAXIN OF PLANTS42
SYP42	SYNTAXIN OF PLANTS43
TAE	Tris-acetate-EDTA
T-DNA	Transfer DNA
TE	Tris-EDTA
TEMED	Tetramethylethylenediamine
TGN	*trans*-Golgi network
Tween	Polyoxyethylene sorbitan monolaurate
v	Vesicle
V	Valin
V	Volt

VAMP711	VESICLE-ASSOCIATED MEMBRANE PROTEIN711
VAMP72	VESICLE-ASSOCIATED MEMBRANE PROTEIN72
VHA-a1	VACUOLAR PROTON ATPASE A1
VHS	Vps-27, Hrs, and STAM
VSR	VACUOLAR SORTING RECEPTOR
VTI	VESICLE TRANSPORT V-SNARE 11
X-Gluc	5-Bromo-4-chloro-3-indolyl-β-D-glucuronide
Y	Tyrosin
Y2H	Yeast two hybrid
YEB	Yeast Extract Beef
YFP	YELLOW FLUORESCENT PROTEIN
ZIP4	ZIG SUPPRESSOR4
α	alpha
β	beta
γ	gamma
δ	delta
ε	epsilon
ζ	zeta
YIP4a	YPT/RAB GTPase Interacting Protein 4a
YIP4b	YPT/RAB GTPase Interacting Protein 4b

Abstract

In plant cells, subcellular transport of cargo proteins relies to a large extent on *post*-Golgi transport pathways, many of which are mediated by clathrin-coated vesicles (CCVs). Vesicle formation is facilitated by different factors like accessory proteins and adaptor protein complexes (APs), the latter serving as a bridge between cargo proteins and the coat protein clathrin. One type of accessory proteins is defined by a conserved EPSIN N-TERMINAL HOMOLOGY (ENTH) domain and interacts with APs and clathrin via motifs in the C-terminal part. In *Arabidopsis thaliana*, there are three closely related ENTH domain proteins (EPSIN1, 2 and 3) and one highly conserved but phylogenetically distant outlier, termed MODIFIED TRANSPORT TO THE VACUOLE1 (MTV1). In case of the *trans*-Golgi network (TGN) located MTV1, clathrin association and a role in vacuolar transport have been shown previously (Sauer et al. 2013). In contrast, for EPSIN1 and EPSIN2 limited functional and localization data were available; and EPSIN3 remained completely uncharacterized prior to this study (Song et al. 2006; Lee et al. 2007). The molecular details of ENTH domain proteins in plants are still unknown. In order to systematically characterize all four ENTH proteins *in planta,* we first investigated expression and subcellular localization by analysis of stable reporter lines under their endogenous promotors. Although all four genes are ubiquitously expressed, their subcellular distribution differs markedly. EPSIN1 and MTV1 are located at the TGN, whereas EPSIN2 and EPSIN3 are associated with the plasma membrane (PM) and the cell plate. To examine potential functional redundancy, we isolated knockout T-DNA mutant lines and created all higher order mutant combinations. The clearest evidence for functional redundancy was observed in the *epsin1 mtv1* double mutant*,* which is a dwarf displaying overall growth reduction. These findings are in line with the TGN localization of both MTV1 and EPS1. In contrast, loss of *EPSIN2* and *EPSIN3* does not result in a growth phenotype compared to wild type, however, a triple knockout of *EPSIN1*, *EPSIN2* and *EPSIN3* shows partially sterile plants. We focused mainly on the *epsin1 mtv1* double mutant and addressed the functional role of these two genes in clathrin-mediated vesicle transport by comprehensive molecular, biochemical, and genetic analyses. Our results demonstrate that EPSIN1 and MTV1 promote vacuolar transport and secretion of a subset of cargo. However, they do not seem to be involved in endocytosis and recycling. Importantly, employing high-resolution imaging, genetic and biochemical experiments probing the relationship of the AP complexes, we found that EPSIN1/AP1 and MTV1/AP4 define two spatially and molecularly distinct subdomains of the TGN. The AP4 complex is essential for MTV1 recruitment to the TGN, whereas EPSIN1 is independent of AP4 but presumably acts in an AP1-dependent framework. Our findings suggest that this ENTH/AP pairing preference is conserved between animals and plants.

Zusammenfassung

In pflanzlichen Zellen hängt der Transport von Proteinen von vielen dem Golgi-Apparat nachfolgenden Transportwegen ab, welche zum Großteil durch Clathrin-bedeckte Vesikel (CCV) vermittelt werden. Die Vesikelbildung wird durch verschiedene Helferproteine und Adapterproteinkomplexe (AP) ermöglicht. Letztere dienen als Brücke zwischen den Transportproteinen und dem Hüllprotein Clathrin. Eine Gruppe von Hilfsproteinen interagiert mit APs und Clathrin mittels des C-Terminus und ist durch eine konservierte EPSIN N-TERMINAL HOMOLOGY (ENTH)-Domäne definiert. In *Arabidopsis thaliana* wurden drei eng verwandte ENTH-Domänenproteine (EPSIN1, 2 und 3) sowie ein stark konservierter phylogenetischer Außenseiter MODIFIED TRANSPORT TO THE VACUOLE1 (MTV1), gefunden. Im Falle des im *trans*-Golgi Netzwerk (TGN) lokalisierten MTV1 wurde die Assoziation mit Clathrin und eine Rolle im vakuolären Transport nachgewiesen (Sauer et al. 2013). Im Vergleich dazu gab es für EPSIN1 und EPSIN2 nur limitierte Daten und EPSIN3 war bisher unerforscht (Song et al. 2006; Lee et al. 2007). Die Funktionen der ENTH-Domänenproteine in Pflanzen blieben unklar. Um die vier ENTH-Proteine *in planta* zu charakterisieren, untersuchten wir zunächst deren Expression sowie subzelluläre Lokalisation anhand stabiler Reporterlinien, welche Fusionsproteine vom jeweils endogenen Promotor exprimierten. Obwohl unsere Ergebnisse zeigten, dass alle ENTH-Domänenproteine ubiquitär exprimiert wurden, war die subzelluläre Verteilung deutlich unterschiedlich. EPSIN1 und MTV1 lokalisierten am TGN, während EPSIN2 und EPSIN3 in der Nähe der Plasmamembran (PM) und der Zellplatte zu finden waren. Um eine mögliche funktionelle Redundanz zu untersuchen, nutzten wir komplette Funktionsverlust-Mutanten und erzeugten daraus Mutanten höherer Ordnung. Deutliche Hinweise auf funktionelle Redundanz ergab die *epsin1 mtv1*-Doppelmutante, die eine starke Wachstumsreduktion aufwies, was zur Lokalisierung beider Proteine am TGN passte. Im Gegensatz dazu verursachte der Verlust von *EPSIN2* und *EPSIN3* keinen vom Wildtyp abweichenden Phänotyp, jedoch zeigte die *epsin1 epsin2 epsin3*-Dreifachmutante partielle Sterilität. Wir fokussierten uns daher hauptsächlich auf *epsin1 mtv1* und untersuchten die funktionelle Rolle im Clathrin-vermittelten Vesikeltransport durch vergleichende molekulare, biochemische und genetische Analysen. EPSIN1 und MTV1 unterstützten den vakuolären und sekretorischen Transport, waren aber nicht an Endozytose oder Recycling beteiligt. Durch hochauflösende Mikroskopie, genetische und biochemische Analysen der Beziehung zwischen verschiedenen AP-Komplexen und EPSIN1/MTV1 konnten wir zeigen, dass EPSIN1/AP1 und MTV1/AP4 zwei räumlich und molekular distinkte Subdomänen des TGNs definierten. AP4 war essenziell für die MTV1- jedoch nicht die EPSIN1-Rekrutierung zum TGN und EPSIN1 assoziierte bevorzugt mit AP1. Ähnliche Beobachtungen an EPSIN1- und MTV1-Homologen in tierischen Zellen legen eine evolutionär konservierte Paarung von AP-Komplexen und ENTH-Proteinen nahe.

1. Introduction

1.1 Vesicle transport in eukaryotic cells

All eukaryotic cells possess a complex endomembrane system which forms different membrane-enclosed compartments required for specific functions (Figure 1). A newly synthesized protein that contains a signal peptide for sorting to the endoplasmic reticulum (ER) or provides transmembrane domains and is targeted to the plasma membrane (PM) enters the endomembrane system. These proteins pass through the ER and are transported further to the *cis* face of the Golgi apparatus. Within the Golgi apparatus proteins are modified and move from the *cis* to the *trans* face. Most proteins pass through the *trans*-Golgi network (TGN), where they are sorted and packed into vesicles according to their final destination such as PM or multivesicular body (MVB)/pre-vacuolar compartment (PVC) and vacuole. Those cargo proteins enter different trafficking pathways (Roth et al. 1985; Griffiths and Simons 1986). For plants, it has been shown that there are two forms of the TGN (Viotti et al. 2010). Firstly, the Golgi-associated TGN (GA-TGN) and secondly, the free TGN (Kang et al. 2011; Uemura et al. 2014). In addition and in contrast to the situation in animal cells, the plant TGN acts as an early endosome (EE) which indicates a role in multiple trafficking pathways like endocytic and secretory routes (Dettmer et al. 2006).

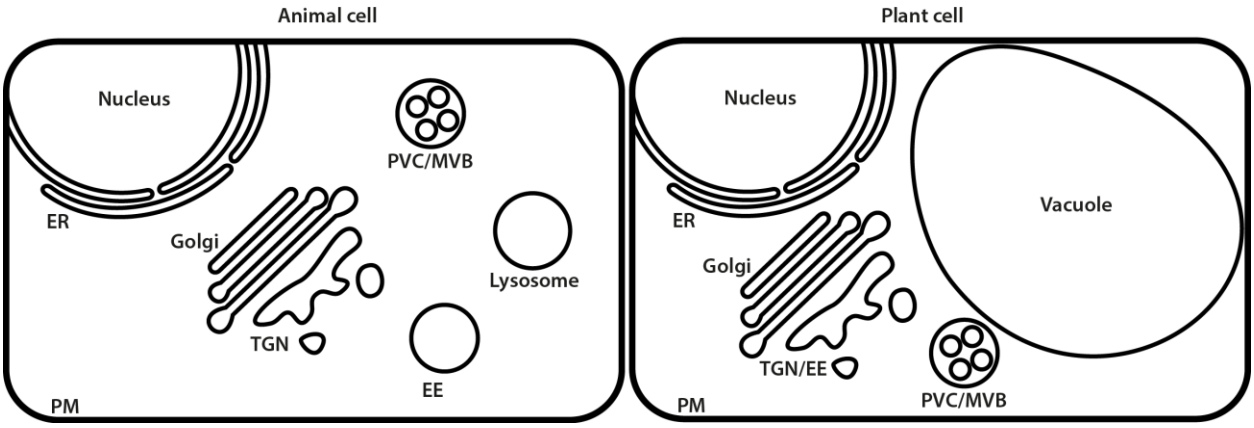

Figure 1: Simplified model of animal and plant endomembrane system. ER: endoplasmic reticulum; TGN: *trans*-Golgi network; EE: early endosome; PVC: pre-vacuolar compartment; MVB: multivesicular body; PM: plasma membrane

In order to execute the specific transport of proteins between different membrane-enclosed compartments, cargos are packed into vesicles at the donor membrane and fuse to the target membrane to release their content. This vesicle transport hypothesis was determined by early electron microscopy (EM) studies. (Roth and Porter 1964; Palade 1975). The first evidence for the vesicle transport was the result of EM studies of yolk proteins. In fact, yolk proteins were detected within invaginations and pits at the PM of oocytes of mosquito *Aedes aegypti* (Roth and Porter 1964). In the early 1970s coated vesicles

were purified and analyzed by biochemical approaches (Kanaseki and Kadota 1969, Pearse 1975). One resulting question was: How are vesicles formed? Many details of this process and factors which are involved in vesicle formation are still unknown. In general, vesicle formation is a stepwise process (Figure 2). In the first step cargo proteins are recognized by sorting receptors and the specific lipid composition of the donor membrane is recognized by lipid binding domains. This initiation leads to the recruitment of additional factors like coat proteins, adaptor proteins and accessory proteins to the donor membrane. It turned out that there are three major coat protein complexes in eukaryotic cells: coatomer protein I (COPI), coatomer protein II (COPII) and clathrin (Bonifacino and Lippincott-Schwartz 2003). COPI is involved in retrograde vesicle transport from the Golgi complex to the ER (Waters et al. 1991; Serafini et al. 1991; Bednarek et al. 1995). COPII mediates the anterograde trafficking from the ER to the Golgi (Barlowe et al. 1994; Barlowe 1998). The third isolated coat component was called clathrin (Pearse 1975). It consists of three clathrin light chains (CLC) and three clathrin heavy chains (CHC) which assemble as a triskelion (Ungewickell and Branton 1981; Kirchhausen et al. 1987). Clathrin mediates most *post*-Golgi trafficking pathways as well as endocytosis and recycling at the PM. The next step is cargo recruitment and membrane bending. The coated vesicle is formed and the last step is the vesicle scission from the donor membrane (Fan et al. 2015; Kaksonen and Roux 2018). Proteins termed dynamins are one example of a scission complex. The multidomain protein dynamin self-assembles into rings and helical stacks of rings around the vesicle neck (Sever et al. 2002). Once the large GTPase dynamin has polymerized it promote membrane fission by using the energy of GTP (Ferguson and De Camilli 2012). Over the last years the role of the cytoskeleton in vesicle formation and vesicle transport has been discussed (Qualmann et al. 2000). The interaction of dynamin proteins and actin or actin-binding proteins can functionally link the vesicle scission process with the cytoskeleton (Kessels et al. 2001). In addition, it has been demonstrated that one class of accessory proteins, epsin N-terminal homology (ENTH) domain proteins, in mammalian and yeast cells directly interact with actin or tubulin (Wendland et al. 1999; Engqvist-Goldstein et al. 1999; Hussain et al. 2003; Messa et al. 2014).

Adaptor proteins are important factors for vesicle formation. The adaptor protein (AP) complexes AP1 and AP2 for instance were isolated from purified clathrin-coated vesicles (CCVs) and extensively studied in the following years (Pearse and Robinson 1984; Keen 1987). Additionally, many accessory proteins were found in purified CCVs. One class of accessory proteins are ENTH domain proteins which are essential elements of the coat formation machinery (De Camilli et al. 2002; Legendre-Guillemin et al. 2004). The role of adaptor proteins and accessory proteins will be of major interest in this thesis and explained in more detail in the following sections.

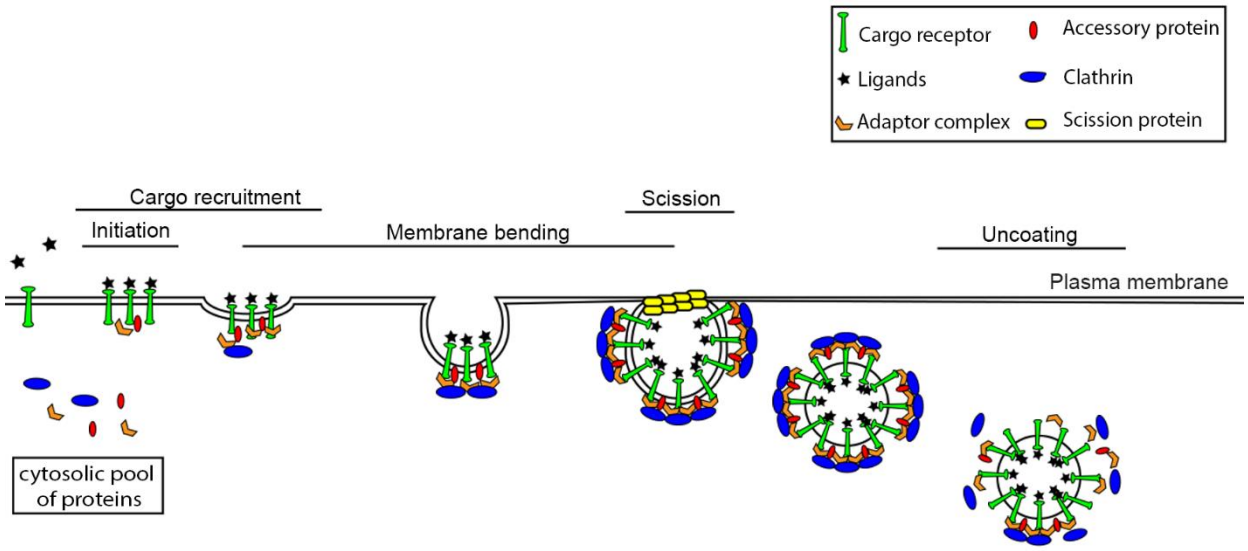

Figure 2: Steps of clathrin-mediated endocytosis

1.2 Adaptor protein (AP) complexes

The identity and function of adaptor protein complexes in eukaryotic cells has been extensively reviewed within the last years (Brodsky et al. 2001; Boehm and Bonifacino 2001; Robinson and Bonifacino 2001; Hirst et al. 2013; Lee and Hwang 2014). AP complexes are heterotetramers composed of two large subunits (β 1-5 and α, γ, δ, ε, ζ), one medium size subunit (μ 1-5) and one small subunit (σ 1-5) (Figure 3). The complexes are built like a head with a core (medium and small subunit as well as parts of the two large subunits) and two ears (appendage domains of the two large subunits) which are connected by a flexible hinge (Heuser and Keen 1988; Collins et al. 2002). The different subunits have different functions. The large β subunit recruits and interacts with clathrin through a binding sequence in its hinge domain. (Gallusser and Kirchhausen 1993; Goodmann and Keen 1995; Morgan et al. 2000). Both, the β and μ subunits are involved in cargo selection (Ohno et al. 1995; Rapoport et al. 1998; Bonifacino and Dell'Angelica 1999). The ear domains have been implicated in recruitment of accessory proteins which may influence the assembly and disassembly of the coat proteins (Hao et al. 1999; Owen et al. 1999; Traub et al. 1999; Duncan et al. 2003).

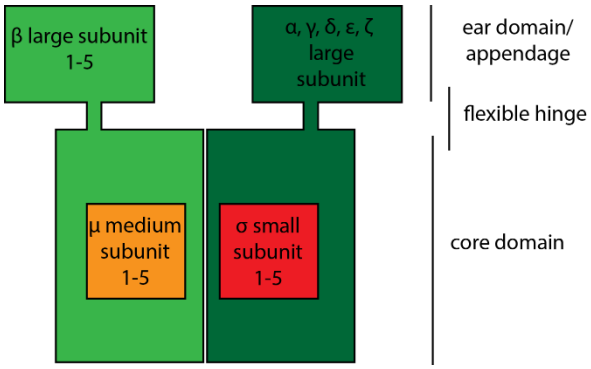

Figure 3: Model of adaptor protein complexes in eukaryotic cells. AP1 with γ subunit, AP2 with α subunit, AP3 with δ subunit, AP4 with ε subunit, AP5 with ζ subunit

In eukaryotic cells the function of AP complexes is highly conserved. The AP1 and AP2 complexes are known for many years and have been characterized extensively in animal and plants cells as well as yeast cells. In plants, AP1 is located at the TGN and mediates the CCV trafficking between TGN, EE and vacuole (Teh et al. 2013; Park et al. 2013; Wang et al. 2013). Genetic analyses suggest that AP1 is the major trafficking component involved in various protein trafficking routes. *Arabidopsis thaliana* (*A. thaliana*) possesses two isoforms of the large β subunit of AP1. Knockout mutants of one isoform of the AP1 β subunit show drastic developmental and morphological defects. Double knockout of both isoforms leads to embryo-lethal mutants which was previously shown in mice as well (Zizioli et al. 1999; Boehm and Bonifacino 2001). The μ subunit of AP1 is also represented by two isoforms in Arabidopsis (AP1M1 and AP1M2). In a genetic screen for developmental or functional haploid gametophyte defects in *A. thaliana*, *HAPLESS13* (*hap13*) was identified which is a loss of AP1 μ subunit mutant (Johnson et al. 2004; Park et al. 2013). Plants lacking AP1 μ subunit showed abnormal root architecture, impaired root length and defects in vacuolar transport as well as secretory trafficking (Park et al. 2013). Endocytosis and recycling were not affected. The severe phenotype of *ap1* mutants can partially be explained by the mis-targeting of the essential KNOLLE syntaxin (Park et al. 2013; Teh et al. 2013) which normally resides at the cell plate and is required for correct cytokinesis (Lukowitz et al. 1996; Lauber et al. 1997). Moreover, it has recently been demonstrated that the AP1 complex is also involved in polarized secretion of mucilage (Shimada et al. 2018). The mucilage layer of seeds in *A. thaliana* consists of pectin polysaccharides which have to be secreted into the seed coat (Western et al. 2000). Thus, besides the KNOLLE syntaxin, pectin polysaccharides or mucilage were identified as cargos of AP1-mediated vesicle transport.

The AP2 complex, located at the PM, directly interacts with clathrin and is involved in endocytosis mediated by CCVs (Gallusser and Kirchhausen 1993; Goodman and Keen 1995). At the PM the complex binds preferentially to phosphatidylinositol-4,5-bisphosphate (PtdIns(4,5)P_2) and phosphatidylinositol-

3,4,5-trisphosphate (PtdIns(3,4,5)P_3) (Gaidarov et al. 1996; Gaidarov and Keen 1999). Knockout of the AP2 µ subunit leads to an embryo-lethal phenotype in mice (Mitsunari et al. 2005). In plants, the direct interaction of AP2 with clathrin has been demonstrated and *ap2* knockout mutants exhibit several developmental defects (Fan et al. 2013; Kim et al. 2013). It has been shown that loss of the AP2 σ subunit causes defects in endocytosis and recycling of auxin efflux carrier protein PIN-FORMED 1 (PIN1). Due to mis-localized PIN1 proteins, *ap2* mutants show defects in their auxin gradient which causes various developmental defects, for instance, reduced vegetative growth and mis-formed cotyledons (Fan et al. 2013). Moreover, mutants of the AP2 µ subunit display multiple phenotypes including abnormal phyllotaxis, altered flower organs, smaller siliques and a defect in pollen production, pollen tube growth and staminal filaments (Kim et al. 2013; Yamaoka et al. 2013). Another cargo of AP2-dependent endocytosis are CELLULOSE SYNTHASE (CESA) proteins. An interaction of AP2 µ subunit with CESA6, 3 and 7 was demonstrated in Yeast two hybrid (Y2H) screen as well as *in planta* studies and biochemical approaches (Gu et al. 2010; Bashline et al. 2013). Importantly, it has been suggested from phylogenetic analysis that the β adaptins and the isoforms of AP1 and AP2 are shared proteins in both complexes (Boehm and Bonifacino 2001; Dacks et al. 2008). Thus, higher order knockout mutations of β adaptins cause loss of AP1 and AP2 which results in embryonic lethality (Zizioli et al. 1999). In contrast, single and higher order knockout mutants of other subunits of the AP1 or AP2 complex only lead to loss of either AP1 or AP2 (Boehm and Bonifacino 2001).

Some years ago, the AP3, AP4 and AP5 complexes were identified in animal and plant cells by sequence analysis. AP3 mediates the transport between EE, lysosomes and PVC (Simpson et al. 1996). In humans, loss of AP3 β subunit leads to defective melanosomes which causes a disease called Hermansky-Pudlak syndrome type 2 (Dell'Angelica et al. 1999a). The direct interaction of AP3 with clathrin has been shown for the mammalian but not the yeast or plant proteins, yet (Dell'Angelica et al. 1998). Yeast mutants of AP3 subunits showed mis-localization of specific vacuolar cargos like ALKALINE PHOSPHATASE (ALP) and the vacuolar soluble N-ethylmaleimidesensitive factor attachment protein receptor (SNARE) protein, termed Vam3p, which indicated a cargo selective role of AP3 in vacuolar transport (Cowles et al. 1997; Stepp et al. 1997). In *A. thaliana*, the first loss of function mutant of an AP3 µ subunit, called *zig suppressor 4* (*zip4*), was isolated by a screen to identify mutants that can suppress the *zig-1* phenotype. AP3 was suggested as a player in transport between TGN and vacuoles (Niihama et al. 2009). One year later another screen was performed in *A. thaliana* in which an AP3 β subunit mutant, termed *protein affected trafficking 2* (*pat2*), was isolated (Feraru et al. 2010). *In planta*, *pat3* did not show any morphological aberrations or growth defects, although various PM proteins and soluble proteins are mis-localized in *pat3*. It was

demonstrated that mis-targeted proteins accumulate as a result of disturbed vacuolar transport and therefore proteins cannot be degraded (Feraru et al. 2010). The *pat4* mutant is a loss of AP3 δ subunit function and showed the same phenotype as *pat3* (Zwiewka et al. 2011). Both, *pat3* and *pat4,* displayed aberrantly shaped lytic vacuoles with multi-membrane enclosures which suggested a role of AP3 in lytic vacuolar biogenesis and identity (Feraru et al. 2010; Zwiewka et al. 2011). Only a few cargos, for instance SUCROSE TRANSPORTER4 (SUC4), PAT10 and VESICLE-ASSOCIATED MEMBRANE PROTEIN711 (VAMP711) have so far been demonstrated to be involved in of AP3-mediated trafficking pathways (Feng et al. 2017).

The function of AP4 is one of the least understood so far (Hirst et al. 2013). Nevertheless, it has been shown in animal and plant cells that the AP4 complex is located at the TGN (Hirst et al. 1999; Dell'Angelica et al. 1999b; Burgos et al. 2010; Fuji et al. 2016). Interestingly, yeast cells and fruit flies do not have an AP4 and AP5 complex (Boehm and Bonifacino 2001). At present, it remains to be determined as to whether AP4 can directly interact with clathrin. In addition, the AP4 β subunit lacks the so-called ear domain where the clathrin-binding box is located in AP1, 2 and 3. This suggests that AP4 is involved in a non-clathrin coated vesicle pathway at the TGN (Hirst et al. 1999; Paolini et al. 2011). In humans, loss of any AP4 subunits leads to severe intellectual disability and neurological disorders (Verkerk et al. 2009; Burgos et al. 2010; Abou et al. 2011; Moreno-De-Luca et al. 2011). Recently, loss of function mutants of the AP4 complex have been identified by a mutant screen in *A. thaliana* (Fuji et al. 2007; Fuji et al. 2016). The GREENFLUORESCENT SEED 4, 5 and 6 (*gfs4*, *gfs5* and *gfs6*) mutants displayed loss of the AP4 β, the μ and the σ subunits, respectively. All *ap4* mutant plants accumulated high levels of VACUOLAR SORTING RECEPTORs (VSRs) which are involved in vacuolar sorting of storage proteins, suggesting a role of AP4 in vacuolar transport (Ahmed et al. 1997; Shimada et al. 2003; Müdsam et al. 2018). In addition, all *ap4* mutants showed reduced growth and shorter root length. Recently, a role of AP4 in plant immunity has been demonstrated (Hatsugai et al. 2018). With inoculation experiments it has been shown that *ap4* mutant plants are less resistant against bacterial infection. In fact, the fusion of vacuolar membrane and PM is abolished and causes defects in hypersensitive cell death as a response to bacterial infection. The molecular mechanism of AP4 in vacuolar fusion is not clear. One hypothesis is that AP4 mediates the transport and sorting of vacuolar located immune-associated cargo proteins or SNARE proteins which are involved in vacuolar fusion processes.

Although some sequence similarities of AP5 subunits were found in *A. thaliana,* the proof for a functional AP5 complex in plants is still lacking (Hirst et al. 2011; Hirst et al. 2013). In animal cells, the AP5 complex was connected to the transport in the late endocytic pathway, however, the subcellular localization of the

AP5 complex remains to be determined (Hirst et al. 2011). The knockout of AP5 causes MVB swelling and an increased number of MVBs in HeLa cells. Moreover, loss of AP5 in humans leads to neurological disorders similar to the AP4 knockout phenotype (Hirst et al. 2013).

1.3 Epsin N-terminal homology domain-containing proteins

The ENTH domain is a highly conserved domain found in proteins of eukaryotic organisms like yeast, plants, mice and humans which consists of approximately 130-150 amino acids forming eight α-helices. It has been characterized as a lipid-binding domain that can influence lipid morphology at the membrane (Ford et al. 2002; Lai et al. 2012). ENTH domain proteins have always been connected to CCV formation (Kay et al. 1999; Rosenthal et al. 1999; Legendre-Guillemin et al. 2004; Zouhar and Sauer 2014). The ENTH domain of mammalian epsin1 was crystallized with its so-called helix zero in complex with PtdIns(4,5)P_2 (Itoh et al. 2001) Moreover, it has been proposed that ENTH domains are specific for certain phosphoinositides (PIs) depending on their head group phosphorylation. For instance, mammalian EpsinR showed a higher affinity to PtdIns(4)P rather than PtdIns(4,5)P_2 (Mills et al. 2003). This observation lead to the hypothesis that the helix zero, which presents many hydrophobic residues on the surface, can be inserted into the cytosolic leaflet of the lipid bilayer thereby inducing membrane curvature (Stahelin et al. 2003; Lai et al. 2012). It has been discussed whether ENTH domain proteins act as oligomers like other accessory proteins, but this has not been demonstrated so far (Ford et al. 2002; Gallop et al. 2006). The C-terminal part of ENTH domain proteins has been described as a large unstructured tail providing multiple interaction platforms for other elements of the vesicle formation machinery (Kalthoff et al. 2002a). One proposed model is that the N-terminal part of ENTH proteins binds to the membrane by interaction with PtdIns and the C-terminal part recruits coat components for vesicle formation (Ford et al. 2002). In this model, ENTH domain proteins are involved in early steps of vesicle formation. In contrast, there is evidence that ENTH domain proteins may be involved in late steps in particular vesicle scission. In fact, mammalian epsins locate at the neck of the forming vesicle at the opposite side of AP complexes (Saffarian et al. 2009; Taylor et al. 2011; Boucrot et al. 2012). In addition, the triple *epsin* mutant in mouse showed impaired CCV formation due to the inability of vesicle scission (Messa et al. 2014). Clathrin-coated pits were built but the force for deep invagination of the vesicle and fission was not provided. As a result, the *epsin* triple-knockout mice displayed drastic defects in clathrin-mediated endocytosis and cell division (Messa et al. 2014). There is clear evidence in mammalian and yeast cells that the ENTH domain can interact with SNARE proteins (Jahn et al. 2003; Chidambaram et al. 2004; Wang et al. 2011; Messa et al. 2014). For instance, the mammalian epsinR/ clathrin-interacting protein localized in the *trans*-Golgi region

(CLINT)/Enthoprotein interacts with vesicle (v-)SNARE vti1b (Vesicle transport through interaction with t-SNAREs homolog 1B) (Hirst et al. 2004; Miller et al. 2007). SNARE proteins are integrated in donor membranes, target membranes and vesicle membranes and mediate recognition and vesicle fusion. This SNARE-ENTH interaction has also been shown in plants (Song et al. 2006; Lee et al. 2007).

Members of the ENTH domain protein family in mammals, budding yeast and plants appear to group into two classes by phylogenetic analysis (Legendre-Guillemin et al. 2004). The first class contains members like mammalian epsin1 as well as budding yeast Ent1p and Ent2p which are involved in vesicle transport at the PM, specifically in endocytosis (Chen et al. 1998; Wendland et al. 1999; De Camilli et al. 2002). Second class contains mammalian epsinR/CLINT/Enthoprotein as well as budding yeast Ent3p and Ent4p which are located at the TGN and mediate *post*-Golgi vesicle transport (Duncan et al. 2003; Costaguta et al. 2006). In plants, seven ENTH domain proteins have been identified (Zouhar and Sauer 2014). According to the protein structure, they group into two clusters with three proteins each (Figure 4). The first group contains EPSIN1, 2 and 3 which possess a long C-terminus, whereas the second group include three proteins with a very short C-terminal tail. In addition, there is one phylogenetic outlier which is highly conserved throughout the plant kingdom and termed MODIFIED TRANSPORT TO THE VACUOLE1 (MTV1) (Sauer et al. 2013).

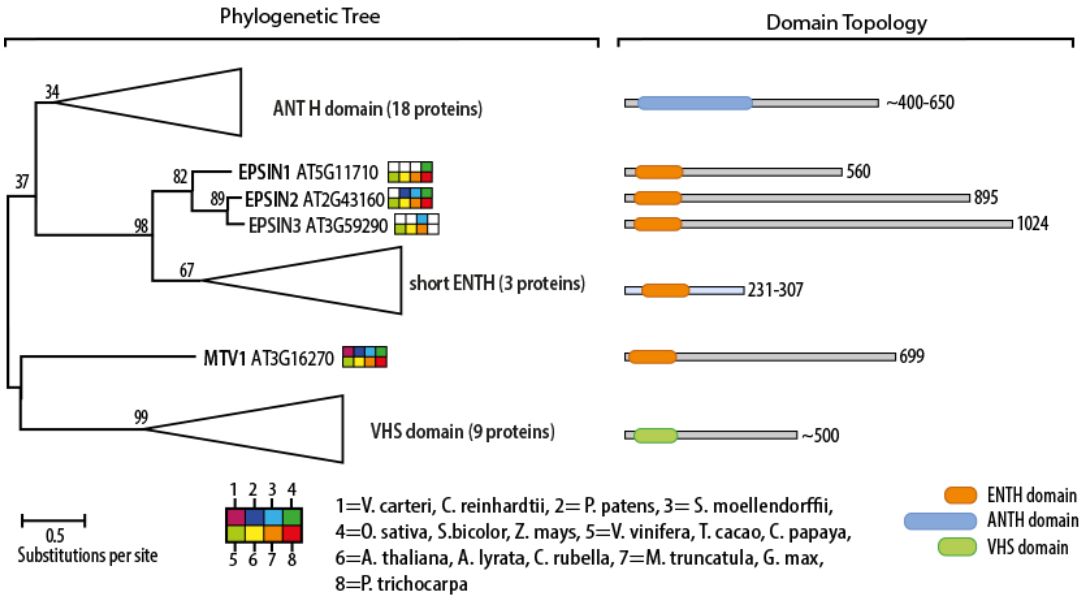

Figure 4: Phylogenetic analysis of ENTH domain proteins in plants (modified from Zouhar and Sauer 2014). Segments of the rainbow-colored bar indicate the presence/absence of a clear homolog in at least one of the species indicated. Rough domain topology is shown on the right, with approximate length and placement of N-terminal domains. Reproduced and modified with permission of Oxford University Press – Journals.

The homolog of mammalian epsinR is EPSIN1/EpsinR1 which was the first plant ENTH domain protein that was investigated in detail (Song et al. 2006). EPSIN1 was reported to display a wide expression range throughout various plant tissues. The subcellular localization was addressed by transient transformation of protoplasts resulting in a network and punctate pattern. The EPSIN1 signal was partially co-localized with a Golgi marker, a TGN marker and a PVC marker. By co-transformed EPSIN1:RFP and GFP:talin protoplasts, which is a F-actin marker, in combination with latrunculin B (actin filament disruptor) drug treatment the network pattern of EPSIN1 and actin filaments was interrupted. However, stable transformation studies as well as tests for functionality of fluorescently tagged EPSIN1 are missing. Again, only limited *in planta* data from a weak T-DNA-insertion mutant allele were presented (Song et al. 2006). Thus, *in planta* localization and loss of function mutant data are still lacking. EPSIN1 interaction with clathrin, AP1, v-SNARE VTI11/AtVTI1a (VESICLE TRANSPORT V-SNARE11) and VSR1 by pull down assay and co-immunoprecipitation was determined (Song et al. 2006). It has been concluded that EPSIN1 is an ENTH domain protein involved in a clathrin- and AP1-mediated vesicle transport pathway at the Golgi and/or *post*-Golgi (Song et al. 2006).

The second ENTH domain protein that was characterized is EPSIN2/EpsinR2 (Lee et al. 2007). By *in vitro* lipid-binding assays it has been demonstrated that EPSIN2 specifically binds to PtdIns(3)P. To examine the subcellular localization, transiently transformed protoplasts were used and EPSIN2 was proposed to be a Golgi protein. Moreover, EPSIN2 was linked to vesicle transport by identifying its interaction partners clathrin, AP3 and, to a lesser extent, AP2 and VTI12/AtVTI1b with pull down assays (Lee et al. 2007). However, reliable *in planta* data of the expression pattern, subcellular localization and general function are not available, yet, and loss of function mutants as well as stable transformation lines have not been investigated until now.

The third ENTH domain protein in plants that has been characterized, so far, is the phylogenetic outsider called MTV1 (Sauer et al. 2013). It was identified in a mutant screen for plants with impaired transport to the vacuole in order to identify factors involved in this trafficking pathway (Sanmartin et al. 2007). MTV1 is expressed throughout the whole plant displaying stronger abundance in root meristem, shoot and leaf vasculature (Sauer et al. 2013). The subcellular localization was addressed by *in planta* studies and the punctate pattern of MTV1-GFP was shown to represent a TGN localization. It has been shown that the *mtv1* loss of function mutant in A. thaliana is slightly smaller than the wild type and displays an impaired transport of storage proteins to the vacuole as well as the mis-localization of endogenous vacuolar cargo in vegetative tissue (Sauer et al. 2013). In addition, MTV1 was directly connected to CCVs by purifying

CCVs and detecting MTV1 with a specific antibody. Importantly, *mtv1* mutant plants did not show any obvious defects in endocytosis and recycling.

The interaction of AP complexes with specific accessory proteins was previously discussed. In case of human AP4, there is only one accessory protein, called tepsin, known to interact directly with AP4 β and ε subunits (Borner et al. 2012; Mattera et al. 2015; Frazier et al. 2016). Interestingly, in human cells AP4 and tepsin co-localize in a punctate pattern which is completely disrupted and cytosolic in *ap4* loss of function mutant cells. In contrast, loss of tepsin had no effect on AP4 localization. Thus, in human cells, AP4 is required for tepsin recruitment to the TGN (Borner et al. 2012). Recently, the structure of the tepsin ENTH domain was resolved by X-ray crystallography (Archuleta et al. 2017). Surprisingly, the ENTH domain of tepsin lacks the zero helix, helix 8 and the binding motifs for PIs. Furthermore, biochemical data using recombinant ENTH domains on PIP strips confirmed the structural predictions (Archuleta et al. 2017). Thus, tepsin is unlikely to be able to bind PIs. Moreover, this data suggests that the special structure causes dependency of tepsin on AP4 for its correct localization. Notably, the tepsin-AP4 β/ε-binding motif is conserved in different eukaryotic groups, for instance, in *A. thaliana.* The tepsin homolog in plants is termed MTV1. Thus far the interaction of AP4 with a specific ENTH domain protein in plants has not been addressed.

1.4 Aim of the project

In plants, the functional roles of ENTH domain proteins remain unclear. Some first data on EPSIN1, EPSIN2 and MTV1 have been published but only in case of MTV1 *in planta* data and functional analysis is available (Song et al. 2006; Lee et al. 2007; Sauer et al. 2013). The aim of the project was to address potential functional redundancy and to perform a comprehensive characterization of the four members of the ENTH protein family in *Arabidopsis thaliana.* The expression, subcellular localization and loss of function mutant phenotypes were to be investigated in this work. The observed interesting genetic interaction between *MTV1* and *EPSIN1* became the main focus of further studies including the examination of their roles in different trafficking pathways. Furthermore, first interaction data of ENTH proteins with AP complexes were available, however, the underlying specificity and functional overlap is not clear, yet (Song et al. 2006). Thus, this project aimed to uncover the molecular link between ENTH domain proteins and specific AP complexes.

2. Materials and Methods

2.1 Materials

All materials (equipment, chemicals, reaction kits as well as software and primer sequences) which were used are summarized in the appendix including the respective manufacture (Supplementary table 1-6).

2.2 Methods

2.2.1 Growth conditions and culturing of organisms

Arabidopsis thaliana (*A. thaliana*) accession Columbia-0 (Col-0) plants and mutant lines were grown on soil in the greenhouse or in growth chambers with long-day conditions (16 h light and 8 h dark) at 22-23°C. Seedlings were grown vertically on plates with 0.5 x Murashige and Skoog (MS) medium (1 l: 10 g sucrose, 2.2 g Murashige and Skoog, 8.0 g plant agar, 0.5 g MES, pH 5.8) including 1% weight per volume (w/v) sucrose and 0.4% (w/v) plant agar. Seeds were incubated for 2 days with 4°C and darkness to synchronize germination before exposure to light. Normally, the experiments were carried out with 5-day-old seedlings, if not otherwise marked. To select transformed plants in the T1 generation, seeds were sowed on MS medium containing appropriate antibiotics (Table 2). Seed sterilization was done under the clean bench. Seeds were mixed with 70% ethanol for maximum 10 min followed by 100% ethanol for maximum 2 min. After 2 h the ethanol was evaporated and seeds were ready to use.

Escherichia coli (*E. coli*) strains BL21 and DH5α were cultivated in liquid Lysogeny broth (LB) medium (1 l: 10 g tryptone/peptone ex casein, 5 g yeast extract, 10 g NaCl pH 7.0) in orbital shaking incubators at 37°C and 220 rpm overnight. Alternatively, petri dishes were used with solid LB medium including bacto agar (15 g/l) overnight at 37°C within an incubator.

Agrobacterium tumefaciens (*A. tumefaciens*) strain GV3101 was incubated with either liquid or solid Yeast Extract Beef (YEB) medium (1 l: 5 g beef extract, 1 g yeast extract, 1 g tryptone/peptone ex casein, 5 g sucrose, 0.49 g $MgSO_4 \cdot 7H_2O$, 15 g agar-agar) at 28°C for 2-3 days.

2.2.2 *In vitro* pollen germination assay

The *in vitro* pollen germination assays were performed as described in detail (Rodriguez-Enriquez et al. 2013). The pollen medium (10% (w/v) sucrose; 1.5% (w/v) low melt agarose; 1 mM $CaCl_2$; 1 mM $Ca(NO_3)_2$; 1 mM KCl; 0.03% (w/v) amicase; 0.01% (w/v) myo-Inositol; 0.01% (w/v) ammonium ferric citrate; 10 mM γ-aminobutyric acid (GABA); 0.1 mM spermidine; 0.01% (w/v) boric acid; pH 8.0) was prepared, instead of autoclaving, it was boiled for a few minutes and stored at -20°C in tubes for several months. Immediately before use, the medium was melted at 65°C for 10 min. On a microscope slide, a rectangle (1.5 cm x 2.0

cm) was drawn with a Circle Writer Liquid Blocker Pen and filled it up with 250 µl pollen medium. Next, the solid medium was covered with a cellulosic cellophane membrane (325P Cellulose). Recently opened flowers were used as pollen donor on the surface of the membrane. Slides with pollen were incubated at 25°C in darkness in small slide chambers with wet tissues inside to generate high humidity for 3 h. The outgrown pollen tubes were imaged at the membrane with Zeiss Axio Zoom.V16 with 32x magnification (objective: Plan-NEOFLUAR Z 1.0x/0.25 FWD 56 mm) and the pollen germination rate calculated using ImageJ.

2.2.3 T-DNA mutant lines and marker lines

Different T-DNA mutant lines were analyzed and higher order mutants were generated by crossing.

Table 1: T-DNA mutant lines with their locus and stock number. Lines which were used in this study are marked in grey.

Name	AGI code	Stock number
epsin1-1	AT5G11710	SALK_049204
epsin1-2	AT5G11710	SAIL_394_G02
epsin1-3	AT5G11710	SALK_200365C
epsin2-1	AT2G43160	SALK_043953
epsin2-2	AT2G43160	SAIL_172_B07
epsin2-3	AT2G43160	GABI_952E04
epsin3-1	AT3G59290	SALK_060957
epsin3-2	AT3G59290	SALK_060957
epsin3-3	AT3G59290	SALK_060899
epsin3-4	AT3G59290	SALK_085179
epsin3-5	AT3G59290	SALK_110999
mtv1-1	AT3G16270	FLAG_276G08
mtv1-2	AT3G16270	SALK_061811
mtv1-3	AT3G16270	GABI_587B11
mtv4-1	AT5G54310	SALK_079928
mtv4-2	AT5G54310	SALK_099679
ap4e-1	AT1G31730	SAIL_866_C01
ap4e-2	AT1G31730	SAIL_60_E03
ap4s1	AT2G19790	SAIL_525_A07
ap4b-1	AT5G11490	SAIL_796_A10
ap4b-2	AT5G11490	SAIL_781_H01
ap4m-1	AT4G24550	SALK_014326
echidna	AT1G09330	SAIL_163_E09
quartet-1	AT5G55590	

In order to study the subcellular localization of ENTH domain proteins in detail, published and well-established marker lines were used: mCherry-RabF2b/ARA7 (ARABIDOPSIS RAB GTPASE HOMOLOG7), mCherry-SYP32, mCherry-Got1p (GOLGI TRANSPORT 1), mCherry-RAB A1g (Geldner et al. 2009); CFP-

SYP61 (Robert et al. 2008); Vha1-a1-RFP (VACUOLAR PROTON ATPASE A1) (Dettmer et al. 2006), PIN2-GFP (PIN-FORMED2) (Abas et al. 2006); CLC-mKO (Ito et al. 2011); secN-R_m-2A-GH and secRFP (Samalova et al. 2006).

2.2.4 Transformation of organisms

To transform electrocompetent *E. coli* (strain BL21) and *A. tumefaciens* cells (Inoue et al. 1990), 50 µl cells and 1 µl plasmid were used within a clean electroporation cuvette (2 mm gap). After 3 min incubation on ice the MicroPulser Electroporator (BioRad) with program 2 was used. Immediately after pulsing, 1 ml super optimal broth (SOB) medium (1 l: 5 g NaCl, 20 g tryptone/peptone ex casein, 5 g yeast extract and 2.5 ml 1 M KCl) was added, transferred to a 1.5 ml tube and placed into the thermomixer at either 37°C (*E. coli*) or 28°C (*A. tumefaciens*) and 350 rpm for 2 h. In order to select for transformed cells, they were plated on solid LB medium (E. coli) or YEB medium (A. *tumefaciens)* with appropriate antibiotics and incubated for one to two days at 37°C or 28°C.

A. thaliana plants were stably transformed employing the floral dip method (Clough and Bent 1998). For this, 4 to 5-week-old plants were used one week after cutting the main inflorescence stem which increases the number of unopened buds. *A. tumefaciens* cells were precultured in liquid YEB medium and antibiotics at 28°C with 220 rpm one day before. The next day an overnight culture was prepared with fresh YEB medium to a final volume of 200 ml. The culture was mixed 2 h at 28°C, acetosyringone added to a final concentration of 100 µM and incubated for 4 h. Immediately before dipping, 4% (w/v) sucrose and 0.05% (v/v) Coatosil 77 were added. Next plants were dipped into the bacterial culture and pots were placed horizontally on a tray. After 5 min the pots were placed upright, the tray was covered and plants were incubated overnight at 4°C. Next day, transformed plants were put into a growth chamber under normal growth conditions.

To C-terminally tag our genes of interest, the Gateway® cloning technique was used. First, entry clones were generated containing the genomic sequence of our gene of interest including its endogenous promotor and without its stop codon and then recombined it into a destination vector containing the respective tag. The pDONR^{TM}221 was used for all constructs and resulted in the entry vector pENT221. Destination vectors pGWB3 (β-GLUCURONIDASE (GUS)), pGWB4 (enhanced GREEN FLUORESCENT PROTEIN (eGFP)) and pGWB401 (modified with an mRuby3 CDS for C-terminal fusion) were used to create binary vectors for plant transformation. Constructs are listed in table 2.

Table 2: Entry vectors and destination vectors used for transformation into different organisms.

Gene of interest		Promotor size [bp]	Gene size [bp]	Antibiotic resistant bacteria	Antibiotic resistant plant	Final construct
EPSIN1	AT5G11710	1400	3333	Kan, Hyg	Kan, Hyg	*pEPSIN1::EPSIN1-eGFP*
				Kan, Hyg	Kan, Hyg	*pEPSIN1::EPSIN1-GUS*
				Spec	Kan	*pEPSIN1::EPSIN1-mRuby3*
EPSIN2	AT2G43160	1569	4381	Kan, Hyg	Kan, Hyg	*pEPSIN2::EPSIN2-eGFP*
				Kan, Hyg	Kan, Hyg	*pEPSIN2::EPSIN2-GUS*
EPSIN3	AT3G59290	1578	4676	Kan, Hyg	Kan, Hyg	*pEPSIN3::EPSIN3-eGFP*
				Kan, Hyg	Kan, Hyg	*pEPSIN3::EPSIN3-GUS*
MTV4	AT5G54310	537	2836	Spec	Kan	*pMTV4::MTV4-mRuby3*

2.2.5 DNA and RNA isolation from plant material

For mid-throughput DNA extraction, autotube racks were used with 96 deep well tubes with 5-10 glass beads of 2 mm diameter and one small young leaf was harvested per tube. After adding 400 ml Edwards extraction buffer (1 l: 200 mM Tris, 250 mM NaCl and 25 mM EDTA pH 8.0) a TissueLyser II was used twice for 1 min with full speed to disrupt plant material (Edwards et al. 1991). Next, sodium dodecyl sulfate (SDS) was added to a final concentration of 0.05% (w/v), mixed by inverting and centrifuged for 4 min at 1,500 g at room temperature. 280 µl of the supernatant were transferred to new tubes with 300 µl 2-propanol, inverted and incubated for 5 min. Afterwards, the tubes were centrifuged for 15 min at 1,500 ga at room temperature. The supernatant was discarded and the non-visible pellet was washed with 500 µl 70% ethanol for 10 min. A last centrifugation step was carried out for 5 min at 1,500 g at room temperature. The supernatant was discarded and the ethanol evaporated overnight. On the next day, the pellet was resuspended in 100 µl TE buffer (10x stock solution: 100 mM Tris and 10 mM EDTA pH 8.0) and directly used for PCR.

To isolate RNA the RNeasy Plant Mini Kit was employed according to the manufacturer's instructions. Plant material was disrupted, which was frozen in liquid nitrogen, using glass beads and an ultramat 2 (high speed multi-use triturator). The RLT buffer was used as lysis buffer. In order to check RNA quality and concentration, Nanodrop 2000 was used and additionally isolated RNA was separated by an agarose gel (section 2.2.7).

2.2.6 Genotyping of plants by polymerase chain reaction

The 5x FIREPol Master Mix 12.5 mM $MgCl_2$ was used for genotyping of plants and primers with a final concentration of 5 µM were used in PCR experiments. Primer combinations, primer sequences and their respective annealing temperature are listed in supplementary table 6 in the appendix. PCR reactions were prepared on ice and performed either in PCR plates (96-well) or PCR strips (8-tubes). The following standard protocol and program was used (Tables 3-4). The annealing temperature was adjusted depending on the primer combination.

Table 3: Standard components per PCR reaction.

Component	Volume [µl]
Water	8
Master mix	3
Primer mix (forward and reverse primer)	2
DMSO	1
DNA template	2

Table 4: Standard PCR program repeating step 2-4 38 times.

Step	Temperature [°C]	Time [min]
1	94	2:30
2	94	0:25
3	55	0:25
4	72	1:20
5	72	7:00
6	15	∞

2.2.7 Agarose gel electrophoresis

15 µl PCR reactions were mixed with 4 µl loading buffer (for 50 ml: 10 mg orange G, 27 ml glycerine, 3 ml 1x TE). For testing the size of PCR products, agarose gel electrophoresis was used with TAE buffer (50x TAE buffer: 2 M Tris pH 8.3, 50 mM EDTA), 4 µl ethidium bromide per 100 ml gel at 120 V for approximately 20 min. The images were taken with GelDoc XR+ system and Image LabTM software. 3 µl RNA was mixed with 4 µl loading buffer and separated by an agarose gel electrophoresis with 70 V for 20 min.

2.2.8 Analysis of gene expression by quantitative polymerase chain reaction

The extraction of total RNA from roots, cotyledons and flowers of all single mutants as well as Col-0 was done in independent experiments. In order to generate cDNA from the isolated RNA, the Revert Aid First Strand cDNA Synthesis Kit was used including the step to remove genomic DNA and always carrying a negative control without Reverse Transcriptase. 1 µg RNA was used and the manufacturer´s protocol was

followed. To check the quality of cDNA and test for genomic DNA contamination, PCRs were performed with three reference genes (AT4G26410 (RHIP1), AT5G60390 (EF1α) and AT5G12250 (TUBULIN6β)). Quantitative PCR was performed using GoTaq qPCR Master Mix with a 1:10 dilution of cDNA. The Standard Cycling Program was used as described in the manufacturer´s protocol and all qPCR reactions were performed with 58°C as the annealing temperature. Every primer pair was tested as technical triplicate and with a water-only control for detection of potential contaminations. The ct-value (Cycle Threshold) is the amount of cycles where the unspecific fluorescence emission was exceeded and a clear fluorescence signal was detected. The resulting ct-values described a relative concentration of the gene of interest in one reaction without a unit. The ct-values were normalized to three reference genes: AT4G26410 (RHIP1), AT5G60390 (EF1α) and AT5G12250 (TUBULIN6β).

2.2.9 Total protein extraction from plant material

Total protein was extracted from plant material by using 3x cracking buffer (for 50 ml: 15 ml 20% (w/v) SDS, 15 ml glycerol, 15 ml Tris 0.5 M pH 6.8, 1.25 ml water, bromophenol blue) with 23 mg/ml dithioerythritol (DTE) and material was disrupted by hand with a pestle. In order to isolate proteins from dry seeds, 40 seeds were disrupted in a tube with seven 2 mm beads. The ultramat 2 (high speed multi-use triturator) was used for 8 s with full speed and after disruption of the plant material 250 µl 3x cracking buffer were added. Next, samples were boiled for 5 min at 94°C and centrifuged at 13,000 g for 3 min. Samples were stored at -20°C.

2.2.10 Sodium dodecyl sulfate–polyacrylamide gel electrophoresis

First, polyacrylamide gels (8-15%) were prepared with the separation phase and stacking phase (Table 5). A Mini Protean Tetrad system was used. Gels were placed into the electrophoresis cell, loaded with samples as well as PageRuler Prestained Protein Ladder and the chamber filled with 1x Laemmli buffer (10x Laemmli buffer: 0.25 M Tris, 1.92 M glycin, 40 mM SDS) (Laemmli 1970). Gels ran for 1.5 h under constant 17 mA per gel. After separation of proteins, protein gels were either stained with Coomassie Brilliant Blue or used for western blot experiments to detect proteins with antibodies. In order to stain proteins directly, gels were incubated with Coomassie solution (0.25% (v/v) Coomassie Brilliant Blue, 45% (v/v) methanol, 9% (v/v) acetic acid) for 10 min and washed twice for 10 min with destaining solution (30% (v/v) methanol and 5% (v/v) acetic acid).

Table 5: Components of a standard 10% acrylamid gel.

Separation phase		**Stacking phase**	
0.75 M Tris pH 8.8	6 ml	0.5 M Tris pH 6.8	2 ml
water	1.8 ml	water	5 ml
10% SDS	120 µl	10% SDS	80 µl
Rotiphorese gel 30 (37.5:1)	4.0 ml	Rotiphorese gel 30 (37.5:1)	0.8 ml
10% APS	40 µl	10% APS	80 µl
TEMED	6 µl	TEMED	6 µl

2.2.11 Western blot experiment and chemiluminescence detection

Proteins were transferred from polyacrylamide gels onto 0.45 nitrocellulose western blotting membranes by the wet blotting system from Bio Rad with transfer buffer (for 1 l: 50 mM Tris, 150 mM glycine, 10% (v/v) methanol, 0.02% (w/v) SDS). Transfer was performed at constant voltage either for 1.5 h at 100 V or overnight at 20 V. Proteins were bound to the membrane after transfer and temporarily stained with Ponceau S (0.25% (w/v) Ponceau S in 1% (v/v) acetic acid) to check transfer efficiency. The following incubation steps were performed in little chambers placed on a rocking shaker. Proteins were blocked on the membranes with 5% (w/v) milk powder in TBS-T buffer (50 mM Tris pH 7.5, 150 mM NaCl, 0.1% (v/v) Tween) for 1 h. Subsequently, membranes were incubated with the first antibody for 1 h at room temperature or overnight at 4°C. Next, membranes were washed 5 times for 5 min with TBS-T buffer. The secondary antibodies were conjugated to horseradish peroxidase and incubated with the membranes for 1 h. Finally, the membranes were washed 5 times for 5 min with TBS-T buffer and SERVA*Light* Polaris CL HRP WB Substrate Kit or for weak signals SERVA*Light* Helios CL HRP WB Substrate Kit were added to the membranes and their luminescence was imaged in a Fujifilm Intelligent Dark Box employing an Atik 460 EX camera.

Table 6: Dilution of antibodies used in western blot experiments.

Antibody	**Dilution**	**Size [kDa]**
EPSIN1	1:2000	61
purified MTV1	1:500	75
12S Globulin	1:1000	55
12-348 Sigma-Aldrich Goat Anti-Rabbit IgG Antibody, HRP-conjugate	1:10000	

2.2.12 Protein expression in *Escherichia coli*

Proteins of interest were expressed in *E. coli* strain BL21 (Table 2). For this, overnight cultures were prepared with a single colony in 5 ml LB medium with appropriate antibiotics at 37°C with 220 rpm. The next day, the main culture was set up with LB medium (800 ml final volume) and appropriate antibiotics. For all cultures, optical density (OD) was measured with a photometer at 600 nm and adjusted to around 0.1. The bacterial culture was incubated at 37°C and 220 rpm agitation until the OD reached around 0.6. The expression of the gene of interest was induced by adding 1 mM IPTG. The temperature and incubation time were adjusted for the next growth phase depending on the protein of interest. Cultures were incubated at either 25°C for 3-4 h after induction and harvested or the culture was grown overnight at 16°C. In order to harvest bacterial cultures, the incubation was stopped, cultures were put on ice for 10 min and a Sorvall centrifuge was used with 400 ml centrifuge beaker at 4°C with 7200 g for 10 min. The supernatant was discarded and the pellet was resuspended with cold sterile water. This step was repeated twice. After the last centrifugation step the supernatant was discarded and the bacterial pellet was stored at -80°C for several weeks.

To confirm successful expression, samples were taken prior to and after induction. Samples were centrifuged at 13,000 g for 3 min and the supernatant was discarded. The pellet was resuspended in 100 µl 3x cracking buffer and boiled for 5 min at 94°C. Expressed proteins were verified by SDS-PAGE and subsequent Coomassie staining. If the expression was successful, a clear pronounced band would be visible at the right molecular size after induction.

2.2.13 Glutathione S-transferase fusion protein affinity purification

Since fragments of EPSIN1, 2 and 3 tagged with glutathione S-transferase (GST) were generated and expressed, the fragments were purified using glutathione sepharose 4B (Sauer et al. 2014). First, bacterial pellets containing GST-tagged EPSIN fragments were resuspended (5 ml per 1 g pellet) in cold lysis buffer (1 mM PMSF, 0.1% Triton and 1 ml Protease-Inhibitor Mix P per 100 ml buffer). To disrupt the cells, the sonicator was used with 5x 30 s, 3 cycles and 40% power. After centrifugation for 20 min at 4°C and 16,000 g, the supernatant was removed and placed on top of the prepared GST-columns. The GST-columns were prepared by an incubation of 329 mg sepharose with 6 ml 1xPBS buffer (1 l 10x PBS buffer: 2 g KCl, 80 g NaCl, 17.8 g $Na_2HPO_4 \cdot 2H_2O$, 2.4 g KH_2PO_4) for 10 min at room temperature on a shaker. 2 ml sepharose were added per Pierce™ Disposable Column. After 5 min the beads had settled and were washed 3 times with 5 ml wash buffer (1x PBS with 0.1% Trition). Next, the supernatant of the bacterial pellet was transferred onto the columns and incubated for 1 h on a revolving rotator. The beads were allowed to

settle for 15 min before the flow-through was discarded. The columns were washed 6 times with 5 ml wash buffer and eluted 5 times with 500 µl elution buffer (10 mM glutathione and 50 mM Tris pH 8.0). Samples were collected at three predefined time points, precisely, (1) total protein from bacterial pellet supernatant, (2) flow through post-incubation of 1 h and (3) elution steps 1 to 5. In each case 100 µl sample was mixed with 50 µl 3x cracking buffer and boiled for 5 min at 94°C. To analyze samples after purification, they were subjected to SDS-PAGE followed by either Coomassie staining or western blot experiments employing an anti-GST antibody.

2.2.14 Dialysis and Bradford assay

The purified EPSIN fragments needed to be rebuffered in 1x PBS buffer. To this end, Slide-A-Lyzer™ Dialysis Cassettes (0.5-3 ml volume range and 10K MWCO) were used according to the manufacturer's instructions. The aim was to generate antibodies in rabbits against EPSIN1, 2 and 3 and the stability of all three protein fragments was tested by an incubation for 90 h at 40°C followed by a subsequent check as to whether proteins were degraded employing SDS-PAGE in combination with Coomassie staining. This revealed that all protein fragments were stable.

Protein concentration was measured by Bradford assay by adding 200 µl Bradford Reagent, 780 µl water and 20 µl sample. In case of the control 200 µl Bradford Reagent and 800 µl water were used. After mixing and incubation of the reaction mixtures for 10-15 min the absorbance was determined at 595 nm with a photometer. The concentrations were calculated from a standard curve generated with BSA.

2.2.15 Antibody generation

There were no commercial antibodies available for detection of EPSIN 1, 2 and 3. Due to the fact that EPSIN2 and EPSIN3 display high sequence similarity, polyclonal antibodies were raised against short less conserved fragments of all three EPSINs (Table 7). These plasmids were previously cloned in the lab of Dr. Sauer by N. Freimuth (unpublished results) as destination vectors pGEX-2T-GW with an N-terminal GST tag and the coding sequence of the protein of interest. They were cloned with Gateway® cloning technique using pDONR™221 and pENT221. The final bleeds after 4 months of immunization protocol (Pineda Antibody-Service) were used and the serum was tested against full plant proteins from Col-0 compared to the respective mutant. In case of MTV1, the previously generated antibody was used (Sauer et al. 2013).

Table 7: Protein fragments used for antibody generation.

Name/Vector	AGI code	Protein fragment	Resistance in bacteria	Size [kDa]
GST-EPSIN1	AT5G11710	from V163 to N434	Amp	56
GST-EPSIN2	AT2G43160	from R265 to P692	Amp	73
GST-EPSIN3	AT3G59290	from Y619 to S726	Amp	38

2.2.16 β-glucuronidase activity staining

To gain insight into the expression pattern of all ENTH domain proteins, C-terminally tagged proteins with β-GLUCURONIDASE (GUS) under their endogenous promotor were used (Table 2). The GUS assays were performed on seedlings (5 days after germination (DAG) and 10 DAG) and adult flowering plants. The flowers and leaves were fixed with 90% (v/v) acetone at -20°C for 1 h and washed twice with 1x GUS buffer (10x GUS buffer for 50 ml: 1 M phosphate buffer pH 7.0, 100 mM EDTA, 20 mM $K_3Fe(CN)_6$), 10 mM $K_4Fe(CN)_6 \cdot 3H_2O$, 1% (v/v) Triton). Seedlings and roots were used without fixation. First, plant tissue was incubated in 6-well or 12-well tissue culture plates with 1x GUS buffer under vacuum for 5 min. X-Gluc was added to a final concentration of 1 mg/ml, incubated for 5 min under vacuum and at 37°C in darkness for 2-3 h. To stop the reaction, 100% ethanol was added followed by a stepwise rehydration (100%, 90%, 70%, 50%, 25% ethanol and water). Finally, water was replaced with clearing solution (80 g chloral hydrate, 30 ml water and 8 ml glycerol) and samples were incubated for 2 days. Sample imaging was performed in 6-well or 12-well plates with stereomicroscope Stemi 2000-C or seedlings were mounted onto slides and imaged with an Axiophot I Microscope.

2.2.17 Immunolocalization

An immunocytochemical technique was performed for localization of endogenous proteins in whole-mount plant roots. 5-day-old seedlings were analyzed and examined as described (Boutté and Grebe 2014).

Table 8: Antibodies and plant material used for immunolocalization experiments.

Plant material	First antibody	Dilution	Second antibody	Dilution
Col-0	α-ECHIDNA anti-Rabbit (Gendre et al. 2011)	1:1000	Dylight550 anti-Rabbit	1:600
echidna				
epsin1 mtv1				
Col-0	α-MTV1 anti-Rabbit (Sauer et al. 2013)	1:1000		
mtv1				
echidna				
Col-0	α-EPSIN1 anti-Rabbit	1:1000		
epsin1				
echidna				

2.2.18 Imaging and microscopy

To address root length, seedlings grown vertically on plates were scanned with HP Scanjet G4050 (scan resolution 1200 dpi) and measurements were done with ObjectJ which is a plugin for ImageJ. Plants were grown on soil in Multipot Propagation Trays, imaged with a Nikon D750 camera on a tripod with fixed settings and ImageJ (ROI Manager) with color threshold tool was used to measure rosette area. The pollen germination assay was imaged with Zeiss Axio Zoom.V16 with 32x magnification (objective: Plan-NEOFLUAR Z 1.0x/0.25 FWD 56mm).

All confocal laser scanning microscopy applications like subcellular co-localization studies were performed using a Zeiss LSM 880 Airyscan Fast. The LD LCI Plan-Apochromat 40x/1.2 Imm Korr DIC M27 objective was used if not indicated otherwise. In order to excite different fluorophores, these laser lines were used: DPSS laser at 405 nm (CFP), Argon laser at 488 and 514 nm (GFP and YFP) and DPSS laser at 561nm (RFP/mCherry/mKO). Depending on the purpose, either the spectral GaAsP detector or the AiryScan detector were used. All subcellular localization studies with co-localization of GFP lines with marker lines were done with the AiryScan detector. AiryScan mode superresolution, detector gain between 850 and 900 V, pinhole around 3 airy units (the AiryScan detector has an internal pinhole array equivalent of 0.2 airy units), dwell time around 2 µs, 2-fold line averaging, optimal resolution as suggested by the ZENblack imaging software and the automatic AiryScan processing mode were used. Depending on the laser lines utilized, appropriate beam splitters were employed. The localization of fluorescence markers within different mutant backgrounds was studied by using the Quasar 34 channel spectral GaAsP detector with 4-fold line averaging and detector gain levels between 600 – 800 V. The autofluorescence of protein storage vacuoles in seeds was exited at 405 nm, MBS 405/505 beam splitter, 620 – 680 detector gain, 2-fold averaging and objective LD LCI Plan-Apochromat 20x/0.8 Imm Korr DIC M27. In all experiments, laser attenuation (often referred to as power) was kept between 0.2% and 5% and optimized for the best compromise of signal-to-noise ratio, acquisition speed and photobleaching.

2.2.19 Quantification of co-localization experiments

In order to address quantification of two different fluorophores in *A. thaliana* root cells, ImageJ with the Distance Analysis (DiAna) plugin was used (Gilles et al. 2016). All analyzed images were taken with the AiryScan detector. First, either Median or Gaussian blur was used as denoise filter. Next, objects needed to be segmented and last the center-to-center distance was calculated by object-based co-localization. For every image the segmentation parameter Volume min 16 and Volume max 500 were used. The center-to-center distance between larger objects can fall below the theoretical resolution limit of ~150 nm in

our setup. When the distances were close to or smaller than 150 nm objects were considered as co-localized.

Table 9: Summary of DiAna settings used for quantification of co-localization studies. EPSIN1-GFP and MTV1-GFP were crossed with different marker lines and their F1 offspring was directly analyzed.

Line	Denoise filter	Segmentation parameter A channel	Segmentation parameter B channel	Number of roots
EPSIN1x Got1p	Median 1.0 Pixel	min Threshold 200 STEP value 200	min Threshold 5 STEP value 5	9
MTV1x Got1p				5
EPSIN1x SYP32	Gaussian 1.0 Pixel	min Threshold 200 STEP value 200	min Threshold 200 STEP value 130	5
MTV1xSYP32				
EPSIN1xVHA-a1	Median 2.0 Pixel	min Threshold 200 STEP value 200	min Threshold 200 STEP value 200	5
MTV1xVHA-a1		min Threshold 30 STEP value 30		8
EPSIN1x RabF2b/ARA7	Median 1.0 Pixel	min Threshold 200 STEP value 200	min Threshold 5 STEP value 5	12
MTV1x RabF2b/ARA7				8
EPSIN1xCLC	Median 2.0 Pixel	min Threshold 200 STEP value 230	min Threshold 200 STEP value 200	10
MTV1xCLC				8
EPSIN1xMTV1	Median 1.0 Pixel	min Threshold 200 STEP value 200	min Threshold 100 STEP value 100	9
EPSIN1xMTV4	Median 2.0 Pixel	min Threshold 200 STEP value 230	min Threshold 200 STEP value 200	8
MTV1xMTV4				10
EPSIN1xAP4	Median 2.0 Pixel	min Threshold 200 STEP value 200	min Threshold 200 STEP value 200	10
MTV1xAP4				
EPSIN1xAP1	Median 2.0 Pixel	min Threshold 200 STEP value 200	min Threshold 200 STEP value 200	10
MTV1xAP1				

2.2.20 Staining methods and inhibitor treatments

5-day-old seedlings were incubated in 6-well plates or 12-well plates with liquid MS medium and the appropriate dye or drug. Vacuole morphology was studied by 25 µM MDY-64 staining of roots up to 5 min (Scheuring et al. 2015). Propidium iodide was used to stain cell walls in root cells. To address endocytosis defects a commonly used method is the staining of seedlings with the styryl dye FM4-64. Firstly, the dye lables the PM. After being internalized by endocytosis, it reaches the tonoplast membrane via endosomes (Bolte et al. 2004; Dettmer et al. 2006). In this study 5-day-old seedlings were either shortly incubated with 2 µM FM4-64 on ice or were treated for 3 h. Afterwards the seedlings were washed two times with liquid MS medium and imaged immediately. To investigate endocytosis defects the constant circulation of PIN2 auxin transporter between the PM and EE was analysed. The treatment with Brefeldin A (BFA) leads to the aggregation of PIN2 in so called BFA-Bodies, by blocking the exocytotic step of the recycling

processes in root epidermal cells (Geldner et al., 2003; Langhans et al., 2011). We investigated BFA washout experiments in order to determine whether PIN2 is recycled from the BFA bodies back to the PM. Seedlings were incubated for 1 h with 50 µM BFA in liquid MS medium. After washing two times, incubation for 2 h and additional staining with propidium iodide, the root meristem was imaged. The experiment was conducted in presence of 50 µM cycloheximide (CHX) to exclude effects resulting from *de novo* protein synthesis.

To determine the meristem size of *epsin1* and *mtv1* single and double mutants, 5 DAG seedlings were fixed, cleared and stained with Calcofluor White as previously described (Ursache et al. 2018).

To address secretion defects, the mucilage layer of seeds was stained with ruthenium red (McFarlane et al. 2014). For this, dry seeds were incubated with water for 2 h at 200 rpm on a GFL 3005 orbital shaker at room temperature and the water was replaced with ruthenium red solution for 1 h. Afterwards, the solution was removed and seeds were imaged in water with a Stemi 2000-C stereomicroscope. Quantification of the mucilage layer was done with ImageJ (ROI Manager). Therefore, the thickness of the mucilage layer was measured from microscopic images (Heinze et al. 2020)

3. Results

3.1 Ubiquitous expression and distinct subcellular localization of ENTH domain proteins

We investigated the expression pattern of all four ENTH domain proteins in *A. thaliana* in detail by creating stably transformed lines expressing promoter GUS fusions of all four candidates. Of those, we performed GUS activity assays and compared root tips, 11-day-old seedlings and inflorescences (Figure 5). All four ENTH domain proteins, EPSIN1, 2, 3 and MTV1, were ubiquitously expressed and showed a similar pattern. We detected strong signals in root meristems, the leaf vascular system, anthers as well as pollen compared to other floral organs. A similar ubiquitous expression points to a possible functional redundancy within this family.

Besides their expression, we investigated the subcellular localization of all four ENTH domain proteins *in planta* by functional enhanced GFP fusion proteins (*pEPSIN1::EPSIN1-GFP*, *pEPSIN2::EPSIN2-GFP, pEPSIN3::EPSIN3-GFP* and *pMTV1::MTV1-GFP*) (Figure 6A-D). Notably, in root epidermal cells, used as a model system, EPSIN1-GFP and MTV1-GFP showed a punctate pattern in contrast to EPSIN2-GFP and EPSIN3-GFP which were located at the PM and the growing cell plate. Thus, ENTH domain proteins were classified in two possibly functional distinct groups based on their localization.

To investigate the localization of EPSIN2-GFP and EPSIN3-GFP at the cell plate in more detail, we used the common cell plate marker mCherry-RabA1g (RAB GTPASE HOMOLOG A1G) (Figure 6E-F). Although the GFP signal was clearly located at the cell plate, as indicated by co-occurrence with mCherry-Rab A1g, the overlap was limited. The signal of mCherry-Rab A1g was predominantly located at the outgrowing younger parts of the cell plate. Since Rab A1g is known as an early player in cell plate formation, we concluded that EPSIN2 and EPSIN3 may be involved in late steps of cytokinesis.

Figure 5: Expression pattern of ENTH domain proteins fused to GUS expressed from their endogenous gene promotors. I: root tip of 5-day-old seedlings, scale bar: 100 µm; **II:** 11-day-old seedlings, scale bar: 1000 µm; **III:** inflorescence of 36-day-old plants, scale bar: 1000 µm.

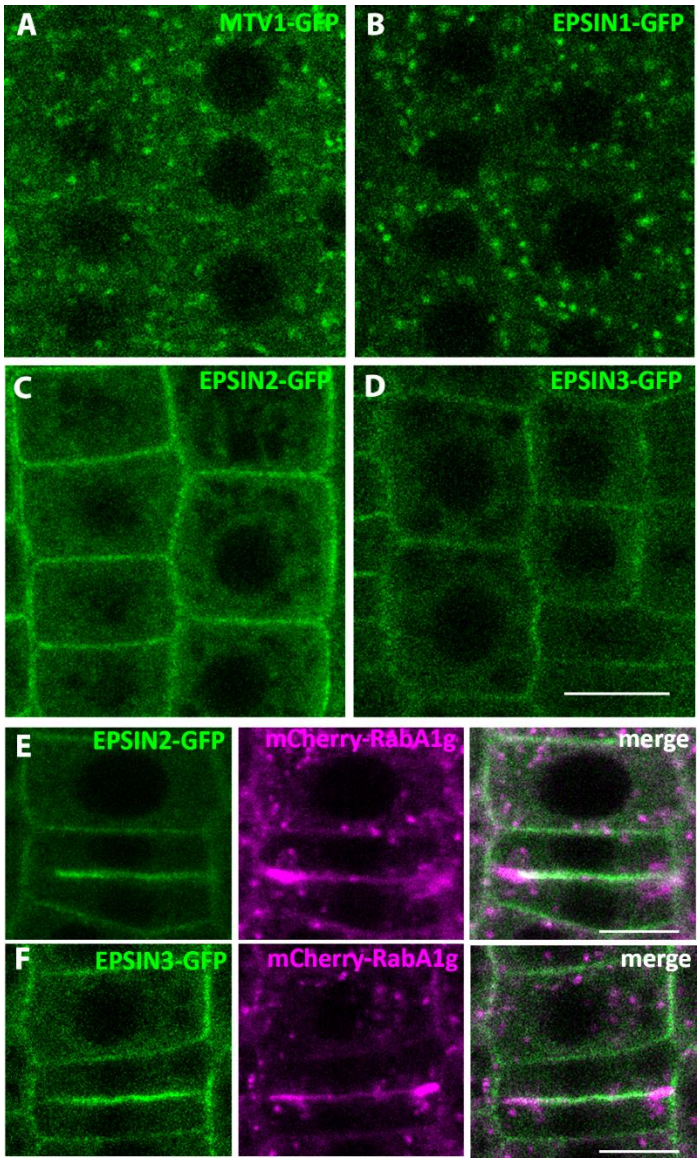

Figure 6: Subcellular localization of ENTH domain proteins fused to GFP expressed under control of the endogenous gene promotors. A-D: GFP signal distribution in root epidermal cells of 5-day-old seedlings, scale bar 10 µm; **E:** co-occurrence of EPSIN2-GFP and mCherry-Rab A1g at the cell plate, scale bar: 10 µm; **F:** co-occurrence of EPSIN3-GFP and mCherry-Rab A1g at the cell plate, scale bar: 10 µm.

In order to identify the punctate pattern of EPSIN1-GFP and MTV1-GFP, we crossed the respective lines with established subcellular marker lines. We used mCherry-Got1p and mCherry-SYP32 (Geldner et al. 2009) as two Golgi markers (Figure 7A-F.). We calculated the center-to-center distance of endosomal punctae as an object-based quantification method and used the median distance of each pair as a readout. We defined distance values around 0.1500 µm (theoretical resolution limit) as co-localization. We discovered EPSIN1-GFP (0.4715 µm) and MTV1-GFP (0.3825 µm) close but with no overlap to mCherry-

Got1p proteins. The second Golgi marker showed similar results with a center-to-center distance of EPSIN1-GFP and mCherry-SYP32 of 0.4502 µm and 0.3769 µm between MTV1-GFP and mCherry-SYP32. As a side effect the high similarity of both ENTH proteins to both Golgi markers showed the robustness of our quantification method. Next, we tested VHA-a1-RFP (Dettmer et al. 2006) as a TGN marker with EPSIN1-GFP and MTV1-GFP. We propose EPSIN1-GFP (0.2242 µm) and MTV1-GFP (0.1319 µm) as TGN located proteins, due to a clear overlap with VHA-a1-RFP (Figure 7G-I).

We used mCherry-RabF2b/ARA7 as a PVC maker and identified 0.3625 µm distance to EPSIN1-GFP and 0.3610 µm to MTV1-GFP (Figure 8A-C). Thus, neither EPSIN1-GFP nor MTV1-GFP co-localized with the PVC marker. In addition, both TGN proteins were co-localized with the coat protein CLATHRIN LIGTH CHAIN (CLC-mKO) (Figure8 D-F). We calculated the center-to-center distance between EPSIN1-GFP and CLC-mKO with 0.1375 µm and between MTV1-GFP and CLC-mKO with 0.2399 µm.

To determine the co-localization of EPSIN1 and MTV1 itself, we crossed EPSIN1-mRuby3 and MTV1-GFP. Although they were both TGN located there was no perfect overlap (Figure 8G-H). The center-to-center distance of EPSIN1-GFP and MTV1-mCherry was 0.2631±0.0115 µm. Surprisingly, both ENTH proteins were closer located to VHA-a1-RFP and CLC-mKO rather than to each other. Our co-localization results indicated EPSIN1-GFP and MTV1-GFP are TGN proteins which differ in their overlap to VHA-a1-RFP and CLC-mKO. We propose that EPSIN1 and MTV1 are located at different subcompartments of the TGN.

Table 10: Quantification of co-localization data by DiAna. Displayed are means with their respective 95% confidence Interval (CI). The theoretical resolution limit is ~0.150 µm in the setup.

Marker	**Center-to-center distance [µm] EPSIN1-GFP**	**Center-to-center distance [µm] MTV1-GFP**
mCherry-Got1p	0.4715±0.0069	0.3825±0.0073
mCherry-SYP32	0.4502±0.0091	0.3769±0.0083
VHA-a1-RFP	0.2242±0.0105	0.1319±0.0036
mCherry-RabF2b/ARA7	0.3625±0.0073	0.3610±0.0097
CLC-mKO	0.1375±0.0034	0.2399±0.0061

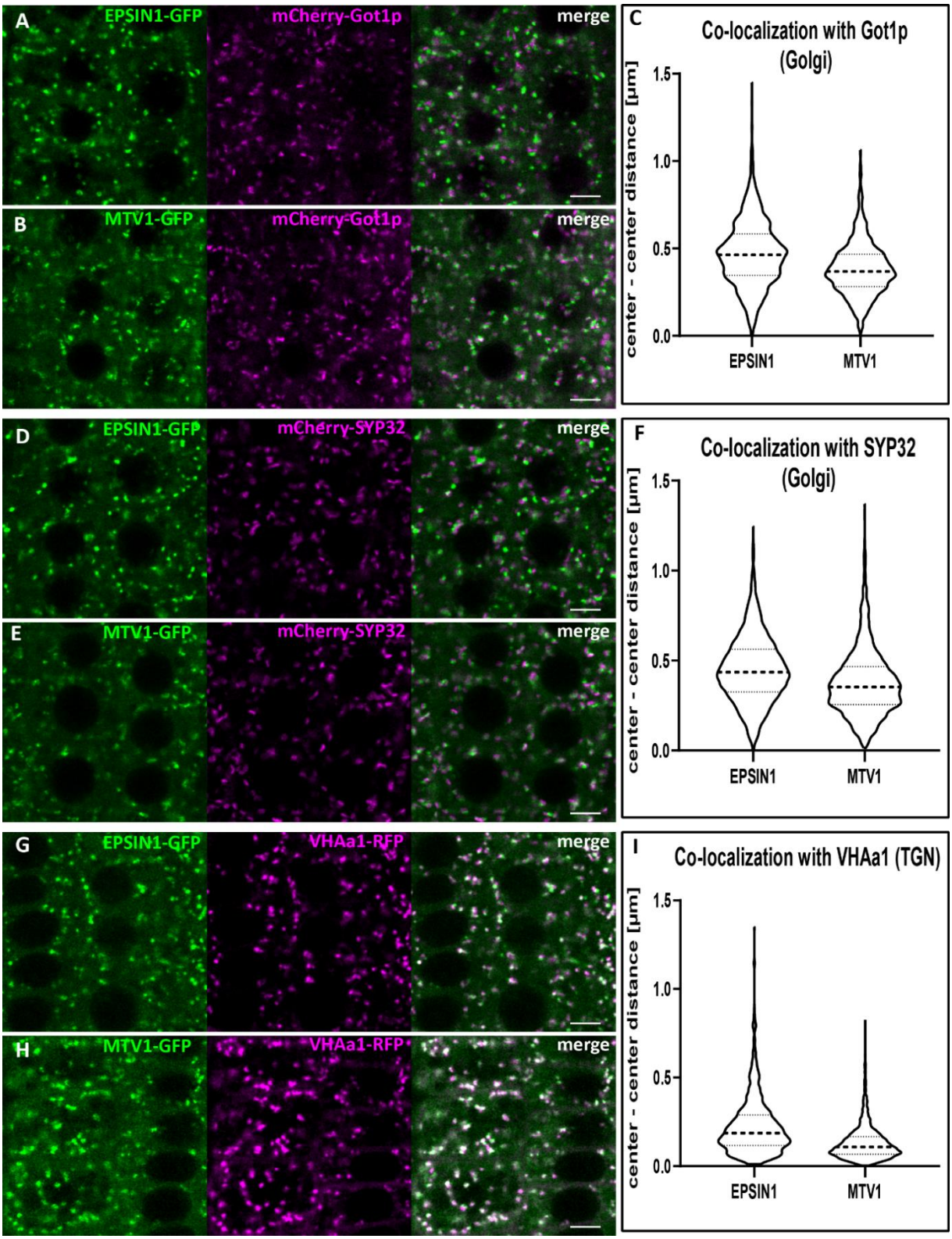

Figure 7: Co-localization of EPSIN1 and MTV1 with subcellular markers in 5-day-old root epidermal cells. A-C: Co-localization with mCherry-Got1p (Golgi) and quantification of center-to-center distance displayed as violin plot, median marked with dashed line. **D-F:** Co-localization with mCherry-SYP32 (Golgi) and quantification of center-to-center distance displayed as violin plot, median marked with dashed line. **G-I:** Co-localization with VHA-a1-RFP (TGN) and quantification of center-to-center distance displayed as violin plot, median marked with dashed line. Scale bar: 5 µm.

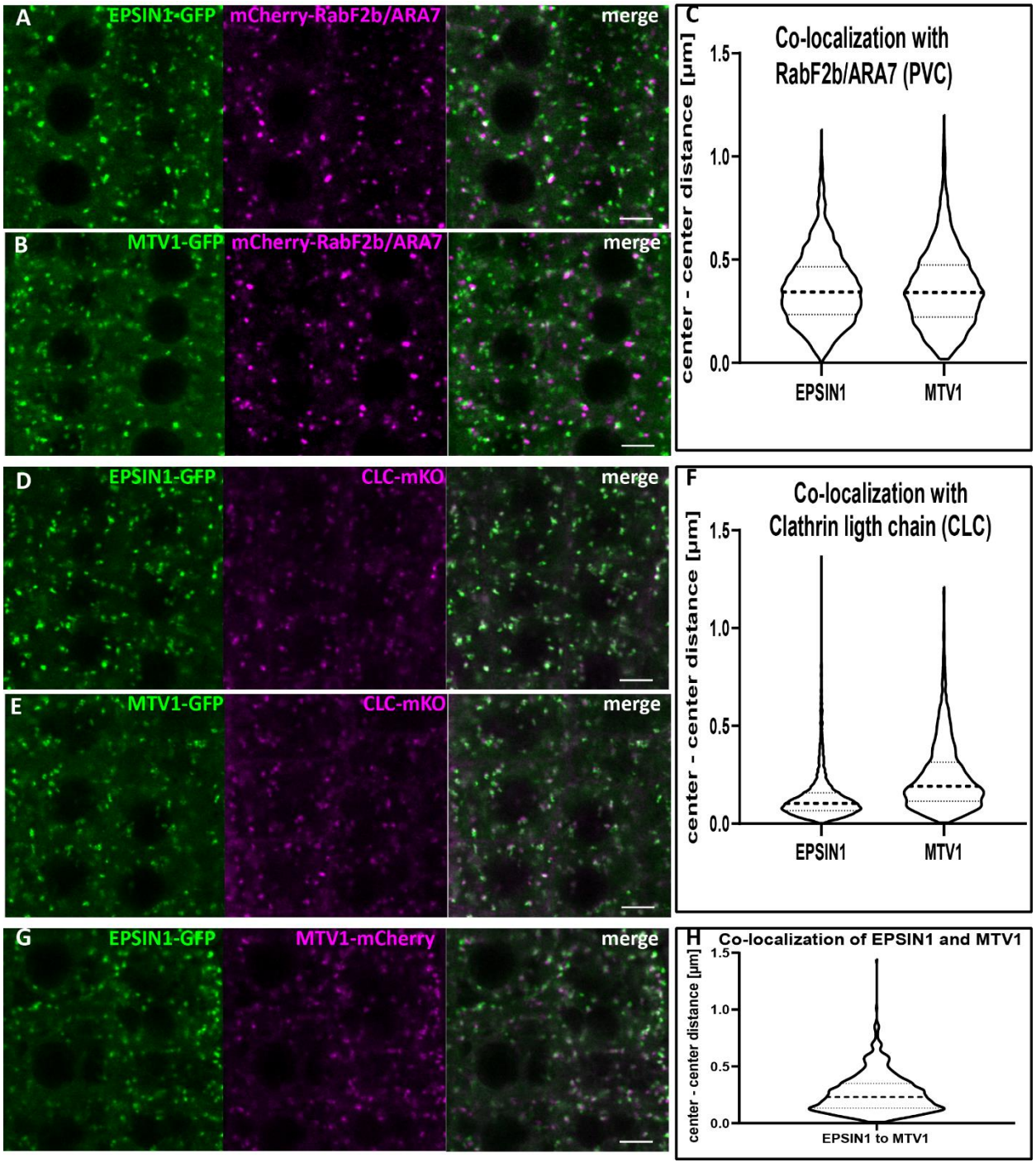

Figure 8: Co-localization of EPSIN1 and MTV1 with subcellular markers and each other in 5-day-old root epidermal cells. A-C: Co-localization with mCherry-RabF2b/ARA7 (PVC) and quantification of center-to-center distance displayed as violin plot, median marked with dashed line. **D-F:** Co-localization with clathrin marker CLC-mKO and quantification of center-to-center distance displayed as violin plot, median marked with dashed line. **G-H:** Co-localization of EPSIN1-GFP and MTV1- mCherry and quantification of center-to-center distance displayed as violin plot, median marked with dashed line. Scale bar: 5 µm.

3.2 Functional redundancies of ENTH domain proteins

Since we divided the ENTH domain proteins into two groups based on their subcellular localization and found similarly ubiquitous expression patterns for all of them, we analyzed their potential functional redundancy. Here, we analyzed knockout T-DNA mutant lines of *epsin1*, *epsin2* and *epsin3* as well as *mtv1* (see Table 1). Although first data about a weak mutant allele of *EPSIN1* were published, *in planta* data of all four members were lacking. In order to confirm the obtained T-DNA mutant lines as full knock out mutants, we analyzed mRNA levels and protein levels of the respective mutant gene and/or protein. We extracted total RNA from roots, cotyledons and flowers of all single mutants as well as Col-0. We analyzed transcript levels by qPCR and used AT4G26410, AT5G60390 and AT5G12250 as reference genes (Figure 9A and Supplementary Figure 1 and 2). First, we quantified the abundance of all *EPSINs* and *MTV1* transcripts in wild type plants. Notably, in all plant organs that we tested, mRNA levels of *EPSIN1* and *MTV1* were higher abundant than *EPSIN2* and *EPSIN3* (Table 11). There was no hint for strong cross regulation. We did not detect transcripts of *EPSIN1*, *EPSIN2* and *EPSIN3* in the respective single mutant plants. Thus, we confirmed our single mutant plants as full knockout mutants. Interestingly, *EPSIN3* was the only one that showed differences in its transcript level of tested plant organs. *EPSIN3* transcript was 10-fold higher in flower organs than in roots or cotyledons.

Furthermore, we analyzed protein levels of EPSIN1 and MTV1 in seedlings by western blot experiment. For this, we used our generated EPSIN1 antibody and the purified MTV1 antibody which was generated previously (Sauer et al. 2013). We clearly detected EPSIN1 as a single band at 75 kDa in protein extracts from Col-0 and *mtv1* single mutant plants, while it was absent in *epsin1* (Figure 9B). Although *mtv1* is already published as a knockout, we confirmed it again with a specific band around 80 kDa in wild type and *epsin1* extracts.

Table 11: Summary of gene expression data in root tissue displayed as the mean of three replicas with their standard deviation (SD) in arbitrary units (a.u.). Normalized to three reference genes AT4G26410, AT5G60390 and AT5G12250. Single knockout mutants are marked in grey.

	EPSIN1	**EPSIN2**	**EPSIN3**	**MTV1**
Col-0	0.710±0.082	0.189±0.027	0.079±0,016	0.478±0.079
epsin1	1.118e-8±1.773e-9	0.145±0.026	0.098±0.017	0.429±0.012
epsin2	0.607±0.058	5.381e-6±2.655e-6	0.089±0.017	0.540±0.109
epsin3	0.543±0.037	0.239±0.021	0.009±0.003	0.394±0.029
mtv1	0.635±0.127	0.338±0.110	0.183±0.091	2.167e-8±1.158e-8

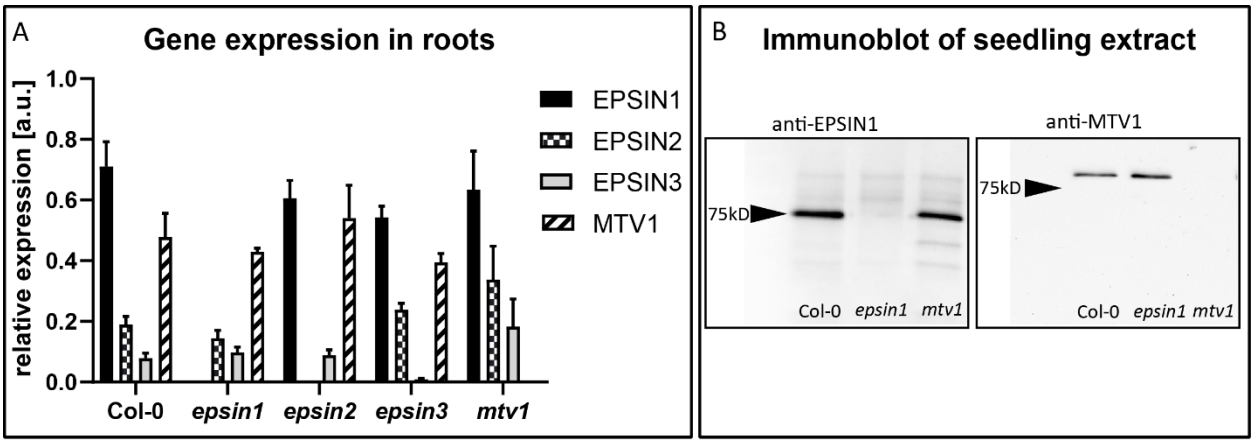

Figure 9: Confirmation of full knockout mutant lines in *A. thaliana*. A: Gene expression of *EPSIN1, 2* and *3* as well as *MTV1* detected in Col-0 and respective single mutant plants by qPCR, normalized to three reference genes AT4G26410, AT5G60390 and AT5G12250. Arbitrary units (a.u.). **B:** Detection of EPSIN1 and MTV1 protein in full protein extract from Col-0, *epsin1* and *mtv1* seedlings with generated EPSIN1 antibody and published MTV1 antibody by western blot experiment.

We identified EPSIN1 and MTV1 as TGN proteins and EPSIN2 and EPSIN3 as PM as well as cell plate-located proteins with ubiquitous expression, which raised the question of redundancy within their respective groups. In order to study functional redundancy, we checked *epsin1*, *epsin2*, *epsin3* and *mtv1* for phenotypes. To address this, we let plants grow on soil and compared their vegetative growth with rosette area as criteria to quantify the phenotype. All plants grew side by side and we took pictures after 16, 18 and 20 DAG. The phenotype of all single mutants did not deviate significantly from wild type (Figure 10A-B). To further examine functional redundancy, we created higher-order mutants and displayed the phenotype the same way as used for single mutants (Figure 10A and C). The double mutants of all *EPSIN* combinations (*epsin1 epsin2*, *epsin1 epsin3* and *epsin2 epsin3*) were not significantly distinguishable from Col-0 plants. Moreover, we generated an *epsin1 epsin2 epsin3* triple mutant which showed normal vegetative growth. *EPSIN1* and *MTV1* showed a strong genetic interaction which is illustrated by the dwarf phenotype of the double mutant. The 16-day-old *epsin1 mtv1* was approximately five times smaller compared to wild type plants which was significant and resulted in eight times smaller rosettes of 20-day-old plants. 36-day old plants were assessed for their reproductive phenotypes in all mutant combinations (Supplementary Figure 3). In contrast to all other mutant plants, which showed no additional phenotype to their vegetative phenotype, *epsin1 epsin2 epsin3* had shorter siliques and were partially sterile, indicating genetic interaction between *EPSIN1*, *EPSIN2* and *EPSIN3*. Notably, the *epsin1 mtv1* double mutant remained dwarfed and could not catch up to wild type growth level, although formed flowers and siliques, so reproductive development was not affected *per se*.

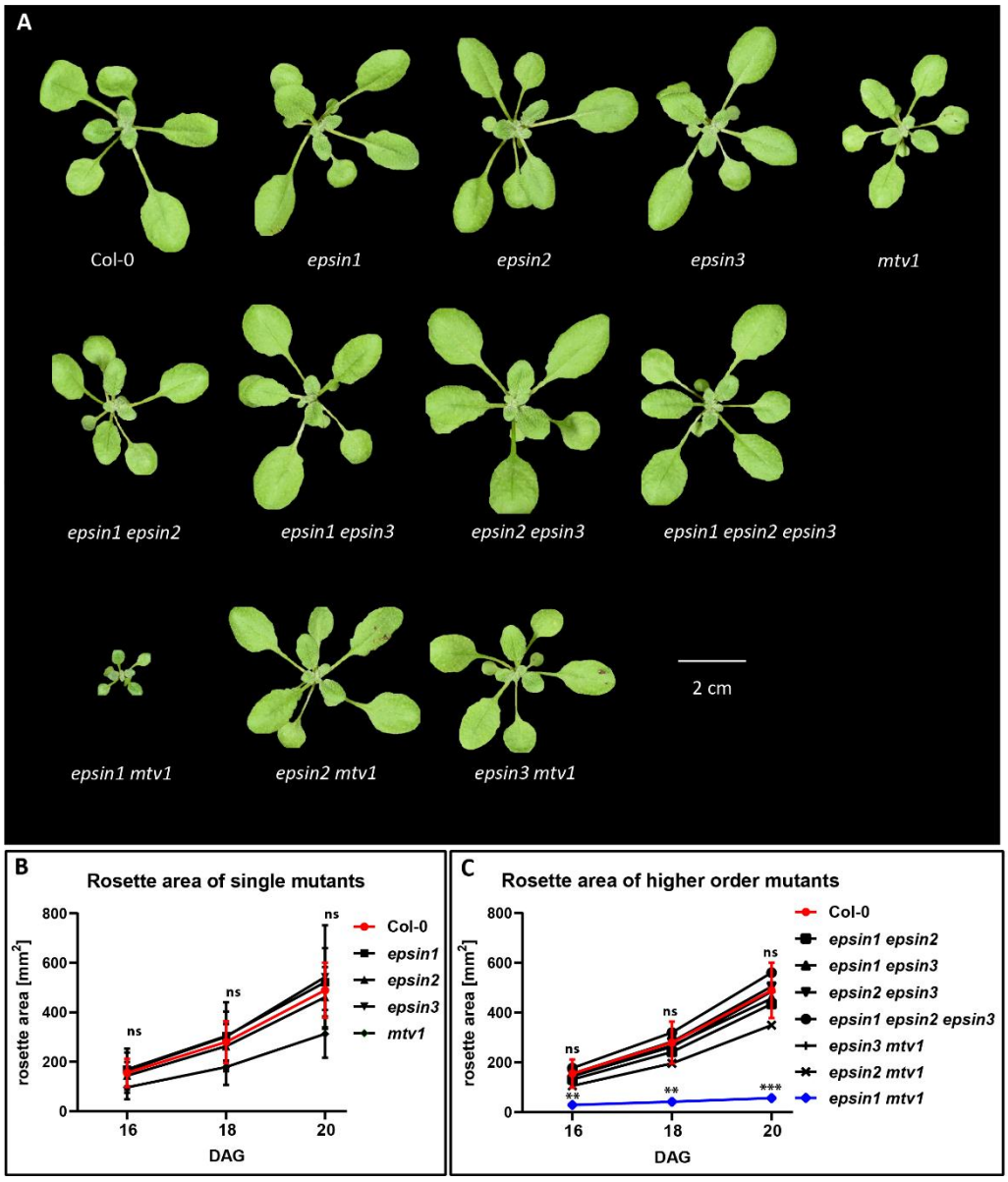

Figure 10: Phenotype of single and higher-order mutant plants. A: Vegetative growth phenotype of 24-day-old plants grown on soil under long day conditions, scale bar: 2 cm. **B:** Quantification of rosette area of single mutants in comparison to Col-0 displayed as mean of mean of three independent experiments, bars indicate range, $6 < n > 8$, 2-way Analysis of variance (ANOVA) with Turkey's multiple comparison test; **C:** Quantification of rosette area of higher-order mutants in comparison to Col-0 displayed as mean of means of three independent experiments, bars indicate rage, $6 < n > 8$, 2-way ANOVA with Turkey's multiple comparison test.

Taken together only *epsin1 mtv1* double mutant and *epsin1 epsin2 epsin3* triple mutant plants showed a phenotype which was very different from each other. *epsin1 mtv1* displayed a reduced overall growth phenotype and the triple mutant was partially sterile. A more detailed analysis of both phenotypes will be presented in sections 3.3 and 3.4 of this thesis.

3.3 Genetic interaction of *epsin* mutants leads to partially sterile plants with pollen germination defects

The loss of all three EPSINs in *A. thaliana* does not impair normal vegetative growth. However, in the reproductive growth phase *epsin1 epsin2 epsin3* (*e1 e2 e3*) mutants exhibited shorter siliques (Figure 11A). Interestingly, the flower morphology itself had no obvious defects (Figure 11 B-G). The anther formation, length and dehiscence as well as the stigma formation was wild type-like. We investigated the shorter silique phenotype by opening the siliques and obtained less fertilized ovules per silique in comparison to Col-0 (Figure 11H-J).

The *QUARTET 1* (*qrt-1*) mutant has a peculiarity in pollen development, resulting in incomplete separation of the pollen grains after maturation and a so-called tetrad pollen phenotype (Preuss et al. 1994). Due to the fact that the triple mutant showed tetrad pollen caused from a *qrt-1* mutation from the sail mutant background, we included *qrt-1* as a control (Sessions et al. 2002). Nevertheless, *qrt-1* mutants developed a normal seed set with no fertilization defect (Preuss et al. 1994).

Figure 11: Phenotype of Col-0, *epsin1 epsin2 epsin3* and *qrt-1* mutant plants in the reproductive growth phase. A: Inflorescence with normal siliques and shorter siliques are marked with arrow, scale bar: 2 cm; **B-D**: Flower morphology, scale bar: 500 µm; **E-G:** Opened anthers, scale bar: 500 µm; **H-J:** Opened siliques with fertilized and unfertilized ovules (arrowheads), scale bar: 500 µm.

To investigate whether this phenotype originates from a male or a female gametophytic defect, we performed reciprocal crosses between *epsin1 epsin2 epsin3* and Col-0 plants. We counted fertilized ovules per silique of the F1 offspring plants from the reciprocal cross (Figure 12A and Table 12). When Col-0

plants were the pollen donor, this resulted in 49.00 (Col-0 x Col-0) and 37.62 (*epsin1 epsin2 epsin3* x Col-0) fertilized ovules per silique (Table 12).

Table 12: Count of fertilized ovules per silique from reciprocal crosses of *epsin1 epsin2 epsin3* and Col-0 plants. Displayed are the means with SD. Col-0 x Col-0 (n = 2) and all other combinations n = 6.

female\male	**Col-0**	***epsin1 epsin2 epsin3***
Col-0	49.00 ± 1.414	4.76 ± 6.157
epsin1 epsin2 epsin3	37.62 ± 10.03	7.75 ± 7.743

Whenever the triple mutant provided the pollen, plants ended up with a drastically reduced set of fertilized ovules per silique which was in all combinations significantly ($p < 0.001$) different to combinations in which Col-0 provided the pollen. Thus, the strongly reduced fertilization of ovules was caused by a male gametophytic defect in the triple mutant.

We performed *in vitro* pollen germination assays with *epsin1 epsin2 epsin3*, Col-0 and the *qrt-1* mutant to study the fertilization defect in more detail (Figure 12B). In these assays, we calculated a germination rate of 72.78% for Col-0 pollen, *qrt-1* showed 50.68% and *epsin1 epsin2 epsin3* was reduced to 12.75%. Both Col-0 and *qrt-1* mutant pollen germination was significantly ($p < 0.0001$) different to *epsin1 epsin2 epsin3*. This data suggested that the pollen germination defect of *epsin1 epsin2 epsin3* results in less fertilized ovules.

The subcellular localization of EPSINs within pollen tubes had not been examined, so far. Thus, we used lines expressing EPSINs fused to GFP for *in vitro* pollen germination assays and imaged the pollen tube with confocal laser scanning microscopy. We detected a punctate pattern of EPSIN1-GFP localization whereas EPSIN2-GFP as well as EPSIN3-GFP displayed a more diffuse signal at the tip of the pollen tube (Figure 12C). We generated complementation lines of *epsin1 epsin2 epsin3* expressing either EPSIN1-GFP, EPSIN2-GFP or EPSIN3-GFP and found that in all three combinations the ovule fertilization defect of the triple mutant was rescued (Figure 12D). To this end, we counted fertilized ovules per silique in comparison to Col-0 (60.20 per silique) and triple mutant (13.25 per silique) itself. EPSIN1-GFP, EPSIN2-GFP and EPSIN3-GFP fusion proteins succeeded to rescue the fertility rate up to 55.8 per silique, 57.4 per silique and 57.2 per silique, respectively, which is indicated by no significant difference between Col-0 and the rescue lines.

Taken together, the genetic interaction of all three *EPSINs* resulted in a male gametophytic phenotype caused by pollen germination defects.

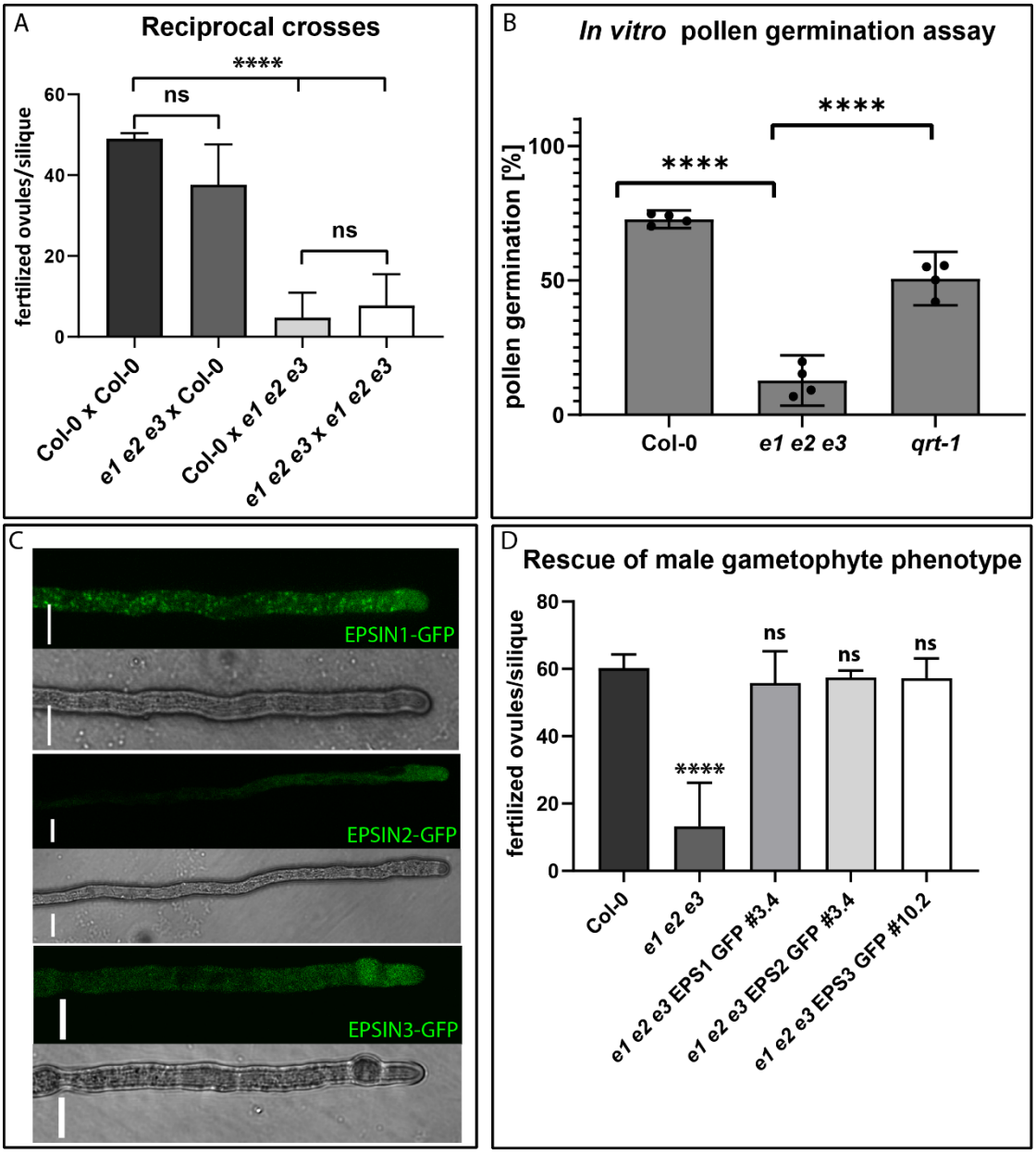

Figure 12: Quantitative analysis of gametophytic defects of the *EPSIN* triple mutant in *A. thaliana*. A: Count of fertilized ovules of reciprocal crosses of Col-0 and *epsin1 epsin2 epsin3* (*e1 e2 e3*), Col-0 as the pollen donor behaved significantly ($p < 0.0001$) different from *e1 e2 e3* as the pollen donor, one-way ANOVA with Tukey's multiple comparison test **B**: *In vitro* pollen germination assay at 25°C for 3 h, displayed are four experiments ($716 < n > 1334$) with mean and 95% CI and *e1 e2 e3* is significantly ($p < 0.0001$) different to Col-0 and *qrt-1* mutant; **C**: Subcellular localization of GFP fusion proteins of EPSIN1, 2 and 3 in pollen tubes, scale bars: 10 µm; **D:** Count of fertilized ovules per silique of Col-0, triple mutant and rescue lines with *pEPSIN1::EPSIN1-GFP, pEPSIN2::EPSIN2-GFP, pEPSIN3::EPSIN3-GFP* ($5 < n > 25$), Col-0 is significantly ($p < 0.0001$) different to *e1 e2 e3* tested with Kruskal-Wallis test.

3.4 Strong genetic interaction of epsin1 and mtv1 mutants results in a dwarf phenotype

The *epsin1 mtv1* double mutant was the only mutant combination of those observed which displayed a drastic growth phenotype already at the vegetative phase (Figure 10A-C). As mentioned before, we measured the rosette area at 20 DAG and *epsin1 mtv1* achieved a growth of 57.03 mm^2 which was significantly smaller compared to the wild type (155.37 mm^2). We generated rescue lines by introducing *pEPSIN1::EPSIN1-GFP* or *pMTV1::MTV1-GFP* constructs into *epsin1 mtv1*. Both rescue lines grew on soil side by side with the respective single mutants, wild type as well as *epsin1 mtv1* and both compensated for the existing dwarf phenotype of *epsin1 mtv1* (Figure 13A).

In order to analyze more growth criteria, we measured root length of *epsin1*, *mtv1*, the double mutant and the rescue lines of 7-day-old plants in three independent experiments and the values were normalized to Col-0. Roots of the double mutant were significantly ($p < 0.0001$) shorter than wild type roots (Figure 13B and Table 13). Both *epsin1 mtv1* MTV1-GFP and *epsin1 mtv1* EPSIN1-GFP showed significantly longer roots compared to the double mutant. Importantly, both rescue lines were not significantly different to their respective single mutant which indicated the functionality of both constructs.

Table 13: Calculation of P values by one-way ANOVA and Tukey's multiple comparisons test of root length data. Three independent experiments values normalized to the respective control.

	p value
Col-0 vs. *epsin1*	0.1584
Col-0 vs. *mtv1*	0.5862
Col-0 vs. *epsin1 mtv1*	<0.0001
epsin1 vs. *epsin1 mtv1* MTV1-GFP	0.0519
mtv1 vs. *epsin1 mtv1* EPSIN1-GFP	0.9668
epsin1 mtv1 vs. *epsin1 mtv1* EPS1-GFP	<0.0001
epsin1 mtv1 vs. *epsin1 mtv1* MTV1-GFP	0.0004

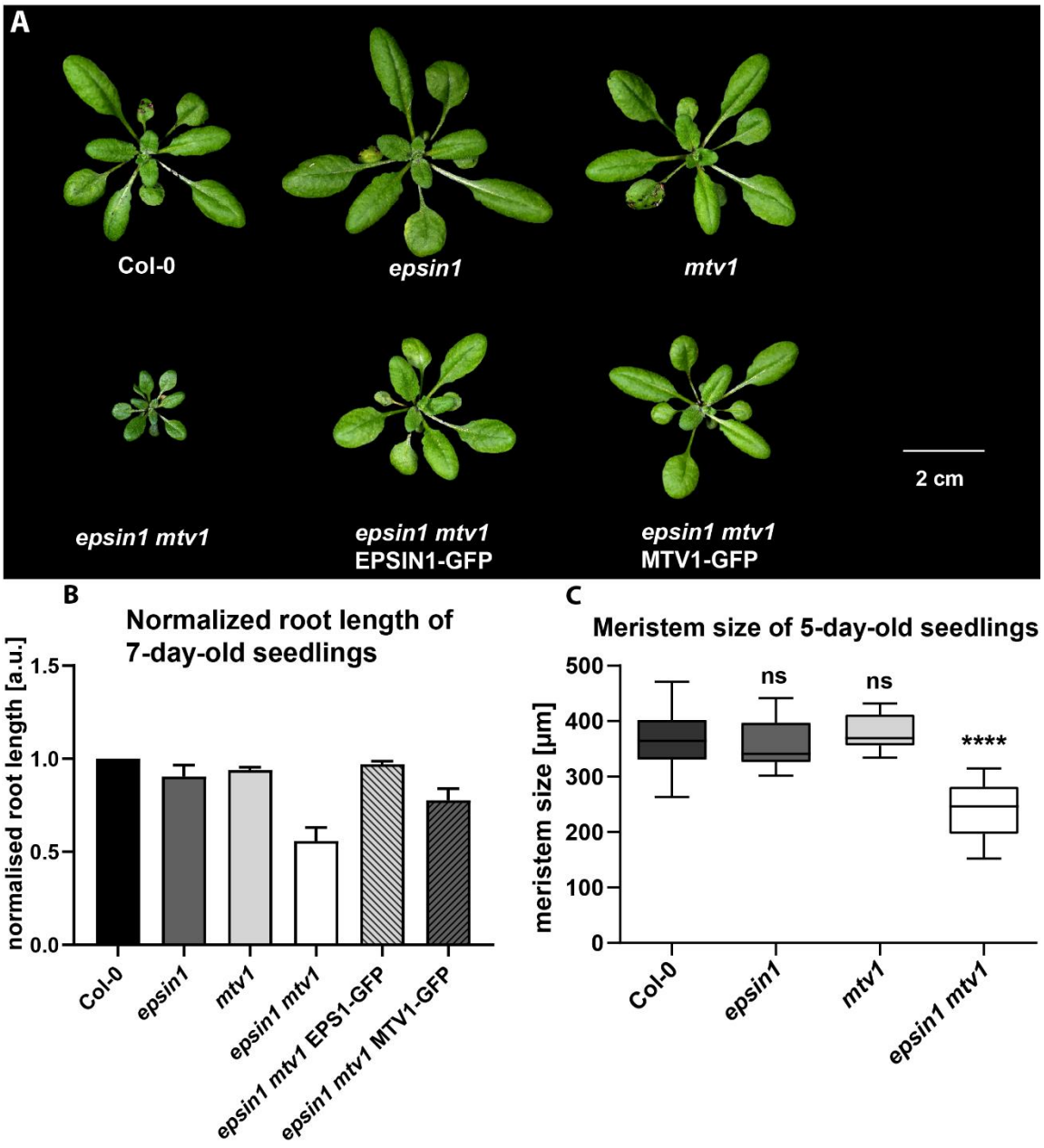

Figure 13: Growth phenotype of *epsin1 mtv1* and rescue lines. A: 21-day-old plants grown side-by-side on soil under long day conditions, scale bar: 2 cm; **B:** Root length measurement of 7-day-old seedlings including rescue lines. Four independent experiments normalized to the respective control ($15 < n > 25$). **C:** Meristem size measurement of 5-day-old seedlings ($n = 20$) stained with Calcofluor White displayed as Box and whiskers with Tukey.

We used root meristem size as an approximation for meristem activity. Therefore, we analyzed root meristem size of 5-day-old seedlings which were fixed, cleared and stained with Calcofluor White. *epsin1* (357.5 µm) and *mtv1* (375.1 µm) were not different from Col-0 (362.7 µm). In line with the reduced growth phenotype, we observed a significantly shorter root meristem size for *epsin1 mtv1* (235.6 µm) compared to the wild type (Figure 13C).

A few years ago it has been shown that *MTV1* interacts genetically with *MTV4,* which is a plant specific ADP ribosylation factor GTPase-activating protein (ARF GAP) localized at the TGN (Liljegren et al 2009; Sauer et al. 2013). To determine whether *EPSIN1*, *EPSIN2* or *EPSIN3* also interact genetically with *MTV4*, we created double mutants and compared their overall growth. 28-day-old plants were grown side-by-side on soil under long day conditions and images were taken (Figure 14A). Neither *epsin2 mtv4* nor *epsin3 mtv4* phenotypically deviated from wild type. Strikingly, *epsin1 mtv4* mutant plants were dwarfed similar to *mtv1 mtv4* mutant plants. Thus, both *MTV1* and *EPSIN1* strongly interact genetically with *MTV4*. We quantified the phenotype by root length measurement of 9-day-old seedlings ($45 < n > 54$) (Figure 14B). *epsin1 mtv4* mutants had significantly shorter roots in comparison to wild type, although *mtv1 mtv4* roots were even shorter. The root phenotype of *epsin1 mtv4* was not fully penetrant indicated by the high variance particularly towards the smaller values. Since EPSIN1 and MTV1 localized to the TGN, we performed co-localization studies of both proteins with stably expressed *pMTV4::MTV4-mRuby3* (Figure 13C-E). The center-to-center distance was calculated as mentioned before. Notably, our quantification data showed that EPSIN1-GFP with a center-to-center distance of 0.1184 ± 0.0037 µm is even closer located to MTV4-mRuby3 than MTV1-GFP which showed a distance of 0.2887 ± 0.007 µm. The distance between EPSIN1 and MTV4 was clearly shifted to smaller values. Although all three proteins are located at the TGN, they do not overlap to the same extent, which we demonstrated precisely with the quantification method.

Taken together, we showed synergistic effects of *EPSIN1* and *MTV1* and a clear genetic interaction of their mutant forms resulting in a dwarf phenotype of double mutant plants. Both introduced constructs, *pEPSIN1::EPSIN1-GFP* and *pMTV1::MTV1-GFP,* are complementing the growth phenotype. Interestingly, both interacted genetically with the ARF GAP MTV4. The double mutants (*epsin1 mtv4* and *mtv1mtv4*) were dwarfs with overall growth reduction and short roots. The co-localization of EPSIN1, MTV1 and MTV4 showed, that EPSIN1 and MTV4 are likely located at the same subdomain of the TGN in contrast to MTV1. This provided a second hint for a functional overlap between EPSIN1 and MTV1, but with different subcellular localization within the TGN.

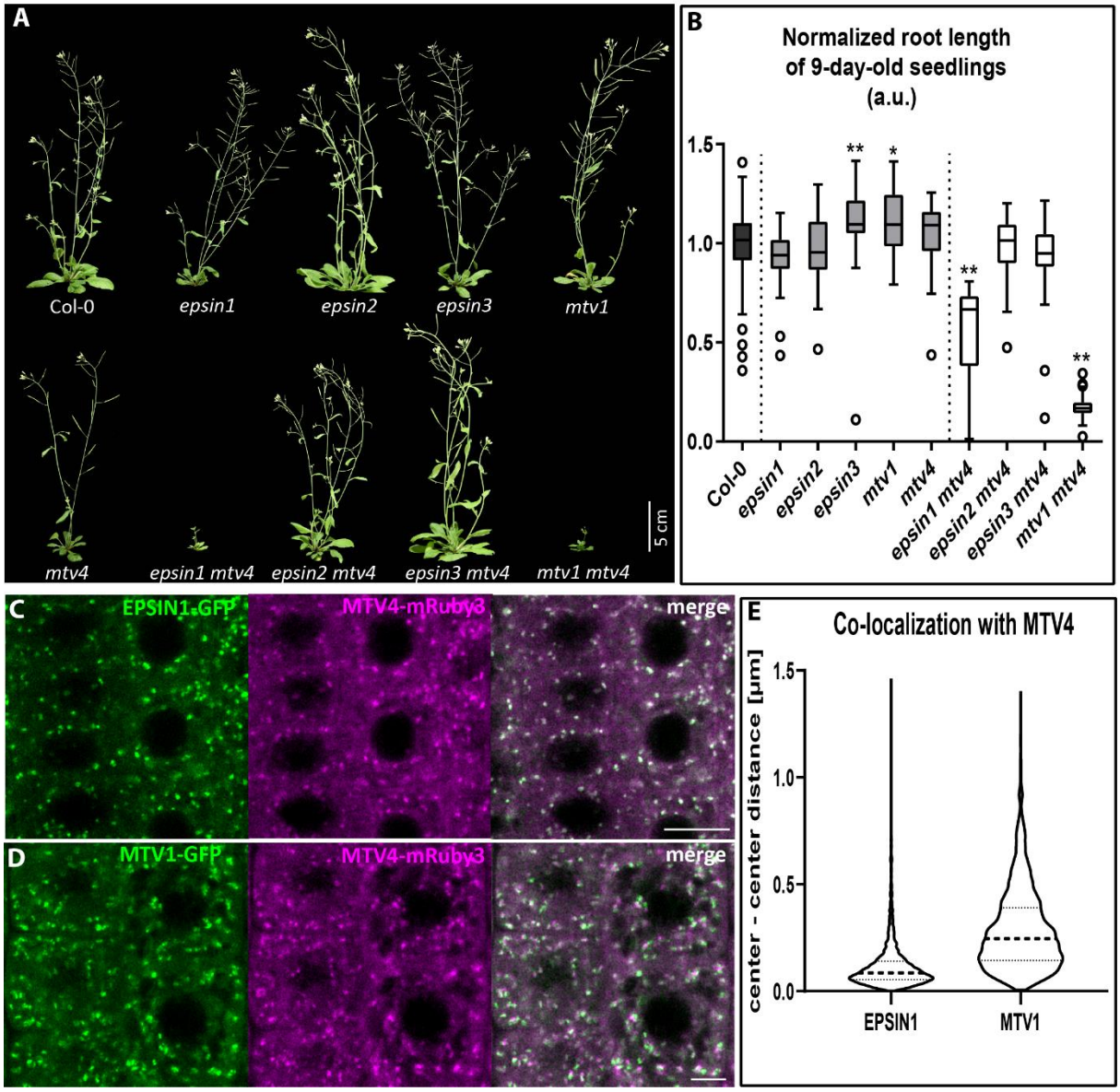

Figure 14: Genetic interaction and co-localization of ENTH proteins with MTV4. A: Comparision of single and double mutant phenotype of 28-day-old plants grown on soil under long day conditions. arbitrary units (a.u.) **B:** Root length measurements of 9-day-old seedlings (45 < n > 54) normalized to the respective Col-0 control displayed as Box and whiskers with Tukey. **C+D:** Co-localization of EPSIN1-GFP and MTV1-GFP with MTV4-mRuby3, scale bar upper panel: 10 µm and scale bar lower panel: 5 µm. **E:** Quantification of center-to-center distance displayed as violin plot, median marked with dashed line.

3.5 Analysis of *post*-Golgi trafficking defects in *epsin1 mtv1* mutant plants

3.5.1 An *epsin1 mtv1* double mutant shows defects in vacuole transport and morphology

In case of the *mtv1* mutant it has been shown that vacuolar transport is impaired and data from a weak mutant allele of *epsin1* also revealed a link to vacuolar transport defects (Song et al. 2006; Sauer et al.

2013). Therefore, we investigated defects in vacuolar transport of cargo proteins by using a polyprotein, which contains signal peptides for sorting into the endomembrane system. The marker, termed secN-R_m-2A-GH, was developed as a secreted-RFP and ER-located GFP dual reporter (Samalova et al. 2006). In wild type cotyledons we observed the GFP part of the polyprotein arrested in the ER and the RFP part transported into the lytic vacuole (Figure 15A). Neither the single nor the double mutant showed affected GFP signal in the ER. Importantly, 27.4% of the analyzed cells from *mtv1* single mutant exhibited RFP signal in the apoplast, indicating impaired protein transport to the lytic vacuole and secretion of RFP by bulk flow (Figure 15B). In contrast, *epsin1* showed 1.3% mis-localized signal which was not significantly different from wild type (2.6%). The double mutant displayed up to 89.4% mis-targeted RFP signal in the apoplast. Our findings thus suggest a strong synergistic interaction between *EPSIN1* and *MTV1* in vacuolar transport of this cargo protein

In line with the affected transport to the lytic vacuole, we observed that the vacuole morphology was altered in *epsin1 mtv1* root epidermal cells at the root tip. 5-day-old seedlings were incubated with MDY-64, which stains the tonoplast, and imaged with confocal laser scanning microscopy (Figure 15C). The root epidermal cells of wild type plants were fully packed with small vacuoles. Those would need to fuse and mature in order to generate the central lytic vacuole later on. The MDY-64 signal was rarely detected inside the forming vacuoles. Root epidermal cells of *epsin1 mtv1* contained less and more rounded vacuoles sometimes with MDY-64 signal inside. Remarkably, we observed multi-membrane regions of the vacuole in the double mutant. Our data suggest that either the vesicle transport of vacuolar proteins is compromised, resulting in altered morphology, or that the membrane fusion itself is affected, probably by mis-localized factors of the fusion machinery.

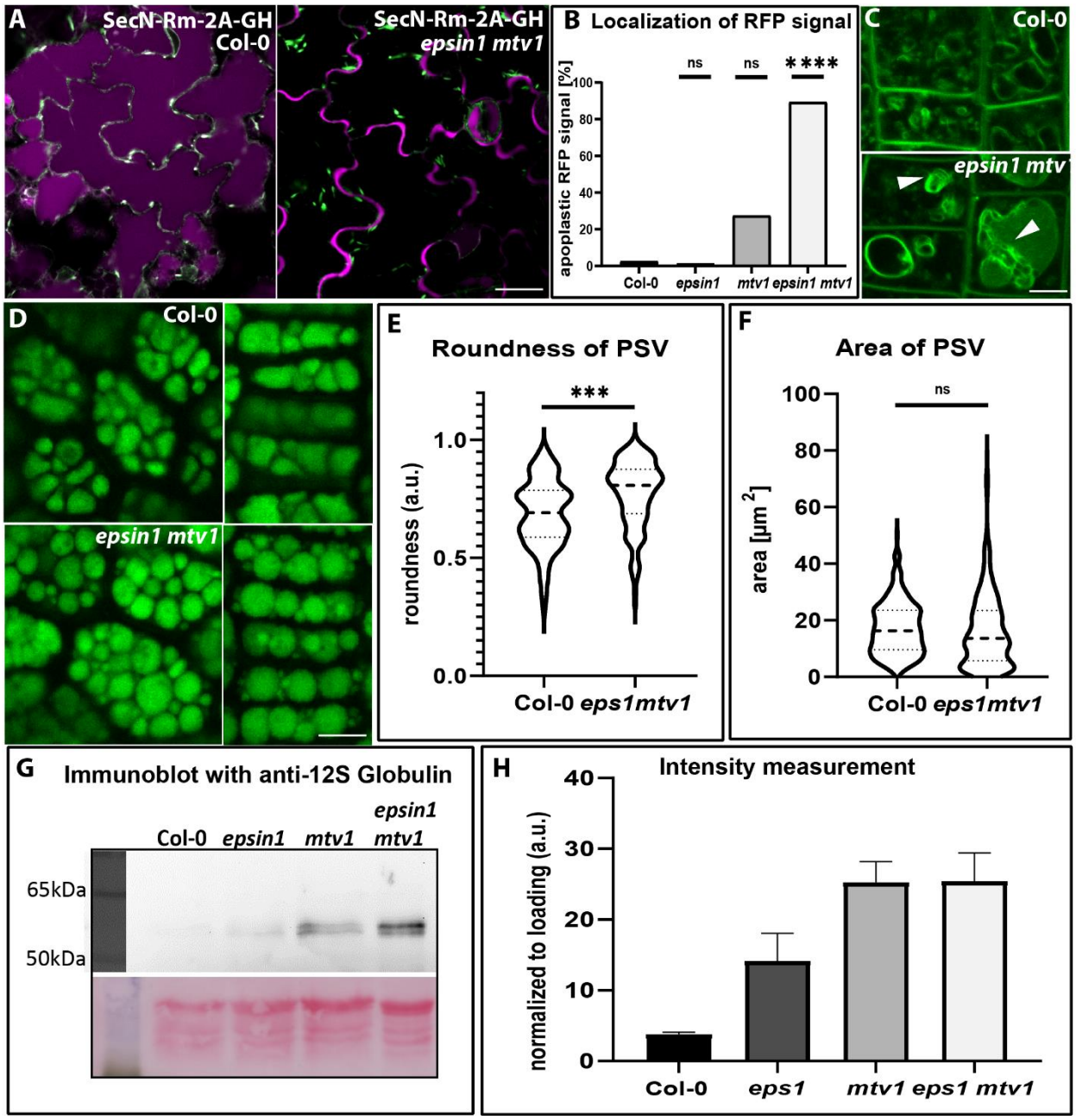

Figure 15: Defects of vacuolar transport and morphology. **A:** Localization of SecN-R_m-2A-GH in cotyledons of 5-day-old seedlings of *epsin1 mtv1* and Col-0, scale bar: 10 µm **B:** Quantification of apoplastic RFP signal in single mutants, double mutant and Col-0 in three independent experiments (227 to 299 total counts per genotype) **C:** Root epidermal cells of 5-day-old seedlings stained with MDY-64. Multi membrane regions are marked with arrows, scale bar: 5 µm. **D:** Morphology of storage vacuoles in seeds, scale bar: 10 µm. **E+F:** Quantification of roundness and area of PSVs in Col-0 and *epsin1 mtv1* mutant displayed as violin plot, median marked with dashed line (220 < n > 312 per genotype). **G:** Immunoblot total of seed protein extracts probed with anti-12S globulin and loading control. **H:** Signal quantification of 12S globulin accumulation of two independent experiments, normalized to loading control displayed as bar chart with SD. Arbitrary units (a.u.).

In addition to lytic vacuoles, protein storage vacuoles (PSVs) have been analyzed in seeds, more precisely in embryos. We imaged the autofluorescence of PSVs in wild type as well as in single and double mutants (Figure 15D). While wild type seeds showed fully packed cells, *epsin1 mtv1* displayed more rounded PSVs with more space in between (Figure 15E-F). We quantified the roundness of PSVs and *epsin1 mtv1* was significantly ($p < 0.001$) different from Col-0. Furthermore, we calculated the area of PSVs and found no significant difference, however, the data set of *epsin1 mtv1* was shifted towards smaller values.

In agreement with the results revealing lytic vacuolar transport defects, we demonstrated mis-sorting and abnormal accumulation of endogenous storage protein precursors in seeds. Storage proteins, such as globulin, are synthesized and their precursor forms targeted to the PSV. At the vacuole the precursors are processed to their mature form. We isolated total protein extracts from single- and double-mutant seeds and used western blot experiments to detect the 12S globulin precursor with a specific antibody (Figure 15G). Quantification of the signal intensity of the specific precursor band demonstrated that the wild type showed almost no and *epsin1* only a small fraction of accumulation. In case of *mtv1* and *epsin1 mtv1*, we detected and quantified a band at around 55 kDa.

Together, our data suggests that EPSIN1 and MTV1 play a strong synergistic role in protein transport to lytic vacuoles as well as storage vacuoles. Moreover, vacuolar morphology of both vacuole types are affected in the *epsin1 mtv1* double mutant.

3.5.2 Endocytosis and recycling seem unaffected in *epsin1 mtv1*

To determine whether the *epsin1 mtv1* double mutant exhibits major defects in endocytosis, we used the uptake of FM4-64, which is a dye being internalized by clathrin-mediated endocytosis, as a readout (Figure 16A). Wild type and mutant seedlings were incubated for 5 min with FM4-64 and immediately imaged with Zeiss LSM 880 Airyscan. We quantified the intensity of endosomal signal (Figure 16B). Due to the fact that *epsin1 mtv1* showed no difference ($p = 0.09$) to wild type, we concluded that EPSIN1 and MTV1 are not required for internalization from the PM mainly.

Some proteins located at the PM, like the auxin efflux carrier PIN2, are constantly endocytosed and recycled by clathrin-coated vesicles between the PM and early endosomes/TGN (Kleine-Vehn et al. 2008; Men et al. 2008). In order to identify defects in this trafficking pathway, we crossed PIN2-GFP into the *epsin1 mtv1* mutant (Figure 16C-E). The polar localization of PIN2-GFP at the PM was quantified by the measurement of the signal intensity distribution between PM and intracellular signal. Between the wild type and the double mutant no significant difference ($p > 0.9999$) was found based on a nested t-test

(unpaired, two-tailed). This localization served as a control for the following drug treatment experiments. To examine endocytosis and recycling defects separately, we treated seedlings with the drug BFA, which blocks the exocytic trafficking step of endocytic recycling, and observed typical BFA compartments in which PIN2-GFP was clustered together. We counted the BFA compartments per cell and there was no significant difference ($p > 0.9999$) between wild type and the double mutant (tested by 2-way ANOVA). To address the recycling process precisely we washed the BFA-treated seedlings for 2 h while blocking *de novo* synthesis of proteins with CHX. PIN2-GFP was restored back to the PM assuming its correct polar localization. We measured the PIN2-GFP signal intensity distribution between PM and intracellular signal in both genotypes and there no significant difference was found ($p > 0.9999$) when tested with a nested t-test (unpaired, two-tailed).

These results suggest that EPSIN1 and MTV1 are not mainly involved in endocytosis from and recycling to the PM.

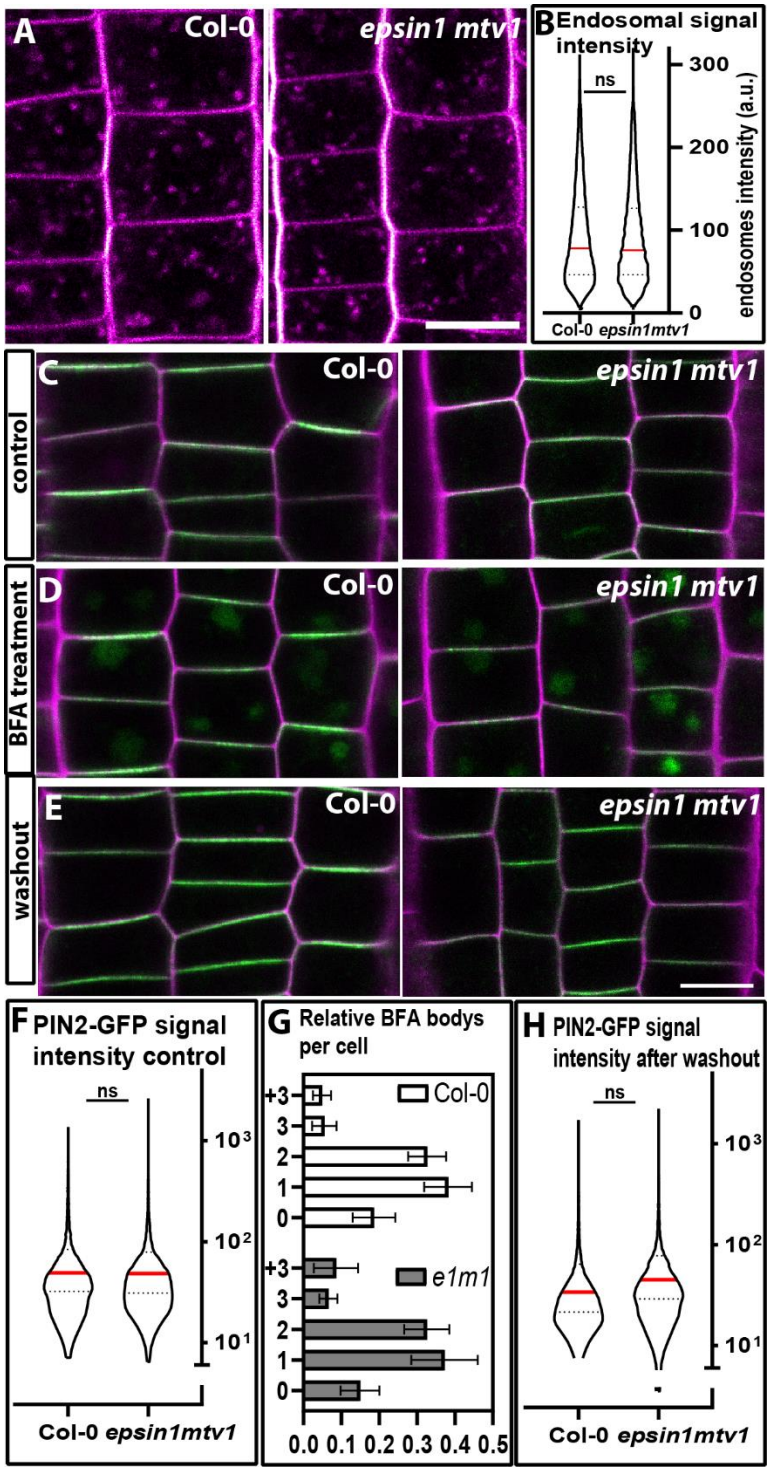

Figure 16: Endocytosis and recycling appear to be unaffected in the *epsin1 mtv1* double mutant. A: FM4-64 uptake after short-term incubation on ice in root epidermal cells of 5-day-old seedlings of *epsin1 mtv1* and Col-0, scale bar: 10 µm. **B:** Quantification of endosomal FM4-64 signal **C:** Localization of PIN2-GFP in *epsin1 mtv1* and wild type root epidermal cells (n = 10). Cell membrane was stained with propidium iodide, scale bar: 10 µm. **D:** Localization of PIN2-GFP after treatment with 50 µM BFA and 50 µM CHX for 1 h (n = 10), scale bar: 10 µm. **E:** Localization of PIN2-GFP after washout and 50 µM CHX for 2 h (n = 10), scale bar: 10 µm.

3.5.3 EPSIN1 and MTV1 play a role in secretion

The involvement of EPSIN1 and MTV1 in *post*-Golgi trafficking pathways, like vacuolar transport, prompted us to further investigate the secretory route. SecRFP is a commonly used marker protein which is secreted to the extracellular space of epidermal cells in wild type cotyledons (Samalova et al. 2006). Mutant plants with major secretion defects accumulate the RFP signal inside the cell. Neither the single mutants nor the double mutant showed abnormal accumulation of RFP signal (Figure 17A). Next, we investigated whether the secretion of complex polysaccharides is affected in *epsin1 mtv1* by staining seeds with ruthenium red and analyzing the thickness of the mucilage layer. Although the exact function of mucilage is not clear, it is known that vesicular transport is involved in secretion of the mucilage components (McFarlane et al. 2014; Gendre et al. 2013). Interestingly, already the single mutants showed a slight reduction of mucilage layer thickness (Figure 17B-C). We quantified the layer thickness and normalized our data to the respective wild type values in each experiment. Except for *epsin1 mtv1* MTV1-GFP, we performed three independent experiments. The single mutants already showed a slight reduction of the mucilage layer thickness down to 86.5% (*epsin1*) and 77.06% (*mtv1*). The thickness was drastically reduced in the *epsin1 mtv1* double mutant (51.28%). The phenotype of the *epsin1 mtv1* double mutant was complemented up to the respective single mutant in the *epsin1 mtv1* EPSIN1-GFP or MTV1-GFP rescue lines, indicating that both fusion proteins were functional and that the phenotype was caused by loss of function of the respective genes. We included an *echidna (ech)* mutant in our analysis as a control due to the fact that it was reported to show almost no mucilage layer (Gendre et al. 2013). The defect of mucilage secretion in *ech* (4.28%) was even stronger compared to the one in the *epsin1 mtv1* (51.28%) double mutant. We further discovered that *epsin1 mtv1* showed cell adhesion defects in roots (Figure 17D). We imaged z-stacks of 7-day-old seedlings stained with propidium iodide and observed root epidermal cells which seemed to lose attachment. Some cells were swollen and sometimes gaps between the epidermal cells and the cell file below were visible. This phenotype was never observed in wild type roots. Furthermore, 5-day-old seedlings were fixed, cleared and stained with Calcofluor White, which is an unspecific dye for cell wall staining (Figure 17E). However, in *epsin1 mtv1* root cells, especially in the quiescent center, we detected internal signal. This cell adhesion defect and internal signal of Calcofluor White were not found in every root, thus the phenotype was not fully penetrant. Based on our results, EPSIN1 and MTV1 are involved in the secretion of a subset of cell wall components. In contrast, other secretory pathways probably independent of clathrin are not affected in *epsin1 mtv1*. Interestingly, we observed similarities to *ech* mutant which is a knockout of a major TGN scaffold protein.

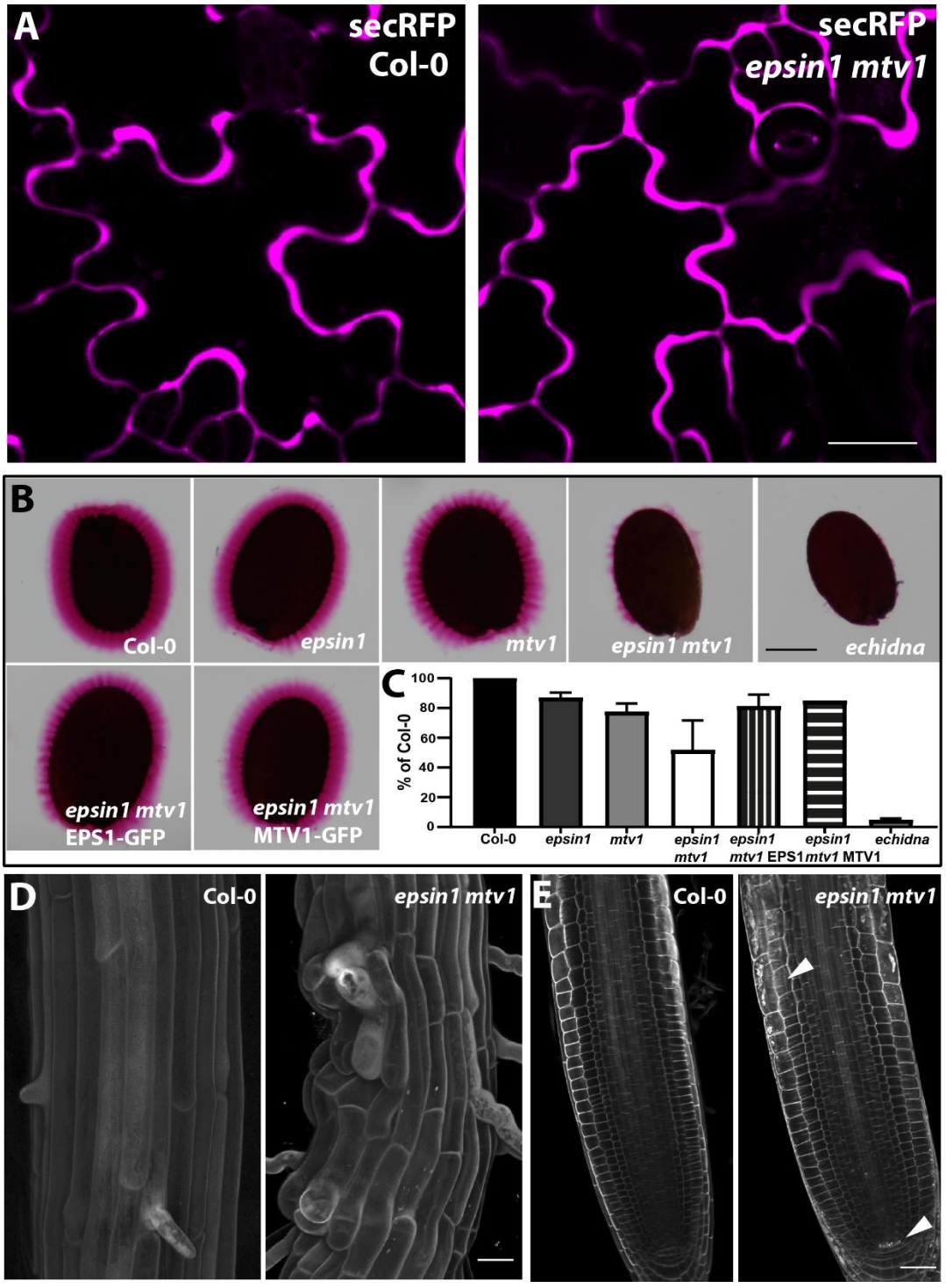

Figure 17: The *epsin1 mtv1* double mutant displays defects in secretion of specific cargo whereas bulk flow remains unaffected. **A:** Localization of secRFP in cotyledons of 7-day-old *epsin1 mtv1* and Col-0, scale bar: 20 µm. **B**: Staining of mucilage layer of hydrated seeds of single as well as double mutants, Col-0 and *echidna* as control by ruthenium red, scale bar: 200 µm. **C**: Measurement of mucilage layer thickness relative to Col-0, bars indicate 95% CI. **D:** 7-day old roots of Col-0 and *epsin1 mtv1* stained with propidium iodide, scale bar: 40 µm. **E:** 5-day-old seedlings fixed and stained with Calcofluor White, abnormal internal signal in *epsin1 mtv1* (arrowheads), scale bar: 20 µm.

3.6 EPSIN1 and MTV1 localization is independent of the *trans*-Golgi network protein ECHIDNA

ECH has been characterized as a TGN located protein involved in various *post*-Golgi trafficking pathways (Gendre et al. 2011). Of note, the *ech* mutant displays a very similar dwarf phenotype to the *epsin1 mtv1* double mutant (Figure 18A). To further define possible similarities to the *ech* mutant, we checked the localization of TGN reside proteins, particularly SYP61 and VHA-a1, due to the fact that both of them are mis-localized in *ech* (Gendre et al. 2013). We crossed CFP-SYP61 and VHA-a1-RFP with *epsin1 mtv1* and imaged 5-day-old root epidermal cells (Figure 18B-C). Both TGN marker proteins were mis-targeted in *epsin1 mtv1*. We observed ring-like structures and multimembrane compartments which were also described in *ech*. In fact, those data raised the question whether the phenotype of *epsin1 mtv1* is a simple phenocopy of *ech* and caused by mis-localization of ECH itself.

It has been shown that *ech* mutants exhibit a TGN with altered morphology (Gendre et al. 2011). In order to rule out mis-localization of ECH in *epsin1 mtv1* mutant out, we investigated the localization of ECH by immunolocalization with ECH antibody (Figure 18D). We stained and imaged roots of Col-0, *epsin1 mtv1* and *ech* side-by-side. ECH is normally distributed in TGN like punctate pattern with only weak background staining in *ech* mutant roots. We tested vice versa whether EPSIN1 or MTV1 were mis-localized in *ech* mutants. Therefore, we used our generated antibodies for immunolocalization on roots of Col-0, *ech* and respective single mutant *epsin1* and *mtv1* (Figure 18E-F). Both antibodies worked in immunolocalization with some background staining in their mutant backgrounds. We detected no differences in ECH distribution between Col-0 and either *epsin1* or *mtv1*. Thus, the phenotype of *epsin1 mtv1* mutants is not caused by ECH mis-localization. Moreover, we concluded that the general morphology of the TGN seems unaffected in *epsin1 mtv1* mutant with ECH as a TGN marker.

Altogether our results indicated that EPSIN1 and MTV1 act either downstream or independent of ECH at the TGN. The dwarf phenotype of *epsin1 mtv1* looked like *ech*. However, similar to *ech* mutant plants, we found TGN cargo proteins like SYP61 and VHA-a1 mis-localized in *epsin1 mtv1*.

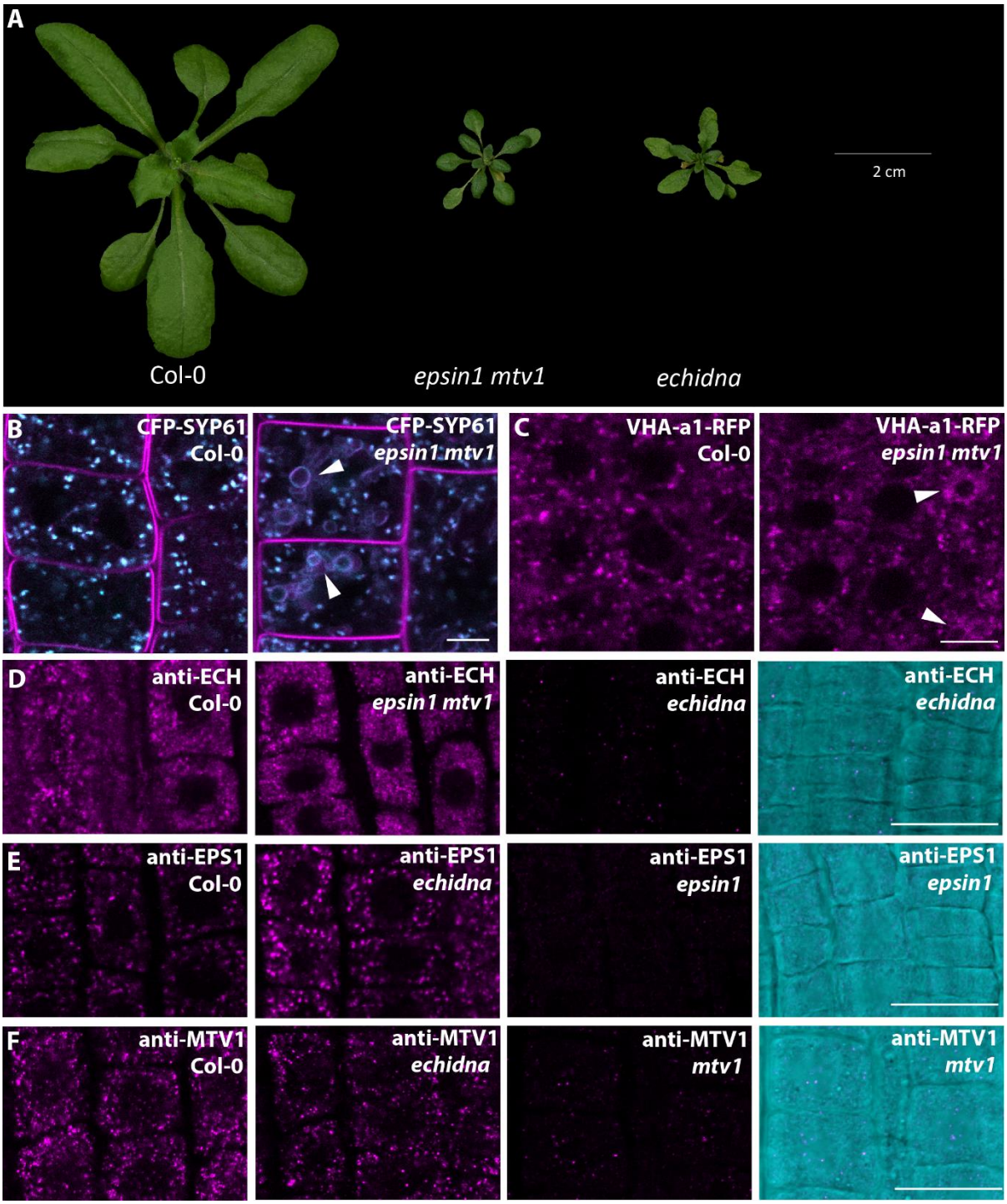

Figure 18: Despite phenotypic similarities between *epsin1 mtv1* double mutant and *echidna* single mutants, localization of EPSIN1 and MTV1 appears to be independent of ECHIDNA function and vice versa. A: Vegetative phenotype of 21-day-old Col-0, *epsin1 mtv1* and *ech*. **B:** CFP-SYP61 localized in a TGN-like pattern in Col-0 background and mis-localized in ring-like structures in *epsin1 mtv1*, FM4-64 dye for PM staining, scale bar: 10 µm **C:** TGN marker VHA-a1-RFP normally distributed in wild type and mis-targeted in *epsin1 mtv1*, scale bar: 5 µm **D:** Immunolocalization of ECH in *epsin1 mtv1* with wild type and *ech* as control, scale bar: 20 µm **E:** Immunolocalization of EPSIN1 in *ech* and controls, scale bar: 20 µm **F:** Immunolocalization of MTV1 in *ech* and controls, scale bar: 20 µm

3.7 MTV1 but not EPSIN1 membrane recruitment depends on AP4 function

We demonstrated that EPSIN1 and MTV1 have overlapping functions in vacuolar transport as well as secretion of cell wall components. However, their subcellular localization at the TGN differed to some extent. In fact, EPSIN1 located preferentially closer to CLC and MTV4. MTV1 was very close to VHA-a1. To investigate the subcellular localization further, we co-localized EPSIN1 and MTV1 with the TGN located adaptor complexes AP1 and AP4. Therefore, we crossed EPSIN1-GFP and MTV1-GFP lines with the AP1-mKO and AP4-mKO lines we had generated in which each protein was expressed under control of its endogenous promotor. All of them displayed the typical punctate TGN pattern (Figure 19A-F). By quantifying the center-to-center distance, we determined that EPSIN1 (0.117 µm) was closer to AP1 in comparison to MTV1 (0.191 µm). In contrast, the distance between MTV1 (0.092 µm) and AP4 was significantly smaller than the one between EPSIN1 (0.225 µm) and AP4. This strongly suggested that we had identified two partially separate TGN subdomains marked by EPSIN1/AP1 and MTV1/AP4, respectively.

To further define the link of ENTH proteins and AP complexes *in planta*, we used a genetic approach and generated double mutants of *epsin1, mtv1* and *ap4* (Figure 20A). The vegetative growth of *epsin1* was similar to wild type, in contrast *mtv1* and *ap4* were slightly smaller than wild type. Notably, *mtv1* and *ap4* were phenotypically indistinguishable. There was no additive effect apparent in the *mtv1 ap4* double mutant, in contrast to the *epsin1 mtv1* double mutant. Importantly, the double mutant *epsin1 ap4* was a dwarf similarly to *epsin1 mtv1* which indicates that the *ap4* mutation phenocopies *mtv1*.

In mammalian cells, it has been published that the recruitment of Tepsin (ortholog to MTV1) depends on AP4 (Borner et al. 2012). To investigate whether a similar relationship occurs in plants, we crossed MTV1-GFP and EPSIN1-mRuby3 into the *ap4* mutant (Figure 20B-C). As a control we imaged EPSIN1-mRuby3 and MTV1-GFP in Col-0 background first. In the next step, we observed a drastic difference between EPSIN1 and MTV1 localization in the *ap4* mutant background. EPSIN1 localization was unchanged in *ap4* with the expected TGN-like punctate pattern, in contrast MTV1 was cytosolic with almost no TGN pattern anymore. This suggests that, in contrast to EPSIN1, MTV1 recruitment to and its proper localization at the TGN require AP4 function.

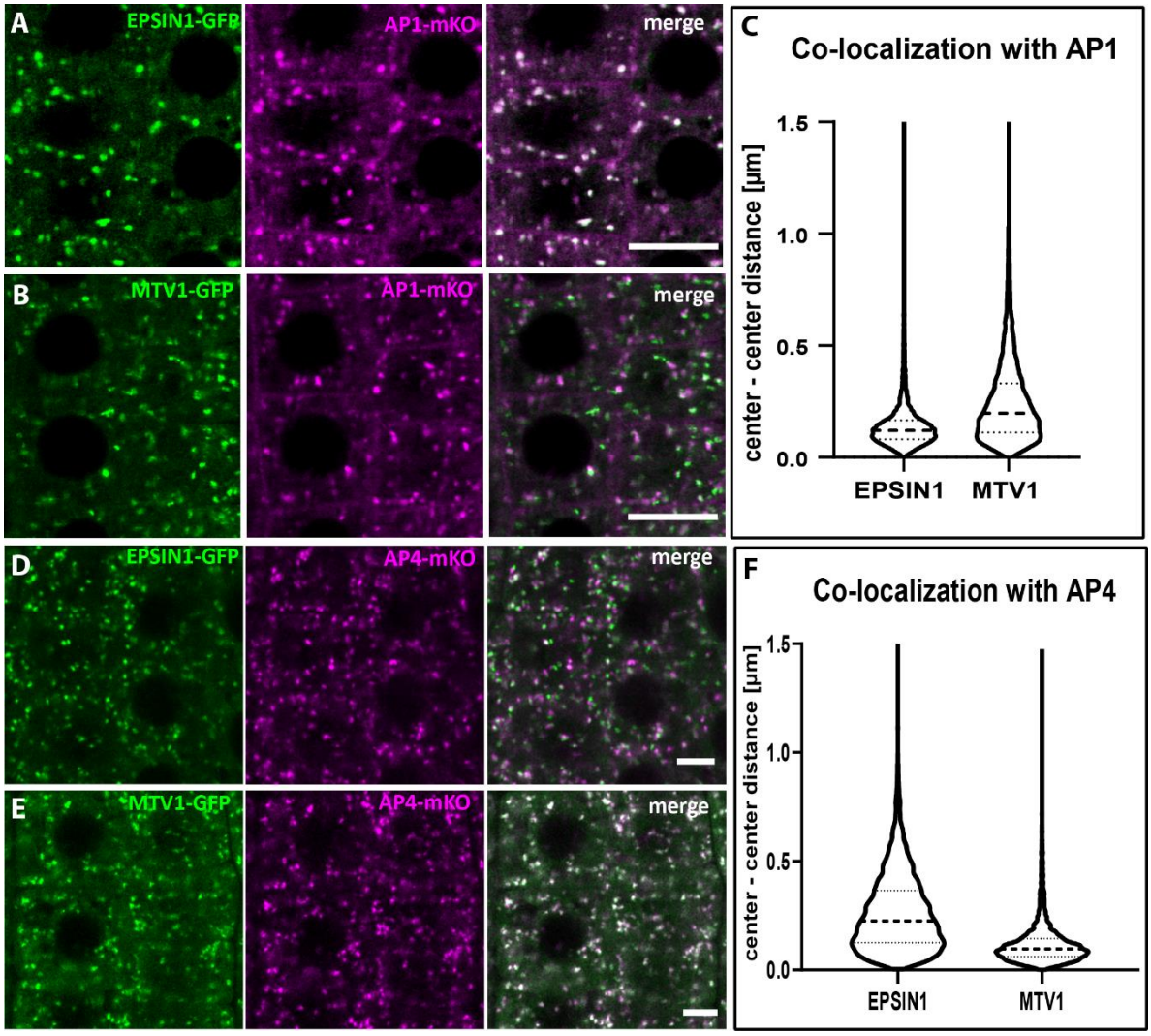

Figure 19: Co-localization of EPSIN1 and MTV1 with AP1 and AP4. A+B: EPSIN1-GFP and MTV1-GFP co-localized with AP1-mKO, root tips of 5-day-old seedlings, scale bar: 10 µm, **C:** Quantification of center-to-center distance, median marked with dashed line. **D+E:** EPSIN1-GFP and MTV1-GFP co-localized with AP4-mKO, root tips of 5-day-old seedlings, scale bar: 10 µm, **F:** Quantification of center-to-center distance, median marked with dashed line.

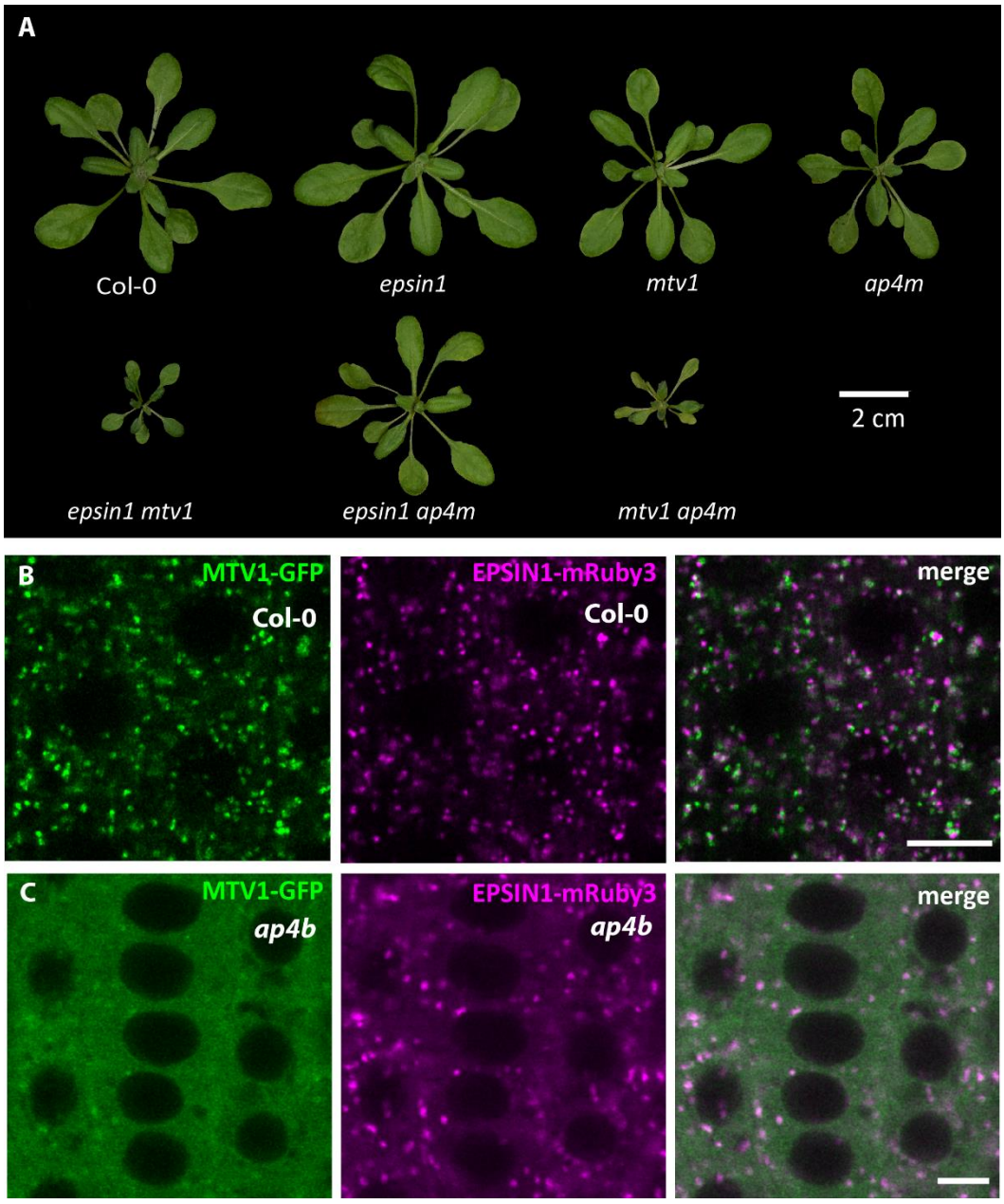

Figure 20: MTV1 and AP4 have overlapping function and depend on each other. A: Growth phenotype of 21-day-old single and double mutant plants grown on soil under long day condition. **B:** Co-localization of EPSIN1-mRuby3 and MTV1-GFP in Col-0 background, scale bar: 10 µm. **C:** Co-localization of EPSIN1-mRuby3 and MTV1-GFP in *ap4* mutant background, scale bar 5 µm.

In summary, we proposed that MTV1 and AP4 are functionally dependent on each other. The recruitment of MTV1 to the TGN is controlled by AP4. In contrast, EPSIN1 localization is independent of AP4. We conclude that EPSIN1 and AP1 are forming one subcompartment and MTV1 and AP4 another subcompartment of the TGN where they appear to have overlapping functions.

4. Discussion

4.1 ENTH domain proteins form two groups based on their subcellular localization

All ENTH proteins investigated in this study were found ubiquitously expressed throughout the whole plant. Importantly, owing to their subcellular localization, the four ENTH proteins can be split into two groups: EPSIN1 and MTV1 are clearly TGN localized, whereas EPSIN2 and EPSIN3 associate with the PM and the growing cell plate. All proteins additionally display cytosolic localization to some extend, which is typical for soluble proteins with transient recruitment to the endomembrane system. In mammalian and yeast cells, ENTH proteins cluster similarly in at least two distinct functional groups with different subcellular localization (Legendre-Guillemin et al. 2004). Members of the first group, such as mammalian epsin1 or yeast Ent1p as well as Ent2p, are located at the PM and mostly involved in clathrin-mediated endocytosis (CME) (Chen et al. 1998; Wendland et al. 1999; De Camilli et al. 2002).

Epsin1 was the first well characterized ENTH domain protein which plays an essential role in endocytosis (Chen et al. 1998). In mammalian cells, the interaction of epsin1 with AP2 and clathrin has been demonstrated (Mills et al. 2003). With the ENTH domain, epsin1 can bind to PIs preferentially to PtdIns(4,5)P_2 which are most abundant at the PM (Itoh et al. 2001). The functionally redundant pair Ent1p and Ent2p are ENTH domain proteins in yeast (Wendland et al. 1999). It has been shown that Ent3p, Ent4p as well as Ent5p cannot substitute the function of Ent1p and Ent2p. The localization studies were done by GFP fusion constructs in yeast and additionally by differential centrifugation fractionation studies (Wendland et al. 1999). The group described the subcellular localization of Ent1p Ent2p as peripheral and with internal punctate structures.

The second class contains mammalian epsinR/CLINT/Enthoprotein and yeast Ent3p and Ent4p which are located at the Golgi, TGN and potentially other endosomal structures (Kalthoff et al. 2002b; Wasiak et al. 2002; Mills et al. 2003; Duncan et al. 2003; Costaguta et al. 2006). The transport network between Golgi and endosomes in yeast and mammalian cells depends on three major players: AP1, Gga proteins and ENTH domain proteins. AP1 is an adaptor protein complex and Gga proteins (Golgi-localizing, gamma-adaptin ear homology domain, ARF-binding proteins) are monomeric adaptors (Boehm and Bonifacino 2001; Robinson and Bonifacino 2001; Boman 2001; Ghosh and Kornfeld 2004). In case of epsinR/CLINT/Enthoprotein (further referred to as epsinR) the interaction with clathrin, AP1 and Gga2 protein was demonstrated (Kalthoff et al. 2002b; Wasiak et al. 2002; Mills et al. 2003; Hirst et al. 2003; Saint-Pol et al. 2004). It is involved in clathrin-mediated transport, for instance, for the transport of the mannose-6-phosphate receptor between TGN and EE. The TGN localization has been shown, by

immunohistochemical localization with a specific epsinR antibody (Kallthoff et al. 2002b). Moreover, the expression was addressed by protein extraction of different mouse organs followed by an immunoblot with a specific antibody. In yeast, Ent3p and Ent5p show functional redundancy, however, Ent3p is an ENTH domain protein whereas Ent5p has an AP180 N-terminal homology (ANTH) domain (Duncan et al. 2003). Localization studies were performed with GFP fusion proteins and FM4-64 staining as well as differential sedimentation assay. Ent3p and Ent5p displayed similar localization, but their affinities to AP1 and Gga proteins as interaction partners are different (Eugster et al. 2004; Costaguta et al. 2006). It turned out that Ent3p interacts specifically with Gga2p and its localization depends on Gga2p rather than AP1. In contrast, Ent5p interacts with clathrin, AP1 and Gga2p, however, the localization of ENT5p is independent of AP1 as well as Gga2p (Duncan et al. 2003). The function of Ent4p is largely unknown. Taken together, our localization data and the resulting classification into two functional groups of ENTH domain proteins in *A. thaliana* is in line with the literature. We propose that EPSIN1 and MTV1 are major players in *post*-Golgi trafficking pathways located at the TGN, and EPSIN2 and EPSIN3 reside at the PM and may play a role in endocytosis, recycling and/or cytokinesis.

The phylogenetic outlier MTV1 was reported to be a factor in CCV-mediated trafficking of a subset of cargo proteins at the TGN (Sauer et al. 2013). By use of a stable MTV1-GUS construct under its endogenous promoter, it has been found that MTV1 is ubiquitously expressed throughout the whole plant with the strongest signal observed in root meristem cells and developing as well as mature embryos (Sauer et al. 2013). To determine the subcellular localization of MTV1, *A. thaliana* plants were stably transformed with *pMTV1::MTV1-GFP*. By live cell imaging MTV1 showed punctate structures and no overlap was observed with wave2R/RabF2b/ARA7 (PVC marker), wave22R/SYP32 (Golgi marker) and wave129R/RabA1g (cell plate marker). More importantly, MTV1-GFP co-localized almost perfectly with both the TGN markers SYP61-CFP and VHA-a1-RFP. Hence, the co-localization results obtained in our studies are in accordance with previous data from the literature.

The expression of EPSIN1 had previously been addressed by protein extraction of various plant organs followed by immunoblots with an EPSIN1- specific antibody (Song et al. 2006). It has been shown that EPSIN1 was expressed in all plant organs. The same group also analyzed the subcellular localization using transient expression studies in protoplasts and showed a network pattern with punctate stains (Song et al. 2006). In order to identify the network pattern in more detail, they co-transformed protoplasts with EPSIN1-RFP as well as GFP:talin, a marker for filamentous actin, and observed close overlap. Furthermore, the co-transformed protoplasts were treated with latrunculin B (Lat B), a drug which disrupts actin

filaments, and consequently the fluorescence signal was diffuse (Song et al. 2006). To examine the punctate stains closer, EPSIN1 was co-localized with a Golgi marker (ST:GFP), a PVC marker (PEP12p/SYP2) and the v-SNARE VTI11 which is located at the TGN as well as PVC (Zheng et al. 1999). In summary, Zheng and colleagues proposed EPSIN1 as an ubiquitously expressed protein with a localization in two locations: 1st) a network pattern which was associated with actin and 2nd) a punctate pattern. Although, the co-localization of EPSIN1 and VTI11 showed a clear overlap, the group determined the localization as Golgi and PVC (Song et al. 2006). This is in contrast to our *in planta* co-localization study of EPSIN1 with the Golgi markers Got1p and SYP32, the TGN marker Vha-a1 and the PVC marker RabF2b/ARA7, where EPSIN1 showed a clear TGN location with no network pattern (Dettmer et al. 2006; Geldner et al. 2009). The reasons for this discrepancy will be discussed below.

Only limited *in vitro* data is available for EPSIN2/EPSIN2R and the expression pattern of EPSIN2 in plants had not been addressed. Co-localization studies of EPSIN2 had previously been performed with the Golgi marker ST:GFP, the PVC marker GFP:Rha1 as well as the PVC and TGN markers in protoplasts. However, there was no overlap with any of those marker proteins (Lee et al. 2007). Consequently, Lee and colleagues postulated that EPSIN2 is localized to a novel compartment. This localization data was generated in transient expression experiments of HA:EPSIN2R and marker proteins in protoplasts followed by immunostaining. In strong contrast, we identified EPSIN2 as PM associated with cytosolic background and signal at the growing cell plate by stable *in planta* experiments. In order to examine the subcellular localization, the protoplast has become a commonly used system, however, there are limits (Denecke et al. 2012). In addition, localization experiments in living protoplasts and fixed protoplasts can already lead to differences in signal distribution as shown for EPSIN1 (Song et al. 2006). Again co-localization studies with fluorescence markers in general are limited by the quality and robustness of the marker line itself. For instance, VTI11 as a protein located at TGN and PVC cannot be used to distinguish between those two organelles (Zheng et al. 1999). Aside from that, within different co-localization studies different markers were used to define *post*-Golgi compartments and a direct comparison may not be reliable due to the dynamics and complexity of the system (Richter et al. 2009). In case of EPSIN3, no data was available at all.

In this work, the ENTH protein family in plants was characterized in more detail. We screened single and higher-order mutant plants for phenotypes in order to explore functional redundancies. Strikingly, only two mutant combinations displayed phenotypes deviating from the wild type: the *epsin1 mtv1* double

mutant showed an overall growth reduction and *epsin1 epsin2 epsin3* displayed shorter siliques. We, therefore, examined those mutant combinations more closely.

Furthermore, it has been shown that *MTV1* interacts genetically with *MTV4/NEVERSHED/ARF-GAP5 (MTV4/NEV/AGD5)* which encodes for an ARF GAP (Sauer et al. 2013). MTV4 resides at the TGN and is involved in specific molecular cargo transport required for abscission of floral organs (Liljegren et al. 2009; Sauer et al. 2013). It has been suggested that ARF-GAPs play a role in loading cargo into vesicles and remodelling the actin cytoskeleton by interaction with lipids, coat proteins and cargo receptors (Inoue and Randazzo, 2007). Until now the molecular details of the interaction of ARF GAPs and ENTH proteins in plants remain unclear. The double mutant *mtv1 mtv4* displayed a dwarf phenotype with defects in clathrin-dependent vacuolar transport (Sauer et al. 2013). Interestingly, both single mutants showed no obvious phenotypic deviations from wild type, except the abscission defects of *mtv4*, suggesting functional redundancy with other members of the respective protein families. We addressed this idea by creating double mutants between *mtv4* and mutants defective in all four ENTH domain proteins of *A. thaliana* in this study. To test for potential functional redundancy, we compared growth phenotypes of 28 DAG old plants as well as root length of 9-day-old seedlings. On the one hand, we confirmed the growth reduction phenotype of *mtv1 mtv4*, while on the other hand we discovered that *epsin1 mtv4* displayed a very similar phenotype. Both double mutants had shorter roots and overall growth reduction, however, in case of *epsin1 mtv4* the phenotype was slightly milder and not fully penetrant. In addition to the functional redundancy of EPSIN1 and MTV1 in their cooperation with MTV4, all three are TGN-localized proteins. Of note, we were able to discover differences in their co-localization by high resolution imaging and center-to-center quantification method called DiAna (Gilles et al. 2016). Interestingly, EPSIN1 and MTV4 co-localization was clearly shifted to smaller values compared to MTV1 and MTV4. Taken together *EPSIN1* and *MTV1* interact genetically with *MTV4*. Mutant plants defective of *MTV4* in combination with *EPSIN2* or *EPSIN3* did not display any phenotypic deviations from wild type. EPSIN1, MTV1 and MTV4 localize to the TGN.

4.2 The two plasma membrane-associated ENTH domain proteins EPSIN2 and EPSIN3 in *Arabidopsis thaliana*

In this study, we investigated the subcellular localization of EPSIN2 and EPSIN3 in root epidermal cells by creating stable GFP lines under their endogenous promotors. Both ENTH domain proteins showed the same association with the PM, in addition to cytosolic localization and they accumulated at the growing cell plate. EPSIN2 and EPSIN3 are the only ENTH proteins at the PM in *A. thaliana*, but their additional

cytosolic localization pinpoints towards their soluble nature and a likely transient association with the PM during CCV formation. Similar distributions at the PM of orthologues in animal cells were demonstrated (Chen et al. 1998). To determine the localization at the cell plate in more detail, we crossed the EPSIN2/3-GFP lines with the cell plate-marker line mCherry-RabA1g (Geldner et al. 2009). Interestingly, the overlap of EPSIN2/3-GFP and mCherry-RabA1g at the cell plate was not distinct. The marker mCherry-RabA1g strongly accumulated at the growing margin of the cell plate whereas EPSIN2/3 resided at the middle part of the cell plate.

In order to interpret the localization data, following a brief summary of cytokinesis in plant cells: the newly formed phragmoplast consists of microtubules and actin which marks the division plane where trafficking vesicles get delivered and start to fuse (review Jürgens and Pacher 2003). After several fusion events, a solid disk-shaped membrane enclosed compartment is formed. Due to transformation of microtubules and actin filaments along the lateral margins, new vesicles accumulate at the growing margin of the cell plate. After the cortical division site is reached, the cell plate fuses with the parental membrane. To determine the localization and potential function of EPSIN2 and EPSIN3, it would be necessary to co-localize them with additional cell plate-localized proteins as well as a more detailed analysis of potential (and subtle) cell division defects. For instance, KNOLLE was identified as an essential cytokinesis specific syntaxin in *A. thaliana* (Lukowitz et al. 1996; Lauber et al. 1997). Interestingly, KNOLLE resides at the cell plate center, however, during cell expansion KNOLLE accumulated at the margin (Lauber et al. 1997). Accordingly, co-localization of EPSIN2 and EPSIN3 with KNOLLE at the cell plate in a time-dependent manner would be worthwhile to investigate.

A. thaliana possesses four ENTH domain proteins and in this study, we created all possible higher order mutant plants. We screened the vegetative and reproductive phenotype under controlled conditions. The knockout of only the two PM localized EPSINs resulted in no obvious phenotypic deviation from the wild type. The *epsin2* and *epsin3* single mutants as well as the resulting double mutant showed no drastic growth defects or mis-formed plant organs. Due to the localization of EPSIN2 and EPSIN3 at the PM and the cell plate, we expected a role in endocytosis or cytokinesis. In fact, it has been demonstrated that defects in endocytosis and cytokinesis lead to growth defects. By a corresponding mutant screen of disrupted embryo or seedling body organization of *A. thaliana* the KNOLLE syntaxin and the GNOM guanine-nucleotide exchange factor on ADP-ribosylation factor G protein (ARF GEF) were identified (Mayer et al. 1991). Both factors are linked to the vesicle transport machinery at the cell plate (Lukowitz et al. 1996; Lauber et al. 1997). Thus, our data and the missing phenotype of *epsin2*, *epsin3* and *epsin2*

epsin3 mutants suggests that EPSIN2 and EPSIN3 have a more specific function probably in other developmental stages or other accessory proteins like ANTH proteins can substitute for EPSIN2 and EPSIN3 function (Zouhar and Sauer, 2014). Successful compensation for the loss of ENTH domain proteins by ANTH domain proteins has been demonstrated in yeast (Duncan et al. 2003). The functional redundancy of Ent3p (ENTH domain protein) and Ent5p (ANTH domain protein) had been discovered, nevertheless both were located at the TGN playing a role in *post*-Golgi transport rather than endocytosis at the PM (Duncan et al. 2003; Costaguta et al. 2006).

Unlike the situation in *A. thaliana,* absence of Ent1 and Ent2 activity in yeast cells, where they are the only ENTH domain proteins at the PM, is lethal (Wendland et al. 1999). In addition, it has been shown that hypomorphic Ent1 or Ent2 mutations lead to stalled CCV formation (Skruzny et al. 2012). As reported, mice possess three PM-located epsins and their triple knockout leads to strong impairment of CME which causes drastic cell division defects (Wendland 2002; Ko et al. 2010). CCV formation and vesicle transport was not successful, but some early and U-shaped pits accumulated at the PM (Messa et al. 2014), so clathrin recruitment to the PM per se was not affected. Thus, when comparing the phenotype of loss of EPSINs at the PM in mammalian or yeast cells to plants cells, the CCV formation machinery of plants might appear more robust. A possible explanation is the existence of two independent adaptor complexes which mediate endocytosis at the PM in plants, the AP2 complex and the TPLATE/TSET complex (Van Damme et al. 2006; Park et al. 2013; Hirst et al 2014; Gadeyne et al. 2014). In fact, animals and yeast lack a functional TPLATE/TSET complex which consequently makes endocytosis completely reliant on the AP2 complex with the respective accessory proteins. Contrarily, in plants, a partial functional overlap of AP2 and TPLATE is conceivable and has been suggested, even though the details remain unclear so far (Wang et al. 2016). The function, composition and possible interaction partners of TPLATE in a heterooctameric complex have been discovered within the last years (Van Damme et al. 2011; Hirst et al 2014; Gadeyne et al. 2014; Yperman et al. 2021). By tandem affinity purification (TAP) experiments, the interaction of TASH3, AtEH1, AtEH2, LOLITA, TML, TWD40-1, and TWD40-2 with TPLATE has been elucidated (Gadeyne et al. 2014). Importantly, the two factors AtEH1 and AtEH2 are able to interact with ANTH domain proteins serving as accessory proteins. This suggests that EPSIN2 and EPSIN3, as ENTH domain proteins, are not essential in endocytosis mediated by the TPLATE complex, however, potential interaction of EPSIN2 and EPSIN3 with one or both adaptor complexes remain to be investigated in further analyzes. It is possible that ANTH domain proteins act as the major accessory proteins at the PM. On the other hand, EPSIN2 and EPSIN3 might have developed rather specialized functions at the PM and cell plate only during certain developmental stages, due to less adaptive pressure in plants. A more detailed analysis of *epsin2*, *epsin3*

and the double mutant with regard to endocytic, recycling and cell division phenotypes, perhaps also in the context of non-standard growth conditions, might shed further light on these questions.

4.3. Knockout of three EPSINs leads to a male gametophytic defect resulting in partial sterility

The *epsin1 epsin2 epsin3* triple mutant displays normal overall growth but exhibits less fertilized ovules per silique. We demonstrated by reciprocal crosses that this is a male gametophyte defect. In fact, the fertilization defect is caused by a drastic pollen germination reduction from 72.7% of wild type pollen down to 12.7% of *epsin1 epsin2 epsin3* pollen. The male gametophyte phenotype of the triple mutant was complemented after introduction of either *EPSIN1-GFP, EPSIN2-GFP* or *EPSIN3-GFP* expressed under control of their respective endogenous promotor. This confirmed that the pollen defect was due to loss of function of all three *EPSINs*.

The pollen germination phenotype raises the question, what role the ENTH domain proteins play in pollen germination and pollen tube growth. Pollen tube tip growth is a very fast polarized process which has been extensively studied as a model system (Franklin-Tong 1999; Hepler et al. 2001; Moscatelli and Idilli 2009; Grebnev et al. 2017; Zhao et al. 2020). The unidirectional outgrowth of the pollen tube is based on massive secretion of Golgi-derived as well as TGN-derived vesicles. They transport proteins, lipids, cell wall and cell membrane material to the side of growth. In general, exocytosis/secretion and endocytosis are the major vesicular trafficking routes to achieve this essential transport of material (Richter et al. 2009). At present, two different models of pollen tube tip growth are discussed: 1.) the classical model and 2.) the alternative model. The classical model suggests that exocytosis is focused at the apical tip and endocytosis takes place at the lateral region of the pollen tube. The alternative model differs in terms of the localization of zones where endocytosis and exocytosis occur (Zonia and Munnik 2008; 2009). Here, endocytosis takes place at the lateral and apical regions whereas exocytosis is restricted to the flanks of the apex. Both models coincide that CCVs are involved in material transport, however, there is evidence that clathrin-independent pathways also occur (Moscatelli et al. 2007).

It has been suggested that pollen tube growth oscillates between an active phase (fast growth) and a resting phase (almost arrested growth) (Moscatelli and Idilli 2009; Damineli et al. 2017). In agreement with this oscillation, clathrin and other factors of CME, for instance ANTH domain proteins, showed different distribution at both phases. Accordingly, the two ANTH domain proteins AtAP180/PICALM6 and Epsin-like Clathrin Adaptor 2 (AtECA2/PICALM5a) have been suggested to play important roles in polar growth of pollen tubes with a highly specific expression and localization (Kaneda et al. 2019). The T-DNA knockout mutants *ateca2* and *ap180* displayed normal silique morphology and seed production, however,

the double mutant showed morphological aberrations of pollen tubes (Kaneda et al. 2019). In addition, the pair of ANTH domain proteins AtECA2/PICALM5a and PICALM5b are specifically required for tip-localization and recycling of ANXUR receptor kinases (Muro et al. 2018). Similar to the phenotype of *epsin1 epsin2 epsin3*, the double mutant *picalm5a picalm5b* exhibits normal overall growth but shorter siliques which are caused by fewer fertilized ovules. Notably, in case of *picalm5a picalm5b* pollen tube length and morphology were altered, a phenotype which we have not addressed or quantified in *epsin1 epsin2 epsin3* so far. Very recently, PICALM1a and PICALM1b were identified as adaptor proteins for CME of the secretory vesicle-associated longin-type R-SNARE VESICLE-ASSOCIATED MEMBRANE PROTEIN72 (VAMP72) group (Fujimoto et al. 2020). Altogether, this indicates that ANTH domain proteins play various important roles in CME which is essential for successful fertility in *A. thaliana.* The possible involvement of PM-located ENTH domain proteins remains to be determined.

For numerous plant mutants with impaired trafficking pathways, defects of the male gametophyte have been published. The four adapter complexes AP1, AP2, AP3 and AP4 have been reported to play a role in *A. thaliana* reproduction for a number of very different reasons. Loss of AP1 leads to male lethality due to defective vacuolar dynamics and acidification which causes defective pollen development (Wang et al. 2017; Feng et al. 2017). The *A. thaliana* mutant *ap2m* displayed defects in endocytosis and mis-targeted auxin-efflux carrier PIN FORMED2 (PIN2) in the stamen filaments (Kim et al. 2013). Thus, multiple developmental aspects of male reproductive organs were affected. The functional loss of AP3 leads to reduced male transmission caused by impaired pollen tube growth, however, the pollen development was unaffected (Feng et al. 2018). Last, specifically male fertility was affected in *ap4* mutant plants by reduced pollen tube length (Müdsam et al. 2018). Another example is loss of ECH which leads to a complex male gametophytic phenotype with shorter anthers and defects in cell wall thickness resulting in impaired anther dehiscence (Fan et al. 2014). ECH is a major TGN scaffold protein involved in *post*-Golgi trafficking pathways like secretion of cell wall components (Gendre et al. 2011; Gendre et al. 2013). Furthermore, loss of the TPLATE complex which is an important adaptor for CME causes pollen germination defects (Van Damme et al. 2006). The mutant shows pollen with drastic internal accumulation of callose and the corresponding pollen is unable to germinate (Van Damme et al. 2006). In summary, the male gametophytic phenotype of *epsin1 epsin2 epsin3* matches with the reported phenotype of other factors of CCV formation and vesicle trafficking. Still, the triple mutant has to be investigated in more detail regarding pollen development, pollen germination and pollen tube morphology, to obtain a more mechanistic understanding of EPSIN function during these processes.

In root epidermal cells, EPSIN1 was clearly localized at the TGN and EPSIN2 and EPSIN3 at the PM as well as the growing cell plate. In pollen tube tips, the localization was slightly different. EPSIN1 showed its typical TGN distribution, in contrast, EPSIN2 and EPSIN3 appeared to be more cytosolic rather than PM associated. Notably, EPSIN2-GFP localized to endosomes in pollen tubes. Our data could suggest a tissue-dependent localization of ENTH domain proteins. Due to the oscillation of growth in pollen tubes the localization of EPSIN1, EPSIN2 and EPSIN3 should be re-investigated by live cell imaging in a time-dependent manner with CLC or other marker proteins in order to compare the exact localization.

To gain quantitative insight into the expression of ENTH domain protein transcripts, we performed qPCR on cDNA from flowers, cotyledons and roots. *EPSIN1* and *MTV1* were highest abundant in all tissues, least expressed was *EPSIN3*. Interestingly, only *EPSIN3* transcript level changed between the different tissues. When compared to roots and cotyledons, *EPSIN3* transcript was 10-fold higher abundant in floral tissues. According to this data, EPSIN3 could be a specific player in flowers. Taken together, the role of *EPSIN1* and the functional overlap with *EPSIN2* and *EPSIN3* in pollen germination and pollen tube growth remains unclear. It is possible that the phenotype of the triple mutant is only an additive result of independent events which cannot be compensated to sufficient levels by putative buffering mechanisms anymore.

4.4 EPSIN1 and MTV1 are key accessory proteins in vacuolar and secretory transport rather than endocytosis

We identified EPSIN1 and MTV1 as TGN-located proteins with overlapping functions in *post*-Golgi vesicle transport. Double knockout of both ENTH proteins in *A. thaliana* led to a drastic overall growth reduction with eight times smaller rosettes compared to wild type plants. Moreover, the root length as well as root meristem size was significantly reduced. The dwarf phenotype of *epsin1 mtv1* was fully complemented by *pEPSIN1::EPSIN1-GFP* and *pMTV1::MTV1-GFP* and thus, the growth phenotype was caused by loss of EPSIN1 and MTV1. TGN function as well as morphology and TGN trafficking pathways are essential for plant development (Uemura 2016). Thus, mutant plants with altered TGN morphology and/or defects in TGN transport pathways often show growth reduction similar to the *epsin1 mtv1* double mutant. There is published precedence to support this idea; the TGN localized membrane protein CONTINUOUS VASCULAR RING (COV1) is involved in vacuolar trafficking as well as TGN morphology and its deficiency leads to drastic overall growth reduction, however the molecular function has to be investigated (Shirakawa et al. 2014). The adaptor complexes serve as a bridge between clathrin and the membrane lipids which is crucial for CCV formation. Loss of functional AP1 leads to cell division defects and consequently to arrested plant growth with aberrant plant organ architecture (Park et al. 2013). Plants lacking a functional AP4 complex,

exhibited abnormal development and a dwarfed phenotype (Fuji et al. 2016). In short, the growth phenotype caused by loss of EPSIN1 and MTV1 which are two ENTH domain proteins involved in CCV formation, is consistent with published data on mutant phenotype of *ap1* and *ap4*.

We addressed *post*-Golgi trafficking defects in *epsin1 mtv1* with endogenous and transgenic marker by different experimental designs. Importantly, loss of both TGN-located ENTH proteins leads to strong synergistic effects with drastic defects in vacuolar transport and secretion in *A. thaliana*. For instance, in *epsin1 mtv1* almost 90% of the vacuolar marker (secN-R_m-2A-GH) was mis-localized to the apoplast in cotyledons. In summary, *mtv1* single mutant showed a higher impact on vacuolar transport than *epsin1*. This is in line with previous data on *mtv1* involvement in vacuolar transport (Sauer et al. 2013). Notably, it has been demonstrated that MTV1 is expressed in developing as well as mature embryos and this was linked to transport of proteins to protein storage vacuoles (PSVs). We confirmed these findings with our data. In case of EPSIN1, only a weak allele *epsin1* (SALK_049204) had been analysed, so far (Song et al. 2006). Nevertheless, it has been shown that the marker sporamin:green fluorescent protein (Spo:GFP) was not correctly transported to the vacuole which leads the assumption that EPSIN1 is involved in vacuolar transport. Recently, the expression of EPSIN1 and MTV1 in *A. thaliana* at different stages of seed maturation was compared. Interestingly, MTV1 and a 12S Globulin encoding gene CRB (AT1G03880) were highly co-expressed (Heinze et al. 2020). The different expression levels of EPSIN1 and MTV1 in seed maturation could explain the higher impact of MTV1 on vacuolar trafficking in PSVs.

In addition to the impaired transport to the vacuole, we discovered altered vacuolar morphology of lytic as well as storage vacuoles in *epsin1 mtv1*. This vacuolar morphology phenotype could be caused by either impaired transport of vacuolar proteins or by inefficient vacuolar membrane fusion. In the literature the vacuolar SNARE complex, which contains VTI11, SYNTAXIN OF PLANTS22 (SYP22), SYP51 and VAMP727, has been demonstrated to be crucial for vacuolar biogenesis and vacuolar transport (Ebine et al. 2008; Zheng et al. 2014). Loss of VTI11 resulted in the same rounded PSVs as we observed in *epsin1 mtv1* embryos. Furthermore, the SYP4 group (SYP41, SYP42 and SYP43) have been studied in more detail in *A. thaliana* (Uemura et al. 2012). Members of this group are TGN-resident SNAREs which play a role in secretory and vacuolar transport pathways as well as in Golgi morphology. Single mutants, *syp41 syp42* and *syp41 syp43* double mutants showed no obvious phenotypic deviations from wild type which suggest functional redundancy. In case of the double mutant *syp42 syp43*, plants were dwarfs with short roots and undergoing early senescence. Mounting evidence suggests that ENTH domain proteins interact with SNARE proteins presumably in the process of CCV formation (Chidambaram et al. 2004; Miller et al. 2007;

Wang et al. 2011). The specific interaction of mammalian EpsinR with Vti1b as well as yeast Ent3p with Vti1p has been proven (Hirst et al. 2004; Chidambaram et al. 2004). Moreover, the interaction of EPSIN1 with AtVTI11 and EPSIN2/EpsinR2 with AtVTI12 in *A. thaliana* has been shown (Song et al. 2006; Lee et al. 2007). In light of the dwarf phenotype as well as aberrant PSVs of *epsin1 mtv1*, the lack of ENTH-SNARE interaction could partially cause the downstream defects. Thus, the correct localization of SNARE proteins like VTI11, SYP22, SYP51, VAMP727 and SYP4 group should be addressed in *epsin1 mtv1* double mutant in order to see whether the phenotype may be a result from mis-targeted SNARE proteins.

At present the TGN has been associated with the secretory pathway, the endocytic pathway, the recycling pathway and the vacuolar transport pathway (Inada and Ueda 2014; Uemura 2016). Notably, a special feature of plant TGN is that it serves as an early endosome (Dettmer et al. 2006). Thus, some PM components are first transported to the TGN and subsequently recycled back to the PM or further transported to the vacuole. Recently, EPSIN1 was identified as a modulator of plant immunity by modulating the abundance of PM-located receptors like FLAGELLIN SENSING2 (FLS2) and BRASSINOSTEROID INSENSITIVE1-ASSOCIATED KINASE1 (BAK1) (Collins et al. 2020). However, the transport of FLS2 was only reduced in an *epsin1* mutant rather than completely abolished. Thus, EPSIN1 is not essential in this pathway. It would be worthwhile to analyze *epsin1 mtv1* double mutant in terms of plant immunity defects. Probably, there would be a synergistic effect as we have seen in vacuolar and secretion pathways. Still this very recent study gave a new hint for the involvement of EPSIN1 in trafficking routes to the PM (Collins et al. 2020).

To further corroborate the possible molecular function of EPSIN1 and MTV1 in endocytic as well as recycling pathways, we performed FM4-64 uptake experiments and PIN2-GFP trafficking experiments. After 5 min of incubation of *epsin1 mtv1* as well as Col-0 seedlings with FM4-64, we observed the fluorescence and quantified its intensity. There was virtually no difference between mutant and wild type, indicating that EPSIN1 and MTV1 do not play important roles in endocytosis. To confirm this consideration, we used PIN2-GFP which constantly recycles between TGN and PM and has been established as a marker for endocytosis and recycling pathways (Kleine-Vehn et al. 2008; Men et al. 2008). The polar distribution of PIN2-GFP in root epidermal cells of *epsin1 mtv1* was intact and along with it the signal intensity was the same as measured for wild type roots. We assumed that endocytosis and recycling are not affected, however, we treated seedlings with the toxin brefeldin A (BFA) in order to inhibit the recycling process and this leads to accumulation of endocytosed material in so called BFA bodies (Geldner et al. 2001). This experimental design has been used previously to distinguish between endocytosis and recycling more

precisely (Men et al. 2008; Kitakura et al. 2011). After counting the number of BFA bodies per cell as a quantification method, we found no difference which underpins the assumption that EPSIN1 and MTV1 are not essential players in CME. Of note, the intensity distribution of PIN2-GFP at the PM after washing out BFA was nearly completely recovered with only a minor difference to wild type. In order to block *de novo* synthesis this last step of the PIN2-GFP experiment was performed under presence of the translation inhibitor CHX. In short, although there are first data on EPSIN1 involvement in receptor transport to the PM (Collins et al. 2020), in our hands EPSIN1 and MTV1 do not significantly contribute to endocytosis and recycling.

Prior to this study, neither EPSIN1 nor MTV1 were linked to the secretory pathway which branches off at the TGN and involves factors like SYP42/SYP43, ECH/YIP4A/B and SYP61 (Kim et al. 2016; Sinclair et al. 2018). 20 years ago, the differentiation of specialized cells of the seed coat of *A. thaliana* was analyzed (Western et al. 2000). The group discovered the mucilage secretory cells and implicated them as a model system to study biosynthesis and secretion of complex polysaccharide. Moreover, by transmission electron micrographs these authors observed that developing epidermal cells of wild type seeds were fully packed with vesicles with grainy content which proved to result from the massive secretion of pectic polysaccharides (Western et al. 2000; Young et al. 2008; McFarlane et al. 2013). Indeed, staining of mucilage layer of seeds by ruthenium red has become a common approach to address secretion defects in *A. thaliana* (Western et al. 2001; Gendre et al. 2013; Francoz et al. 2015; Shimada et al. 2018). In terms of EPSIN1 and MTV1, we found a clear synergistic effect on secretion of mucilage components. Already the single mutants showed 15-25% reduced mucilage layer thickness which was enhanced in the double mutant (down to 50%). In contrast, general bulk flow of the transgenic marker secRFP was not affected in *epsin1 mtv1*. We cannot rule out decreased biosynthesis rather than secretion defects causing reduced mucilage layer thickness. However, importantly, a similar phenotype has been shown for other mutants with a role in vesicle transport. The loss of ADAPTOR COMPLEX 1 (AP1), which is located at TGN and involved in post-Golgi trafficking pathways, leads to reduced mucilage layer thickness (Shimada et al. 2018).

In order to analyze root architecture and to measure root meristem size we fixed, cleared and stained 5-day-old seedlings with Calcofluor White (Ursache et al. 2018). This dye is an established marker for cell walls, however, it stains rather unspecific the β-glucan structures. Thus, all three major polysaccharide classes of cell wall components are stained with Calcofluor White (Sauter et al. 1993; Anderson et al. 2010). Importantly, in *epsin1 mtv1* roots we detected Calcofluor White fluorescence signal inside the cells

especially the quiescent center cells. None of the wild type roots ever showed internal signal. Currently, we have no explanation for this phenotype but it could be possible that this internal signal monitored secretion defects of *epsin1 mtv1* due to abnormal accumulation of β-glucan structures of polysaccharides.

Surprisingly, but in accordance with the mucilage defects, *epsin1 mtv1* displayed an interesting cell adhesion defect in roots. During microscopic analysis, we discovered that the root epidermal cells were disordered, twisted, with gaps exposing the underlying cell file. This phenotype never appeared in wild type roots and was not fully penetrant in *epsin1 mtv1*. Loss of synthase proteins for proper pectin establishment in the cell wall resulted in similar cell adhesion defects in *A. thaliana*. In the literature, *QUASIMODO1-3 (QUA1-3)*, for instance, had been described in more detail. *QUASIMODO1 (QUA1)* encodes a putative membrane-bound glycosyltransferase (Bouton et al. 2002; Leboeuf et al. 2005). The loss of QUA1 results in less pectin and consequently in cell adhesion defects. The pectin methyltransferase mutant *quasimodo2 (qua2)* showed the same phenotype with cells losing attachment (Du et al. 2020). In case of QUASIMODO3, which is a putative S-adenosyl-L-methionine (SAM)-dependent methyltransferase, a cell adhesion phenotype has not been reported, yet (Miao et al. 2011). The analysis of the *qua* mutant phenotype was done in etiolated hypocotyls and not in roots, hence we cannot compare the phenotype of *epsin1 mtv1* directly. It would be interesting to test cell adhesion defects in *epsin1 mtv1* in direct comparison to *qua* mutants, to create higher order mutants and/or to check the correct localization of QUA1-3 in *epsin1 mtv1* mutant background. Different scenarios could be envisaged; first, QUA1-2 and EPSIN1/MTV1 may act in parallel on pectin synthesis and transport of pectic polysaccharides respectively, and loss of both components may independently lead to cell adhesion defects, second, *epsin1 mtv1* may play a specific role in pectic polysaccharides secretion and knockout of EPSIN1/MTV1 may phenocopy the *qua* mutant phenotype due to impaired transport. The question arises as to whether a triple mutant *epsin1 mtv1 qua1* would show an enhancement of the pectic polysaccharides related cell adhesion phenotype.

To gain further evidence into what role EPSIN1 and MTV1 may play in secretion of cell wall components, most likely pectic polysaccharides, a next step could be to check the polysaccharide composition of the cell wall of *epsin1 mtv1* mutants. This could give a hint towards the cargos contained in EPSIN1 MTV1 vesicles. Moreover, immunostaining with antibodies specifically recognizing different pectin types such as JIM5 and JIM7, that detect homogalacturonan, and LM19, that detects unesterified or sparsely methylated homogalacturonan, may reveal a mis-targeting of pectin within the cell (Voiniciuc et al. 2018).

We conclude that EPSIN1 and MTV1 have overlapping functions and can functionally replace each other to some extent. As the only TGN-located ENTH domain proteins in *A. thaliana* they play a role in the secretory and vacuolar transport pathway, however, there is first evidence that transport of receptors to the PM also involves EPSIN1. Of note, our data indicate that EPSIN1 and MTV1 act in two independent pathways with overlapping cargos. This will be discussed later on in this thesis, since we have evidence that EPSIN1 and MTV1 reside at different TGN subdomains where they interact with AP1 and AP4, respectively.

4.5 EPSIN1 and MTV1 are independent of the *trans*-Golgi network protein ECHIDNA

During the last years ECH has drawn attention as a very interesting factor of the TGN and has been functionally characterized to a good extent (Gendre et al. 2011). ECH forms a complex at the TGN with YPT/RAB GTPase Interacting Protein 4a (YIP4a) and YIP4b/YIP2, which are functional redundant (Gendre et al. 2013; Gendre et al. 2019). Loss of ECH leads to a complex phenotype resulting in a bushy dwarfed plant, which is semisterile with reduced male fertility (Fan et al. 2014). Defects in TGN-mediated secretion of pectin and hemicellulose leads to altered cell wall composition in *ech*. Moreover, altered TGN structure in ECH-defective plant cells has been observed by TEM analysis (Gendre et al. 2011). In line with this, TGN located proteins, particularly VHA-a1 and SYP61 where mis-localized in *yip4a yip4b* mutants (Gendre et al. 2013). In contrast, the TGN localization of RabA2a was unaffected. Gendre and colleagues assumed that ECH/YIP4 define a functional subdomain of the TGN which was believed to be distinct from endocytic and vacuolar trafficking pathway (Gendre et al. 2013). However, very recently it has been shown that ECH contributes to vacuolar transport as well as vacuolar morphology (Ichino et al. 2020). In summary, *ech* single and *yip4a yip4b* double mutants display a complex phenotype with some similarities to *epsin1 mtv1*. The dwarfed phenotype with altered vacuolar morphology and defects in secretory as well as vacuolar transport could hint towards a functional overlap with EPSIN1 and MTV1.

The TGN morphology in *epsin 1 mtv1* was recently monitored by TEM and there was no evidence for any changes (Heinze et al. 2020). To investigate TGN alterations further we observed VHA-a1 and SYP61 localization in *epsin1 mtv1*. Notably, both TGN proteins were mis-localized into vacuolar ring-shaped multilaminar compartments. It has previously been reported that *vha-a1* mutant plants display severe phenotypes since loss of *VHA-A* function leads to altered Golgi structure in pollen resulting in a male gametophytic defect (Dettmer et al. 2005; Brüx et al. 2008). In fact, V-ATPase mutants like *det3* show a dwarf phenotype which is caused by a reduction of cell expansion (Schumacher et al. 1999). Thus, *ech* as well as *epsin1 mtv1* phenocopy partially the mutant phenotype of overall growth reduction.

Mis-localization of SYP61 in *epsin1 mtv1* could partially explain the secretion phenotype because it has been shown that SYP61 vesicles are involved in secretion by proteomic analysis (Drakakaki et al. 2012, Wilkop et al. 2019). SYP61 vesicles were isolated, their glycome profile was measured and diverse glycans like pectin, xyloglucan and arabinogalactan were detected. Moreover, a weak *syp61* mutant (also called *osm1*) has been described to display no phenotypic deviations under control conditions, however *syp61/osm1* is hypersensitive for ionic and non-ionic stress (Zhu et al. 2002). Metabolic labeling data showed that *syp61/osm1* has altered cell wall composition with a reduction of pectin and arabinogalactan content (Wilkop et al. 2019). This strongly suggests a role for SYP61 in secretion of cell wall components from the TGN. The mis-localization of SYP61 in *epsin1 mtv1* could lead to the same secretion phenotype. It would be interesting to address the co-localization of SYP61 with EPSIN1 and MTV1 including quantification by DiAna analysis. Probably one could define the TGN subdomain with SYP61, ECH and YIP4 additionally with EPSIN1 or MTV1 (Sinclair et al. 2018). Furthermore, a potential interaction of SYP61 (SNARE protein) with an ENTH protein could be investigated by creating knockout mutant plants or *in vitro*/*in vivo* interaction studies (interaction of ENTH proteins and SNAREs was discussed above).

Nevertheless, loss of EPSIN1 and MTV1 could lead to mis-localization of ECH and/or YIP4 which would explain the similarities to *ech* and *yip4* phenotype to that of *epsin1 mtv1*. We investigated this hypothesis by immunolocalization experiments of ECH in *epsin1 mtv1* and Col-0 roots. However, ECH localization displayed a punctate pattern indistinguishable from wild type in *epsin1 mtv1*, indicating that EPSIN1 and MTV1 are not required for TGN morphology and structure. Furthermore, we showed that EPSIN1 and MTV1 are normally distributed in *ech* by immunolocalization with specific anti-EPSIN1 and anti-MTV1 antibodies. The data suggested that, although *ech* and *yip4* mutants showed altered TGN morphology, EPSIN1 and MTV1 localization, and therefore likely also their function, stayed intact. In order to investigate possible functional subdomains at the TGN marked by ECH, YIP4, EPSIN1 and MTV1 *in planta* future co-localization studies with DiAna quantification would be helpful.

Taken together, the phenotype of *epsin1 mtv1* double mutant is not caused by TGN disruption and/or mis-localization of ECH or YIP4. In fact, it would be worthwhile to create an *epsin1 mtv1 ech or epsin1 mtv1 yip4* triple mutant to address interaction of those factors. It may be possible that a triple mutant is embryo lethal due to the fact that several probably independent *post*-Golgi trafficking pathways would be disrupted.

4.6 EPSIN1 and MTV1 are defining molecularly distinct *trans*-Golgi network subdomains via interaction with different AP complexes

We demonstrated major functional overlap between EPSIN1 and MTV1, however, we gained evidence that they reside at different subdomains of the TGN. By high-resolution imaging and powerful quantification of co-localization data, we revealed that EPSIN1 and MTV1 define two different TGN subdomains, one of them is occupied by EPSIN1 and MTV4 the other is characterized by MTV1 and VHA-a1 localization. The potential existence of TGN subdomains and/or subsets marked with specific molecular makeups has found more support within the last years (Sanderfoot et al. 2001; Drakakaki et al. 2012; Uemura et al. 2014; Renna et al. 2018; Müdsam et al. 2018). For example, two SNARE proteins, the SYP41 and SYP42 syntaxins have been localized at distinct domains of the TGN by immunogold EM and the authors hypothesized that this suggests different function for the two syntaxins in vesicle trafficking (Bassham et al. 2000; Uemura et al. 2012).

In plants the adaptor complexes 1, 3 and 4 have been located at the TGN, however, they contribute to vacuolar transport, secretion and recycling to a different extent (Robinson 2004). So far, comparative co-localization studies of all three TGN-located AP complexes have not been performed. Recently, the four AP β subunits were tested for interaction with EPSIN1 and MTV1 by an Y2H screen. Interestingly, MTV1 was linked to AP4 but EPSIN1 displayed clear interaction with AP1 as well as AP2 and slightly with AP4 (Heinze et al. 2020). The interaction of AP1 and AP2 is not distinguishable in this Y2H experiment, because AP1 and AP2 can share their β-subunit and associate into heterologous complexes (Boehm and Bonifacino 2001; Dacks et al. 2008). In accordance with this postulated interaction of EPSIN1 and MTV1 with AP1 and AP4 respectively, we demonstrated by quantitative co-localization studies that MTV1 was significantly closer located to AP4 compared to EPSIN1 with AP4. Moreover, we determined a smaller distance between EPSIN1 and AP1 when compared to AP1 with MTV1. We localized EPSIN1 to the TGN and demonstrated strong overlap with AP1; therefore, the interaction with the PM-localized AP2 seems unlikely. Direct interaction of AP and ENTH proteins in plants has been implicated for EPSIN1 and AP1 as well as EPSIN2 with AP3 and/or AP2 (Song et al. 2006; Lee et al. 2007). Neither EPSIN1 nor MTV1 showed significant interaction with AP3 in the recently published Y2H experiment, although AP3 resides at the TGN also (Heinze et al. 2020). In *A. thaliana* the functional role of AP3 has not been fully uncovered until now. Although AP3 has been found to localize to the TGN and to endosomes, few interaction partners have been described, except for a heterotrimeric G-protein which modulates hormonal and stress responses (Kansup et al. 2013). This suggest that EPSIN1 and MTV1 act independently of AP3, but detailed co-localization studies and/or *in planta* interaction approaches would still be interesting.

In mammalian cells, the specific interaction of AP4 with Tepsin, the closest ortholog of MTV1, has been shown by a multivariate proteomics approach of CCVs. Notably, AP4 interacted exclusively with Tepsin as an ENTH domain protein (Borner et al. 2012; Mattera et al. 2015). This is similar to the situation observed in plants, where MTV1 interacts preferentially with AP4 (Heinze et al. 2020). To investigate the link between EPSIN1, MTV1 and AP4 in *A. thaliana* we created double mutant plants of *epsin1* as well as *mtv1* with loss of *AP4* mutant plants. The *ap4* mutant plants have recently been reported to display an overall growth reduction as well as a short root phenotype (Fuji et al. 2016; Müdsam et al. 2018). Indeed, in our hands *ap4* and *mtv1* single mutants were smaller compared to wild type and *epsin1*. Importantly, simultaneous knockout of AP4 and MTV1 did not cause additional effects. The double mutant *epsin1 mtv1* showed overall growth reduction and interestingly *epsin1 ap4* displayed a similar dwarf phenotype. This means that loss of AP4 has a similar functional outcome to loss of MTV1. Thus, we conclude that AP4 and MTV1 act in the same functional pathway.

In *A. thaliana* complete loss of *AP1* function is embryo-lethal and partial loss of *AP1* leads to drastic developmental phenotypes and defects in *post*-Golgi transport like secretion and vacuolar transport (Boehm and Bonifacino 2001; Park et al. 2013; Teh et al. 2013; Shimada et al. 2018). In contrast, the *epsin1* single mutant does hardly display any phenotypic deviations from wild type, which may indicate that EPSIN1 is a more specific player for a subset of cargo. Therefore, we assumed that AP1 acts rather independently of EPSIN1 probably with other accessory proteins. To find out more about the interaction of ENTH domain proteins and AP1, one could generate double knockout mutant plants. In case of *AP1*, an inducible promotor would be one way to overcome the embryo lethality or one could work with weak alleles. The hypothesis of AP1 and AP4 acting in overlapping but independent pathways at the TGN in plants has been previously been put forward (Müdsam et al. 2018). The group discovered similarities between both loss of function mutants. Furthermore, in mammalian cells cross-regulation of AP1 vesicles and AP4 vesicles has been implicated by a knocksideway approach (Robinson et al. 2010; Hirst et al. 2012).

In summary, our data suggest that EPSIN1 and MTV1 define two molecular distinct pathways with functional overlap in secretion and vacuolar transport. MTV1 and AP4 are indispensable players independent of EPSIN1 which is presumably AP1-dependent.

4.7 Recruitment of ENTH proteins to donor membranes and connection to the cytoskeleton

In plants, the TGN serves as the major sorting hub for various trafficking pathways: endocytosis, vacuolar transport, secretion and recycling (reviewed Uemura 2016; LaMontagne and Heese 2017). In fact, there are several trafficking routes in parallel in order to guarantee robustness of the complex machinery,

however, it is not clear how specificity is ensured. The RAB GTPases family and the SNARE proteins, for instance, were discussed as membrane identity factors (Uemura et al. 2004; Park and Jürgens 2012; Zhen and Stenmark 2015; Rosquete et al. 2018). By sequence analysis combined with transient expression assays SNARE families in *A. thaliana* have been investigated (Uemura et al. 2004; Sanderfoot 2007). In those families some proteins reside at one specific endomembrane compartment whereas others appear to shuttle between two or more organelles. Moreover, it has been shown that some SNAREs are expressed in a specific tissue or at certain developmental stages which indicates a tightly controlled machinery (Park and Jürgens 2012). The KNOLLE/SYP111 syntaxin is one prominent example which is expressed during cell division only and, aside from the TGN, specifically located at the cell plate (Lauber et al. 1997). In addition, the SYP1 family in *A. thaliana* contains among other the SYP124, SYP125 and SYP131 proteins which act exclusively in pollen (Enami et al. 2009). The specific distribution of SNAREs in plant cells could be one way to mark certain kind of membranes and recruit specific adaptors and/or accessory proteins from the CCV formation machinery. As mentioned earlier, the interaction of SNARE proteins with ENTH domain proteins was discovered in mammalian, yeast and plants cells.

There is another hypothesis how membrane identity is established, based on the specific distribution of PIs which can be reversibly phosphorylated by PI kinases (PIKs) and dephosphorylated by PI phosphatases (Vicinanza et al. 2008; D'Angelo et al. 2012). Structural analyses by X-ray crystallography have shown that AP2 and different ENTH as well as ANTH domain proteins can interact directly with PtdIns(4,5)P_2 in mammalian cells (Gaidarov et al. 1996; Ford et al. 2001; Collins et al. 2002). PtdIns(4,5)P2 is mostly generated at the inner leaflet of the PM and is essential for recruitment of the coat machinery (Robinson 2004). In contrast, PtdIns(4)P is preferentially found at the TGN and mammalian EpsinR as well as the AP1 complex interact with PtdIns(4)P (Wasiak et al. 2002; Hirst et al. 2003; Mills et al. 2003; Wang et al. 2003). In addition, yeast Ent3 binds to PtdIns(3,5)P2 which is usually at the membrane of MVBs (Friant et al. 2003). Those data were mostly generated by *in vitro* protein-lipid overlay assays. Currently, the situation in plant cells is not clear. It has been suggested that EPSIN2 (named EpsinR2) binds to PtdIns(3)P and EPSIN1 did not bind any PIs in these kind of assays (Lee et al. 2007). The idea of PI-dependent recruitment of the CCV machinery seems attractive, however, it cannot fully explain the specificity, due to the fact that AP complexes are even more restricted than PIs (Vicinanza et al. 2008). Of note, the phylogenetic outsider Tepsin, the ortholog of plant MTV1, has been investigated by X-ray crystal structures analysis and unexpectedly the ENTH domain of mammalian Tepsin lacks the lipid-binding pocket which has been identified in EPSIN1, for example (Archuleta et al. 2017).

In contrast to the hypothesis postulating membrane identity to be conferred by specific PIs, the ENTH domain protein Tepsin in mammalian cell is recruited by AP4 complex interaction (Borner et al. 2012; Mattera et al. 2015). Therefore, another possible scenario would be that the distribution of AP complexes at different compartments of the endomembrane system could also serve as a membrane identity and recruiting factor for accessory proteins like ENTH domain proteins (Vicinanza et al. 2008; Tan et al. 2019). As discussed before, we have recently established interaction between plant MTV1 and AP4 (Heinze et al. 2020). Thus, we addressed the dependency of AP4 and MTV1 in *A. thaliana* by localization studies of *pMTV1::MTV1-GFP* in loss of *AP4 β* mutant (*ap4b)*. The punctate distribution of EPSIN1-mRuby3 was unchanged in *ap4* mutant, in contrast, MTV1-GFP was almost completely cytosolic rather than TGN-associated. Our results demonstrate that correct localization of MTV1 at the TGN depends on AP4. In contrast, EPSIN1 localization was independent of AP4. The next step should be to investigate AP4 localization in *mtv1* mutant background as well as investigation of a potential dependency of EPSIN1 on AP1.

The coat protein clathrin itself neither binds to the membrane nor to the actin cytoskeleton. Consequently, many accessory proteins are needed in order to perform the different steps of vesicle formation: invagination of the membrane, formation of clathrin-coated pits and finally scission and detachment of the newly formed vesicle. The molecular connection between the actin cytoskeleton and clathrin has been investigated extensively in mammalian cells and yeast cells within the last 25 years (Qualmann and Kessels 2002; Gottfried et al. 2010; Kaksonen and Roux 2018). The mammalian Huntingtin-interacting protein 1 (HIP1) and Huntingtin-interacting protein 1-related protein (HIP1R) were the first components that provided a molecular link between F-actin, clathrin-coated pits and adaptor complex (DiFiglia et al. 1995; Gutekunst et al. 1995; Seki et al. 1998; Waelter et al. 2001; Legendre-Guillemin et al. 2002). The yeast HIP1-homologues Sla2p protein exhibits the same actin-binding and its involvement in endocytosis was proven (McCann et al. 1997). Importantly, the interaction of ANTH as well as ENTH domain proteins with actin was demonstrated (Skruzny et al. 2012). For instance, yeast epsin Ent1p directly interacts with actin (Skruzny et al. 2012). The same holds true for mammalian Epsin1 and actin (Messa et al. 2014). In *Dictyostelium* epsin (ENTH domain protein) interacts with Hip1r to regulate actin dynamics at clathrin-coated pits (Repass et al. 2007; Brady et al. 2010). Taken together, there is strong evidence that the actin cytoskeleton is involved in vesicle formation and/or scission which is a conserved molecular model in mammals, yeast and ameba. However, endocytosis is not dependent on actin-binding. Likewise, in plants first data on actin-binding by ENTH domain proteins have been published. In *A. thaliana,* the localization of EPSIN1 may be dependent on actin because EPSIN 1 distribution was changed

by treatment with the actin-depolymerizing drug Latrunculin B (Song et al. 2006). In order to investigate this topic in plants it would be interesting to perform co-localization studies, including drug treatment, of actin marker combined with ENTH domain proteins. However, this has to be investigated in further studies.

5. Outlook

The results obtained during this project provide a more comprehensive characterization of ENTH domain proteins in *A. thaliana*. Interestingly, the function of EPSIN2 and EPSIN3, as the only PM-associated ENTH domain proteins, seems to be different from what has been shown for animal and yeast cells. Thus, we provide a starting point for further analysis of functional overlap of ENTH domain proteins with putative ANTH domain proteins. The TGN-located EPSIN1 and MTV1 interact genetically and define a molecularly distinct pathway with largely overlapping function. We demonstrated that EPSIN1 and MTV1 define two subdomains of the plant TGN which also provides both as marker proteins for two molecularly different pathways branching at the TGN for future studies. Moreover, this thesis presents a direct functional link between AP complexes and their accessory proteins, providing one more piece towards solving the complex puzzle of plant TGN function.

6. Literature

Abas, L., Benjamins, R., Malenica, N., Paciorek, T., Wiśniewska, J., Moulinier-Anzola, J. C., Sieberer, T., Friml, J., and Luschnig, C. (2006). Intracellular trafficking and proteolysis of the Arabidopsis auxin-efflux facilitator PIN2 are involved in root gravitropism. Nat. Cell Biol., 8, 3, 249–256.

Abou Jamra, R., Philippe, O., Raas-Rot hschild, A., Eck, S.H., Graf, E., Buchert, R., Borck, G., Ekici, A., Brockschmidt, F.F., Nöthen, M.M., Munnich, A., Strom, T.M., Reis, A. and Colleaux, L. (2011). Adaptor protein complex 4 deficiency causes severe autosomal-recessive intellectual disability, progressive spastic paraplegia, shy character, and short stature. Am. J. Hum. Genet., 88, 6, 788-795.

Ahmed, S. U., Bar-Peled, M. and Raikhel, N. V. (1997). Cloning and Subcellular Location of an Arabidopsis Receptor-Like Protein That Shares Common Features with Protein-Sorting Receptors of Eukaryotic Cells. Plant Physiol., 114, 1, 325-336.

Anderson, C.T., Carroll, A., Akhmetova, L. and Somerville, C. (2010). Real-time imaging of cellulose reorientation during cell wall expansion in Arabidopsis roots. Plant physiol., 152, 2, 787–796.

Archuleta, T.L., Frazier, M.N., Monken, A.E., Kendall, A.K., Harp, J., McCoy, A.J., Creanza, N. and Jackson, L.P. (2017). Structure and evolution of ENTH and VHS/ENTH-like domains in tepsin. Traffic, 18, 590–603.

Barlowe, C. (1998). COPII and selective export from the endoplasmic reticulum. Biochim. Biophys. Acta., 1404, 1-2, 67-76.

Barlowe, C., Orci, L., Yeung, T., Hosobuchi, M., Hamamoto, S., Salama, N., Rexach, M.F., Ravazzola, M., Amherdt, M. and Schekman, R. (1994). COPII: A membrane coat formed by Sec proteins that drive vesicle budding from the endoplasmic reticulum. Cell, 77, 895–907.

Bashline, L., Li, S., Anderson, C. T., Lei, L., and Gu, Y. (2013). The endocytosis of cellulose synthase in Arabidopsis is dependent on μ2, a clathrin-mediated endocytosis adaptin. Plant physiol., 163, 1, 150–160.

Bassham, D. C., Sanderfoot, A. A., Kovaleva, V., Zheng, H. and Raikhel, N. V. (2000). AtVPS45 complex formation at the trans-Golgi network. Mol. Boil. Cell, 11, 7, 2251–2265.

Bednarek, S.Y., Ravazzola, M., Hosobuchi, M., Amherdt, M., Perrelet, A., Schekman, R. and Orci, L. (1995). COPI- and COPII-coated vesicles bud directly from the endoplasmic reticulum in yeast. Cell, 83, 1183–1196.

Boehm, M. and Bonifacino, J.S. (2001). Adaptins: the final recount. Mol. Biol. Cell, 12, 10, 2907-2920.

Bolte, S., Talbot, C., Boutte, Y., Catrice, O., Read, N. D., & Satiat-Jeunemaitre, B. (2004). FM-dyes as experimental probes for dissecting vesicle trafficking in living plant cells. J Microsc , *214*(Pt 2), 159–173.

Boman, A.L. (2001). GGA proteins: new players in the sorting game. J. Cell Sci., 114, 19, 3413-3418.

Bonifacino, J. S., and Dell'Angelica, E. C. (1999). Molecular bases for the recognition of tyrosine-based sorting signals. J. Cell Biol., 145, 5, 923–926.

Bonifacino, J.S. and Lippincott-Schwartz, J. (2003). Coat proteins: shaping membrane transport. Nat. Rev. Mol. Cell Biol., 4, 409–414.

Borner, G.H., Antrobus, R., Hirst, J., Bhumbra, G.S., Kozik, P., Jackson, L.P., Sahlender, D.A. and Robinson, M.S. (2012). Multivariate proteomic profiling identifies novel accessory proteins of coated vesicles. J. Cell Biol., 197, 1, 141-160.

Boucrot, E., Pick, A., Çamdere, G., Liska, N., Evergren, E., McMahon, H.T. and Kozlov, M.M. (2012). Membrane Fission Is Promoted by Insertion of Amphipathic Helices and Is Restricted by Crescent BAR Domains. Cell, 149, 124–136.

Bouton, S., Leboeuf, E., Mouille, G., Leydecker, M., Talbotec, J., Granier, F., Lahaye, M., Höfte, H., Truong, H. (2002). QUASIMODO1 Encodes a Putative Membrane-Bound Glycosyltransferase Required for Normal Pectin Synthesis and Cell Adhesion in Arabidopsis. Plant Cell, 14, 10, 2577-2590.

Boutté, Y. and Grebe, M. (2014). Immunocytochemical fluorescent in situ visualization of proteins in Arabidopsis. Methods Mol Biol., 1062, 453–472.

Brady, R.J., Damer, C.K., Heuser, J.E. and O'Halloran, T.J. (2010). Regulation of Hip1r by epsin controls the temporal and spatial coupling of actin filaments to clathrin-coated pits. J. Cell Sci., 123, 21, 3652–3661.

Brodsky, F.M., Chen, C.-Y., Knuehl, C., Towler, M.C. and Wakeham, D.E. (2001). Biological Basket Weaving: Formation and Function of Clathrin-Coated Vesicles. Annu. Rev. Cell Dev. Biol., 17, 517–568.

Brüx, A., Liu, T.Y., Krebs, M., Stierhof, Y.D., Lohmann, J.U., Miersch, O., Wasternack, C. and Schumacher, K. (2008). Reduced V-ATPase activity in the trans-Golgi network causes oxylipin-dependent hypocotyl growth Inhibition in Arabidopsis. Plant Cell, 20, 4, 1088–1100.

Burgos, P.V., Mardones, G.A., Rojas, A.L., daSilva, L.L.P., Prabhu, Y., Hurley, J.H. and Bonifacino, J.S. (2010). Sorting of the Alzheimer's Disease Amyloid Precursor Protein Mediated by the AP-4 Complex. Dev. Cell, 18, 425–436.

Chen, H., Fre, S., Slepnev, V.I., Capua, M.R., Takei, K., Butler, M.H., Di Fiore, P.P. and De Camilli, P. (1998). Epsin is an EH-domain-binding protein implicated in clathrin-mediated endocytosis. Nature, 394, 6695, 793-797.

Chidambaram, S., Müllers, N., Wiederhold, K., Haucke, V. and von Mollard, G.F. (2004). Specific interaction between SNAREs and epsin N-terminal homology (ENTH) domains of epsin-related proteins in trans-Golgi network to endosome transport. J Biol. Chem., 279, 6, 4175–4179.

Clough, S. J., and Bent, A. F. (1998). Floral dip: a simplified method for Agrobacterium-mediated transformation of Arabidopsis thaliana. Plant J., 16, 6, 735–743.

Collins, B.M., McCoy, A.J., Kent, H.M., Evans, P.R. and Owen, D.J. (2002). Molecular architecture and functional model of the endocytic AP2 complex. Cell, 109, 4, 523–535.

Collins, C.A., LaMontagne, E.D., Anderson, J.C., Ekanayake, G., Clarke, A.S., Bond, L.N., Salamango, D.J., Cornish, P.V., Peck, S.C. and Heese, A. (2020). EPSIN1 Modulates the Plasma Membrane Abundance of FLAGELLIN SENSING2 for Effective Immune Responses. Plant Physiol., 182, 4, 1762-1775.

Costaguta, G., Duncan, M.C., Fernández, G.E., Huang, G.H. and Payne, G.S. (2006). Distinct Roles for TGN/Endosome Epsin-like Adaptors Ent3p and Ent5p. Mol. Biol. Cell, 17, 3907–3920.

Cowles, C.R., Odorizzi, G., Payne, G.S. and Emr, S.D. (1997). The AP-3 adaptor complex is essential for cargo-selective transport to the yeast vacuole. Cell, 91, 1, 109-118.

Dacks, J.B., Poon, P.P. and Field, M.C. (2008). Phylogeny of endocytic components yields insight into the process of nonendosymbiotic organelle evolution. Proc. Natl. Acad. Sci USA, 105, 588–593.

Damineli, D.S.C., Portes, M.T. and Feijo, J.A. (2017). Oscillatory signatures underlie growth regimes in Arabidopsis pollen tubes: computational methods to estimate tip location, periodicity, and synchronization in growing cells. J. Exp. Bot., 68, 3267–3281.

D'Angelo, G., Vicinanza, M., Wilson, C. and De Matteis, M.A. (2012). Phosphoinositides in Golgi complex function. Subcell. Biochem., 59, 255–270.

De Camilli, P.D., Chen, H., Hyman, J., Panepucci, E., Bateman, A. and Brunger, A.T. (2002). The ENTH domain. FEBS Letters, 513, 11–18.

Dell'Angelica, E.C., Klumperman, J., Stoorvogel, W. and Bonifacino, J.S. (1998). Association of the AP-3 Adaptor Complex with Clathrin. Science, 280, 431–434.

Dell'Angelica, E.C., Mullins, C. and Bonifacino, J.S. (1999b). AP-4, a Novel Protein Complex Related to Clathrin Adaptors. J. Biol. Chem., 274, 7278–7285.

Dell'Angelica, E.C., Shotelersuk, V., Aguilar, R.C., Gahl, W.A. and Bonifacino, J.S. (1999a). Altered Trafficking of Lysosomal Proteins in Hermansky-Pudlak Syndrome Due to Mutations in the β3A Subunit of the AP-3 Adaptor. Mol. Cell, 3, 11–21.

Denecke, J., Aniento, F., Frigerio, L., Hawes, C., Hwang, I., Mathur, J., Neuhaus, J.M. and Robinson, D.G. (2012). Secretory pathway research: the more experimental systems the better. Plant Cell, 24, 4, 1316-1326.

Dettmer, J., Hong-Hermesdorf, A., Stierhof, Y.D. and Schumacher, K. (2006). Vacuolar H+-ATPase Activity Is Required for Endocytic and Secretory Trafficking in Arabidopsis. Plant Cell, 18, 715–730.

Dettmer, J., Schubert, D., Calvo-Weimar, O., Stierhof, Y.D., Schmidt, R. and Schumacher K. (2005). Essential role of the V-ATPase in male gametophyte development. Plant J., 41, 1, 117-124.

DiFiglia, M., Sapp, E., Chase, K., Schwarz, C., Meloni, A., Young, C., Martin, E., Vonsattel, J.P., Carraway, R. and Reeves, S.A. (1995). Huntingtin is a cytoplasmic protein associated with vesicles in human and rat brain neurons. Neuron, 14, 5, 1075–1081.

Drakakaki, G., van de Ven, W., Pan, S., Miao, Y., Wang, J., Keinath, N.K., Weatherly, B., Jiang, L., Schumacher, K., Hicks, G. and Raikhel N. (2012). Isolation and proteomic analysis of the SYP61 compartment reveal its role in exocytic trafficking in Arabidopsis. Cell Res., 22, 413–424.

Du, J., Kirui, A., Huang, S., Wang, L., Barnes, W.J., Kiemle, S.N., Zheng, Y., Rui, Y., Ruan, M., Qi, S., Kim, S.H., Wang, T., Cosgrove, D.J., Anderson, C.T. and Xiao, C. (2020). Mutations in the Pectin Methyltransferase QUASIMODO2 Influence Cellulose Biosynthesis and Wall Integrity in Arabidopsis. Plant Cell. 32, 11, 3576-3597.

Duncan, M.C., Costaguta, G. and Payne, G. (2003). Yeast epsin-related proteins required for Golgi–endosome traffic define a γ-adaptin ear-binding motif. Nat. Cell Biol., 5, 77–81.

Ebine K., Okatani Y., Uemura T., Goh T., Shoda K., Niihama M., Morita M.T., Spitzer C., Otegui M.S., Nakano A. and Ueda T. (2008). A SNARE complex unique to seed plants is required for protein storage vacuole biogenesis and seed development of Arabidopsis thaliana. Plant Cell, 20, 11, 3006-3021.

Edwards, K., Johnstone, C. and Thompson, C. (1991). A simple and rapid method for the preparation of plant genomic DNA for PCR analysis. Nucleic Acids Res., 19, 1349.

Enami, K., Ichikawa, M., Uemura, T., Kutsuna, N., Hasezawa, S., Naka-gawa, T., Nakano, A. and Sato, M.H. (2009). Differential expression control and polarized distribution of plasmamembrane-resident SYP1 SNAREs in Arabidopsis thaliana. Plant Cell Physiol., 50, 280–289.

Engqvist-Goldstein, A. E., Kessels, M. M., Chopra, V. S., Hayden, M. R. and Drubin, D. G. (1999). An actin-binding protein of the Sla2/Huntingtin interacting protein 1 family is a novel component of clathrin-coated pits and vesicles. J. Cell Biol., 147, 7, 1503–1518.

Eugster, A., Pécheur, E. I., Michel, F., Winsor, B., Letourneur, F., and Friant, S. (2004). Ent5p is required with Ent3p and Vps27p for ubiquitin-dependent protein sorting into the multivesicular body. Mol. Biol. Cell, 15, 7, 3031–3041.

Fan, L., Hao, H., Xue, Y., Zhang, L., Song, K., Ding, Z., Botella, M. A., Wang, H., and Lin, J. (2013). Dynamic analysis of Arabidopsis AP2 σ subunit reveals a key role in clathrin-mediated endocytosis and plant development. Development, 140, 18, 3826–3837.

Fan, L., Li, R., Pan, J., Ding, Z., and Lin, J. (2015). Endocytosis and its regulation in plants. Trends Plant Sci., 20, 388–397.

Fan, X., Yang, C., Klisch, D., Ferguson, A., Bhaellero, R. P., Niu, X. and Wilson, Z. A. (2014). ECHIDNA protein impacts on male fertility in Arabidopsis by mediating trans-Golgi network secretory trafficking during anther and pollen development. Plant physiol., 164, 3, 1338–1349.

Feng, Q.N., Li, S. and Zhang, Y. (2017). Update on adaptor protein-3 in Arabidopsis. Plant Signal Behav., 12, 8, e1356969.

Feng, Q. N., Liang, X., Li, S. and Zhang, Y. (2018). The ADAPTOR PROTEIN-3 Complex Mediates Pollen Tube Growth by Coordinating Vacuolar Targeting and Organization. Plant physiol., 177, 1, 216–225.

Feraru, E., Paciorek, T., Feraru, M.I., Zwiewka, M., Groodt, R.D., Rycke, R.D., Kleine-Vehn, J. and Friml, J. (2010). The AP-3 β Adaptin Mediates the Biogenesis and Function of Lytic Vacuoles in Arabidopsis. Plant Cell, 22, 2812–2824.

Ferguson, S. M., and De Camilli, P. (2012). Dynamin, a membrane-remodelling GTPase. Molecular cell biology, 13, 2, 75–88.

Ford, M.G., Pearse, B.M., Higgins, M.K., Vallis, Y., Owen, D.J., Gibson, A., Hopkins, C.R., Evans, P.R. and McMahon, H.T. (2001). Simultaneous binding of PtdIns(4,5)P2 and clathrin by AP180 in the nucleation of clathrin lattices on membranes. Science, 291, 5506, 1051–1055.

Ford, M.G.J., Mills, I.G., Peter, B.J., Vallis, Y., Praefcke, G.J.K., Evans, P.R. and McMahon, H.T. (2002). Curvature of clathrin-coated pits driven by epsin. Nature, 419, 361–366.

Francoz, E., Ranocha, P., Burlat, V. and Dunand, C. (2015). Arabidopsis seed mucilage secretory cells: regulation and dynamics. Trends Plant Sci., 20, 8, 515–524.

Franklin-Tong VE. (1999). Signaling and the modulation of pollen tube growth. Plant Cell, 11, 4, 727-738.
Frazier, M.N., Davies, A.K., Voehler, M., Kendall, A.K., Borner, G.H., Chazin, W.J., Robinson, M.S. and Jackson, L.P. (2016). Molecular Basis for the Interaction Between AP4 β4 and its Accessory Protein, Tepsin. Traffic, 17, 400-415.

Friant, S., Pécheur, E.I., Eugster, A., Michel, F., Lefkir, Y., Nourrisson, D. and Letourneur, F. (2003). Ent3p Is a PtdIns(3,5)P2 effector required for protein sorting to the multivesicular body. Dev. Cell, 5, 3, 499–511.

Fuji, K., Shimada, T., Takahashi, H., Tamura, K., Koumoto, Y., Utsumi, S., Nishizawa, K., Maruyama, N. and Hara-Nishimura, I. (2007). Arabidopsis vacuolar sorting mutants (green fluorescent seed) can be identified efficiently by secretion of vacuole-targeted green fluorescent protein in their seeds. Plant Cell, 19, 597–609.

Fuji, K., Shirakawa, M., Shimono, Y., Kunieda, T., Fukao, Y., Koumoto, Y., Takahashi, H., Hara-Nishimura, I. and Shimada, T. (2016). The Adaptor Complex AP-4 Regulates Vacuolar Protein Sorting at the trans-Golgi Network by Interacting with VACUOLAR SORTING RECEPTOR1. Plant Physiol., 170, 211–219.

Fujimoto, M., Ebine, K., Nishimura, K., Tsutsumi, N. and Ueda, T. (2020). Longin R-SNARE is retrieved from the plasma membrane by ANTH domain-containing proteins in Arabidopsis. Proc. Natl. Acad. Sci USA, 117, 40, 25150–25158.

Gadeyne, A., Sánchez-Rodríguez, C., Vanneste, S., Di Rubbo, S., Zauber, H., Vanneste, K., Van Leene, J., De Winne, N., Eeckhout, D., Persiau, G., Van De Slijke, E., Cannoot, B., Vercruysse, L., Mayers, J. R., Adamowski, M., Kania, U., Ehrlich, M., Schweighofer, A., Ketelaar, T., Maere, S., Bednarek, S.Y., Friml, J., Gevaert, K., Witters, E., Russinova, E., Persson, S., De Jaeger, G. and Van Damme, D. (2014). The TPLATE adaptor complex drives clathrin-mediated endocytosis in plants. Cell, 156, 4, 691–704.

Gaidarov, I. and Keen, J.H. (1999). Phosphoinositide-AP-2 interactions required for targeting to plasma membrane clathrin-coated pits. J. Cell Biol., 146, 4, 755–764.

Gaidarov, I., Chen, Q., Falck, J. R., Reddy, K. K., and Keen, J. H. (1996). A functional phosphatidylinositol 3,4,5-trisphosphate/phosphoinositide binding domain in the clathrin adaptor AP-2 alpha subunit. Implications for the endocytic pathway. The Journal of biological chemistry, 271, 34, 20922–20929.

Gallop, J.L., Jao, C.C., Kent, H.M., Butler, P.J.G., Evans, P.R., Langen, R. and McMahon, H.T. (2006). Mechanism of endophilin N-BAR domain-mediated membrane curvature. The EMBO Journal, 25, 2898–2910.

Gallusser, A. and Kirchhausen, T. (1993). The beta 1 and beta 2 subunits of the AP complexes are the clathrin coat assembly components. The EMBO Journal, 12, 5237–5244.

Geldner, N., Anders, N., Wolters, H., Keicher, J., Kornberger, W., Muller, P., Delbarre, A., Ueda, T., Nakano, A. and Jürgens, G. (2003). The Arabidopsis GNOM ARF-GEF mediates endosomal recycling, auxin transport, and auxin-dependent plant growth. Cell, 112, 2, 219–230.

Geldner, N., Dénervaud-Tendon, V., Hyman, D. L., Mayer, U., Stierhof, Y. D., and Chory, J. (2009). Rapid, combinatorial analysis of membrane compartments in intact plants with a multicolor marker set. Plant J., 59, 1, 169–178.

Geldner, N., Friml, J., Stierhof, Y.D., Jürgens, G. and Palme, K. (2001). Auxin transport inhibitors block PIN1 cycling and vesicle trafficking. Nature, 413, 6854, 425–428.

Gendre, D., Baral, A., Dang, X., Esnay, N., Boutté, Y., Stanislas, T., Vain, T., Claverol, S., Gustavsson, A., Lin, D., Grebe, M., & Bhalerao, R. P. (2019). Rho-of-plant activated root hair formation requires *Arabidopsis YIP4a/b* gene function. *Development, 146*, 5, dev168559.

Gendre, D., McFarlane, H. E., Johnson, E., Mouille, G., Sjödin, A., Oh, J., Levesque-Tremblay, G., Watanabe, Y., Samuels, L., and Bhalerao, R. P. (2013). Trans-Golgi network localized ECHIDNA/Ypt interacting protein complex is required for the secretion of cell wall polysaccharides in Arabidopsis. Plant cell, 25, 7, 2633–2646.

Gendre, D., Oh, J., Boutté, Y., Best, J. G., Samuels, L., Nilsson, R., Uemura, T., Marchant, A., Bennett, M. J., Grebe, M., & Bhalerao, R. P. (2011). Conserved Arabidopsis ECHIDNA protein mediates trans-Golgi-network trafficking and cell elongation. Proc. Natl. Acad. Sci USA, 108, 19, 8048–8053.

Ghosh, P. and Kornfeld, S. (2004). The GGA proteins: key players in protein sorting at the trans-Golgi network. Eur. J. Cell Biol., 83, 6, 257-262.

Gilles, J.-F., Dos Santos, M., Boudier, T., Bolte, S., Heck, N. (2016). DiAna, an ImageJ tool for object-based 3D co-localization and distance analysis. Methods.

Goodman, O. B., Jr, and Keen, J. H. (1995). The alpha chain of the AP-2 adaptor is a clathrin binding subunit. The Journal of biological chemistry, 270, 40, 23768–23773.

Gottfried, I., Ehrlich, M. and Ashery, U. (2010). The Sla2p/HIP1/HIP1R family: similar structure, similar function in endocytosis? Biochem. Soc. Trans., 38, 1, 187-191.

Grebnev, G., Ntefidou, M. and Kost, B. (2017). Secretion and Endocytosis in Pollen Tubes: Models of Tip Growth in the Spot Light. Front. Plant Sci., 8, 154.

Griffiths, G. and Simons, K. (1986) The trans Golgi network: sorting at the exit site of the Golgi complex. Science, 23, 438–443.

Gu, Y., Kaplinsky, N., Bringmann, M., Cobb, A., Carroll, A., Sampathkumar, A., Baskin, T.I., Persson, S. and Somerville, C.R. (2010). Identification of a cellulose synthase-associated protein required for cellulose biosynthesis. Proc. Natl. Acad. Sci USA, 107, 12866–12871.

Gutekunst, C.A., Levey, A.I., Heilman, C.J., Whaley, W.L., Yi, H., Nash, N.R., Rees, H.D., Madden, J.J. and Hersch, S.M. (1995). Identification and localization of huntingtin in brain and human lymphoblastoid cell lines with anti-fusion protein antibodies. Proc. Natl. Acad. Sci USA, 92, 8710–8714.

Hao, W., Luo, Z., Zheng, L., Prasad, K. and Lafer, E.M. (1999). AP180 and AP-2 Interact Directly in a Complex That Cooperatively Assembles Clathrin. J. Biol. Chem., 274, 22785–22794.

Hatsugai, N., Nakatsuji, A., Unten, O., Ogasawara, K., Kondo, M., Nishimura, M., Shimada, T., Katagiri, F. and Hara-Nishimura, I. (2018). Involvement of Adapter Protein Complex 4 in Hypersensitive Cell Death Induced by Avirulent Bacteria. Plant physiol., 176, 2, 1824–1834.

Heinze, L., Freimuth, N., Rößling, A.K., Hahnke, R., Riebschläger, S., Fröhlich, A., Sampathkumar, A., McFarlane, H. E. and Sauer, M. (2020). EPSIN1 and MTV1 define functionally overlapping but molecularly distinct *trans*-Golgi network subdomains in *Arabidopsis*. Proc. Natl. Acad. Sci USA, 117*,* 41, 25880–25889.

Hepler, P.K., Vidali, L. and Cheung, A.Y. (2001). Polarized cell growth in higher plants. Annu. Rev. Cell. Dev. Biol., 17, 159-187.

Heuser, J.E. and Keen, J. (1988). Deep-etch visualization of proteins involved in clathrin assembly. J. Cell Biol., 107, 877–886.

Hirst, J., Barlow, L.D., Francisco, G.C., Sahlender, D.A., Seaman, M.N.J., Dacks, J.B., and Robinson, M.S. (2011). The Fifth Adaptor Protein Complex. PLOS Biology 9, e1001170.

Hirst, J., Borner, G.H., Antrobus, R., Peden, A.A., Hodson, N.A., Sahlender, D.A. and Robinson, M.S. (2012). Distinct and overlapping roles for AP-1 and GGAs revealed by the "knocksideways" system. Curr. Biol., 22, 18, 1711–1716.

Hirst, J., Bright, N.A., Rous, B. and Robinson, M.S. (1999). Characterization of a Fourth Adaptor-related Protein Complex. Mol. Biol. Cell, 10, 2787–2802.

Hirst, J., Irving, C. and Borner, G.H.H. (2013). Adaptor Protein Complexes AP-4 and AP-5: New Players in Endosomal Trafficking and Progressive Spastic Paraplegia. Traffic, 14, 153–164.

Hirst, J., Miller, S.E., Taylor, M.J., von Mollard, G.F. and Robinson, M.S. (2004). EpsinR Is an Adaptor for the SNARE Protein Vti1b. Mol. Biol. Cell, 15, 5593–5602.

Hirst, J., Motley, A., Harasaki, K., Peak Chew, S.Y. and Robinson, M.S. (2003). EpsinR: an ENTH domain-containing protein that interacts with AP-1. Mol. Biol. Cell., 14, 2, 625-641.

Hirst, J., Schlacht, A., Norcott, J.P., Traynor, D., Bloomfield, G., Antrobus, R., Kay, R.R., Dacks, J.B. and Robinson, M.S. (2014). Characterization of TSET, an ancient and widespread membrane trafficking complex. Elife. 3:e02866.

Hussain, N.K., Yamabhai, M., Bhakar, A.L., Metzler, M., Ferguson, S.S., Hayden, M.R., McPherson, P.S. and Kay, B.K. (2003). A role for epsin N-terminal homology/AP180 N-terminal homology (ENTH/ANTH) domains in tubulin binding. J. Biol. Chem. 278, 31, 28823-28830.

Ichino, T., Maeda, K., Hara-Nishimura, I. and Shimada, T. (2020). Arabidopsis ECHIDNA protein is involved in seed coloration, protein trafficking to vacuoles, and vacuolar biogenesis. J. Exp. Bot. 71, 3999–4009.

Inada, N. and Ueda, T. (2014). Membrane trafficking pathways and their roles in plant-microbe interactions. Plant Cell Physiol., 55, 4, 672–686.

Inoue, H. and Randazzo, P.A. (2007). Arf GAPs and their interacting proteins. Traffic, 8, 11, 1465-1475.

Ito, E., Fujimoto, M., Ebine, K., Uemura, T., Ueda, T., and Nakano, A. (2012). Dynamic behavior of clathrin in Arabidopsis thaliana unveiled by live imaging. Plant J., 69, 2, 204–216.

Inoue, H., Nojima, H., and Okayama, H. (1990). High efficiency transformation of Escherichia coli with plasmids. Gene, 96, 1, 23–28.

Itoh, T., Koshiba, S., Kigawa, T., Kikuchi, A., Yokoyama, S. and Takenawa, T. (2001). Role of the ENTH Domain in Phosphatidylinositol-4,5-Bisphosphate Binding and Endocytosis. Science, 291, 1047–1051.

Jahn, R., Lang, T. and Südhof, T.C. (2003). Membrane Fusion. Cell, 112, 519–533.

Johnson, M.A., Besser, K. von, Zhou, Q., Smith, E., Aux, G., Patton, D., Levin, J.Z., and Preuss, D. (2004). Arabidopsis hapless Mutations Define Essential Gametophytic Functions. Genetics, 168, 971–982.

Jürgens, G. and Pacher, T. (2004). Cytokinesis: Membrane trafficking by default? In The Golgi Apparatus and the Plant Secretory Pathways, D.G. Robinson, ed (Oxford, UK: Blackwell), pp. 238–254.

Kaksonen, M. and Roux, A. (2018). Mechanisms of clathrin-mediated endocytosis. Nat. Rev. Mol. Cell Biol., 19, 313–326.

Kalthoff, C., Alves, J., Urbanke, C., Knorr, R., and Ungewickell, E.J. (2002). Unusual Structural Organization of the Endocytic Proteins AP180 and Epsin 1. J. Biol. Chem. 277, 8209–8216.

Kalthoff, C., Groos, S., Kohl, R., Mahrhold, S. and Ungewickell, E.J. (2002). Clint: a novel clathrin-binding ENTH-domain protein at the Golgi. Mol. Biol. Cell., 13, 11, 4060-4073.

Kanaseki, T. and Kadota, K. (1969). THE "VESICLE IN A BASKET": A Morphological Study of the Coated Vesicle Isolated from the Nerve Endings of the Guinea Pig Brain, with Special Reference to the Mechanism of Membrane Movements. J. Cell Biol., 42, 202–220.

Kaneda, M., van Oostende-Triplet, C., Chebli, Y., Testerink, C., Bednarek, S.Y. and Geitmann, A. (2019). Plant AP180 N-terminal homolog proteins are involved in clathrin-dependent endocytosis during pollen tube growth in Arabidopsis thaliana. Plant Cell Physiol., 60, 1316–1330.

Kang, B.H., Nielsen, E., Preuss, M.L., Mastronarde, D. and Staehelin, L.A. (2011). Electron tomography of RabA4b- and PI-4Kbeta1-labeled trans Golgi network compartments in Arabidopsis. Traffic, 12, 313–329.

Kansup, J., Tsugama, D., Liu, S. and Takano, T. (2013). The Arabidopsis adaptor protein AP-3μ interacts with the G-protein β subunit AGB1 and is involved in abscisic acid regulation of germination and post-germination development. J. Exp. Bot., 64, 18, 5611–5621.

Kay, B.K., Yamabhai, M., Wendland, B. and Emr, S.D. (1999). Identification of a novel domain shared by putative components of the endocytic and cytoskeletal machinery. Protein Science, 8, 435–438.

Keen, J.H. (1987). Clathrin assembly proteins: affinity purification and a model for coat assembly. J. Cell Biol, 105, 1989–1998.

Kessels, M.M., Engqvist-Goldstein, Å.E.Y., Drubin, D.G. and Qualmann, B. (2001). Mammalian Abp1, a Signal-Responsive F-Actin–Binding Protein, Links the Actin Cytoskeleton to Endocytosis via the Gtpase Dynamin. J. Cell Biol., 153, 351–366.

Kim, S.J. and Brandizzi, F. (2016). The plant secretory pathway for the trafficking of cell wall polysaccharides and glycoproteins. Glycobiology, 26, 9, 940–949.

Kim, S.Y., Xu, Z.Y., Song, K., Kim, D.H., Kang, H., Reichardt, I., Sohn, E.J., Friml, J., Jürgens, G. and Hwang, I. (2013). Adaptor protein complex 2-mediated endocytosis is crucial for male reproductive organ development in Arabidopsis. Plant Cell, 25, 8, 2970-2985.

Kirchhausen, T., Harrison, S.C., Chow, E.P., Mattaliano, R.J., Ramachandran, K.L., Smart, J. and Brosius, J. (1987). Clathrin heavy chain: molecular cloning and complete primary structure. Proc. Natl. Acad. Sci USA, 84, 8805–8809.

Kitakura, S., Vanneste, S., Robert, S., Löfke, C., Teichmann, T., Tanaka, H. and Friml, J. (2011). Clathrin mediates endocytosis and polar distribution of PIN auxin transporters in Arabidopsis. Plant Cell, 23, 5, 1920–1931.

Kleine-Vehn, J., Leitner, J., Zwiewka, M., Sauer, M., Abas, L., Luschnig, C. and Friml, J. (2008). Differential degradation of PIN2 auxin efflux carrier by retromer-dependent vacuolar targeting. Proc. Natl. Acad. Sci USA, 105, 46, 17812-17817.

Ko, G., Paradise, S., Chen, H., Graham, M., Vecchi, M., Bianchi, F., Cremona, O., Di Fiore, P.P. and De Camilli, P. (2010). Selective high-level expression of epsin 3 in gastric parietal cells, where it is localized at endocytic sites of apical canaliculi. Proc. Natl. Acad. Sci USA, 107, 50, 21511-21516.

Laemmli, U.K. (1970). Cleavage of Structural Proteins during the Assembly of the Head of Bacteriophage T4. Nature, 227, 680–685.

Lai, C.-L., Jao, C.C., Lyman, E., Gallop, J.L., Peter, B.J., McMahon, H.T., Langen, R. and Voth, G.A. (2012). Membrane Binding and Self-Association of the Epsin N-Terminal Homology Domain. J. Mol. Biol., 423, 800–817.

LaMontagne, E.D. and Heese, A. (2017). Trans-Golgi network/early endosome: a central sorting station for cargo proteins in plant immunity. Curr. Opin. Plant Biol., 40, 114-121.

Langhans, M., Förster, S., Helmchen, G., and Robinson, D. G. (2011). Differential effects of the brefeldin A analogue (6R)-hydroxy-BFA in tobacco and Arabidopsis. J. Exp. Bot., 62, 8, 2949–2957.

Lauber, M.H., Waizenegger, I., Steinmann, T., Schwarz, H., Mayer, U., Hwang, I., Lukowitz, W. and Jürgens, G. (1997). The Arabidopsis KNOLLE protein is a cytokinesis-specific syntaxin. J. Cell Biol., 139, 1485–1493.

Leboeuf, E., Guillon, F., Thoiron, S. and Lahaye, M. (2005). Biochemical and immunohistochemical analysis of pectic polysaccharides in the cell walls of Arabidopsis mutant QUASIMODO 1 suspension-cultured cells: implications for cell adhesion. J. Exp. Bot., 56, 422, 3171–3182.

Lee, M.H. and Hwang, I. (2014). Adaptor proteins in protein trafficking between endomembrane compartments in plants. J. Plant Biol. 57, 265–273.

Lee, G. J., Kim, H., Kang, H., Jang, M., Lee, D. W., Lee, S. and Hwang, I. (2007). EpsinR2 interacts with clathrin, adaptor protein-3, AtVTI12, and phosphatidylinositol-3-phosphate. Implications for EpsinR2 function in protein trafficking in plant cells. Plant physiology, 143, 4, 1561–1575.

Legendre-Guillemin, V., Metzler, M., Charbonneau, M., Gan, L., Chopra, V., Philie, J., Hayden, M.R. and McPherson, P.S. (2002). HIP1 and HIP12 display differential binding to F-actin, AP2, and clathrin. Identification of a novel interaction with clathrin light chain. J. Biol. Chem., 277, 22, 19897–19904.

Legendre-Guillemin, V., Wasiak, S., Hussain, N.K., Angers, A. and McPherson, P.S. (2004). ENTH/ANTH proteins and clathrin-mediated membrane budding. J. Cell Sci., 117, 9–18.

Liljegren, S.J., Leslie, M.E., Darnielle, L., Lewis, M.W., Taylor, S.M.,Luo, R., Geldner, N., Chory, J., Randazzo, P.A., Yanofsky, M.F. and Ecker, J.R. (2009). Regulation of membrane trafficking and organ separation by the NEVERSHED ARF-GAP protein. Development, 136, 1909–1918.

Lukowitz, W., Mayer, U. and Jürgens, G. (1996). Cytokinesis in the Arabidopsis embryo involves the syntaxin-related KNOLLE gene product. Cell, 84, 61–71.

Mattera, R., Guardia, C.M., Sidhu, S.S. and Bonifacino, J.S. (2015). Bivalent Motif-Ear Interactions Mediate the Association of the Accessory Protein Tepsin with the AP-4 Adaptor Complex. J. Biol. Chem., 290, 52, 30736-30749.

Mayer, U., Torres Ruiz, R. A., Berleth, T., Miséra, S. and Jürgens, G. (1991). Mutations affecting body organization in the Arabidopsis embryo. Nature 353, 402-407.

McCann, R.O. and Craig, S.W. (1997). The I/LWEQ module: A conserved sequence that signifies F-actin binding in functionally diverse proteins from yeast to mammals. Proc. Natl. Acad. Sci USA, 94, 5679–5684.

McFarlane, H., Gendre, D. and Western, T. (2014). Seed Coat Ruthenium Red Staining Assay. BIO-PROTOCOL 4.

McFarlane, H.E., Watanabe, Y., Gendre, D., Carruthers, K., Levesque-Tremblay, G., Haughn, G.W., Bhalerao, R. P. and Samuels, L. (2013). Cell wall polysaccharides are mislocalized to the Vacuole in echidna mutants. Plant Cell physiol., 54, 11, 1867–1880.

Men, S., Boutté, Y., Ikeda, Y., Li, X., Palme, K., Stierhof, Y.D., Hartmann, M.A., Moritz, T. and Grebe, M. (2008). Sterol-dependent endocytosis mediates post-cytokinetic acquisition of PIN2 auxin efflux carrier polarity. Nat. Cell Biol., 10, 2, 237–244.

Messa, M., Fernández-Busnadiego, R., Sun, E.W., Chen, H., Czapla, H., Wrasman, K., Wu, Y., Ko, G., Ross, T., Wendland, B. and De Camilli, P. (2014) Epsin deficiency impairs endocytosis by stalling the actin-dependent invagination of endocytic clathrin-coated pits. Elife, 13, 3:e03311.

Miao, Y., Li, H., Shen, J., Wang, J. and Jiang, L. (2011). QUASIMODO 3 (QUA3) is a putative homogalacturonan methyltransferase regulating cell wall biosynthesis in Arabidopsis suspension-cultured cells. J. Exp. Bot., 62, 14, 5063–5078.

Miller, S.E., Collins, B.M., McCoy, A.J., Robinson, M.S. and Owen, D.J. (2007). A SNARE-adaptor interaction is a new mode of cargo recognition in clathrin-coated vesicles. Nature, 450, 7169, 570–574.

Mills, I.G., Praefcke, G.J., Vallis, Y., Peter, B.J., Olesen, L.E., Gallop, J.L., Butler, P.J., Evans, P.R. and McMahon, H.T. (2003). EpsinR: an AP1/clathrin interacting protein involved in vesicle trafficking. J. Cell Biol., 160, 2, 213-222.

Mitsunari, T., Nakatsu, F., Shioda, N., Love, P.E., Grinberg, A., Bonifacino, J.S. and Ohno, H. (2005). Clathrin Adaptor AP-2 Is Essential for Early Embryonal Development. Mol. Cell Biol., 25, 9318–9323.

Moreno-De-Luca, A., Helmers, S.L., Mao, H., Burns, T.G., Melton, A.M.A., Schmidt, K.R., Fernhoff, P.M., Ledbetter, D.H. and Martin, C.L. (2011). Adaptor protein complex-4 (AP-4) deficiency causes a novel autosomal recessive cerebral palsy syndrome with microcephaly and intellectual disability. J. Med. Gen., 48, 141–144.

Morgan, J.R., Prasad, K., Hao, W., Augustine, G.J. and Lafer, E.M. (2000). A conserved clathrin assembly motif essential for synaptic vesicle endocytosis. J. Neuro. sci., 1, 20, 23, 8667-8676.

Moscatelli, A. and Idilli, A.I. (2009). Pollen tube growth: a delicate equilibrium between secretory and endocytic pathways. J. Integr. Plant Biol., 51, 8, 727-739.

Moscatelli, A., Ciampolini, F., Rodighiero, S., Onelli, E., Cresti, M., Santo, N. and Idilli, A. (2007). Distinct endocytic pathways identified in tobacco pollen tubes using charged nanogold. J. Cell Sci., 120(Pt 21):3804-19.

Müdsam, C., Wollschläger, P., Sauer, N. and Schneider, S. (2018). Sorting of Arabidopsis NRAMP3 and NRAMP4 depends on adaptor protein complex AP4 and a dileucine-based motif. Traffic, 19, 503–521.

Muro, K., Matsuura-Tokita, K., Tsukamoto, R., Kanaoka, M.M., Ebine, K., Higashiyama, T., Nakano, A. and Ueda, T. (2018). ANTH domain-containing proteins are required for the pollen tube plasma membrane integrity via recycling ANXUR kinases. Commun. Biol., 1, 152.

Niihama, M., Takemoto, N., Hashiguchi, Y., Tasaka, M. and Morita, M.T. (2009). ZIP genes encode proteins involved in membrane trafficking of the TGN-PVC/vacuoles. Plant Cell Physiol. 50, 12, 2057-2068.

Ohno, H., Stewart, J., Fournier, M.C., Bosshart, H., Rhee, I., Miyatake, S., Saito, T., Gallusser, A., Kirchhausen, T. and Bonifacino, J.S. (1995). Interaction of tyrosine-based sorting signals with clathrin-associated proteins. Science, 269, 1872–1875.

Owen, D.J., Vallis, Y., Noble, M.E.M., Hunter, J.B., Dafforn, T.R., Evans, P.R. and McMahon, H.T. (1999). A Structural Explanation for the Binding of Multiple Ligands by the α-Adaptin Appendage Domain. Cell 97, 805–815.

Palade, G. (1975). Intracellular Aspects of the Process of Protein Synthesis. Science 189, 347–358.

Paolini, L., Radeghieri, A., Civini, S., Caimi, L. and Ricotta, D. (2011). The Epsilon Hinge-Ear Region Regulates Membrane Localization of the AP-4 Complex. Traffic, 12, 1604-1619.

Park, M. and Jürgens, G. (2012). Membrane traffic and fusion at post-Golgi compartments. Front Plant Sci., 2, 111.

Park, M., Song, K., Reichardt, I., Kim, H., Mayer, U., Stierhof, Y. D., Hwang, I., and Jürgens, G. (2013). Arabidopsis μ-adaptin subunit AP1M of adaptor protein complex 1 mediates late secretory and vacuolar traffic and is required for growth. Proc. Natl. Acad. Sci USA, 110, 25, 10318–10323.

Pearse, B.M. and Robinson, M.S. (1984). Purification and properties of 100-kd proteins from coated vesicles and their reconstitution with clathrin. The EMBO Journal 3, 1951–1957.

Pearse, B.M.F. (1975). Coated vesicles from pig brain: Purification and biochemical characterization. J. Mol. Biol. 97, 93–98.

Preuss, D., Rhee, S.Y. and Davis, R.W. (1994). Tetrad analysis possible in Arabidopsis with mutation of the QUARTET (QRT) genes. Science, 1458-1460.

Qualmann, B. and Kessels, M.M. (2002). Endocytosis and the cytoskeleton. Int. Rev. Cytol., 220, 93-144.

Qualmann, B., Kessels, M.M. and Kelly, R.B. (2000). Molecular Links between Endocytosis and the Actin Cytoskeleton. J. Cell Biol., 150, 111–116.

Rapoport, I., Chen, Y.C., Cupers, P., Shoelson, S.E. and Kirchhausen, T. (1998). Dileucine-based sorting signals bind to the β chain of AP-1 at a site distinct and regulated differently from the tyrosine-based motif-binding site. The EMBO Journal, 17, 2148–2155.

Renna, L., Stefano, G., Slabaugh, E., Wormsbaecher, C., Sulpizio, A., Zienkiewicz, K. and Brandizzi, F. (2018). TGNap1 is required for microtubule-dependent homeostasis of a subpopulation of the plant trans-Golgi network. Nat. Commun., 9, 1, 5313.

Repass, S. L., Brady, R. J. and O'Halloran, T. J. (2007). Dictyostelium Hip1r contributes to spore shape and requires epsin for phosphorylation and localization. J. Cell Sci., 120, 22, 3977–3988.

Richter, S., Voss, U. and Jürgens, G. (2009). Post-Golgi traffic in plants. Traffic, 10, 7, 819–828.

Robert, S., Chary, S.N., Drakakaki, G., Li, S., Yang, Z., Raikhel, N.V. and Hicks, G.R. (2008). Endosidin1 defines a compartment involved in endocytosis of the brassinosteroid receptor BRI1 and the auxin transporters PIN2 and AUX1. Proc. Natl. Acad. Sci. USA, 105, 8464–8469.

Robinson, M.S. (2004). Adaptable adaptors for coated vesicles. Trends Cell Biol. 14, 167–174.

Robinson, M. S., and Bonifacino, J. S. (2001). Adaptor-related proteins. Curr. Opin. Cell Biol., 13, 4, 444–453

Robinson, M.S., Sahlender, D.A. and Foster, S.D. (2010). Rapid inactivation of proteins by rapamycin-induced rerouting to mitochondria. Dev. Cell, 18, 2, 324-331.

Rodriguez-Enriquez, M.J., Mehdi, S., Dickinson, H.G., and Grant-Downton, R.T. (2013). A novel method for efficient in vitro germination and tube growth of Arabidopsis thaliana pollen. New Phytol. 197, 668–679.

Rosenthal, J.A., Chen, H., Slepnev, V.I., Pellegrini, L., Salcini, A.E., Fiore, P.P.D., and Camilli, P.D. (1999). The Epsins Define a Family of Proteins That Interact with Components of the Clathrin Coat and Contain a New Protein Module. J. Biol. Chem. *274*, 33959–33965.

Rosquete, M.R., Davis, D.J., and Drakakaki, G. (2018). The Plant Trans-Golgi Network: Not Just a Matter of Distinction. Plant physiol., 176, 1, 187–198.

Roth, T.F. and Porter, K.R. (1964). Yolk Protein Uptake in the Oocyte of the Mosquito Aedes Aegypti. L. J. Cell Biol., 20, 313–332.

Roth, J., Taatjes, D. J., Lucocq, J. M., Weinstein, J., and Paulson, J. C. (1985). Demonstration of an extensive trans-tubular network continuous with the Golgi apparatus stack that may function in glycosylation. Cell, 43, 1, 287–295.

Saffarian, S., Cocucci, E., and Kirchhausen, T. (2009). Distinct Dynamics of Endocytic Clathrin-Coated Pits and Coated Plaques. PLOS Biology, *7*, e1000191.

Saint-Pol, A., Yélamos, B., Amessou, M., Mills, I.G., Dugast, M., Tenza, D., Schu, P., Antony, C., McMahon, H.T., Lamaze and C., Johannes, L. (2004). Clathrin adaptor epsinR is required for retrograde sorting on early endosomal membranes. Dev. Cell, 6, 4, 525-38.

Samalova, M., Fricker, M., and Moore, I. (2006). Ratiometric fluorescence-imaging assays of plant membrane traffic using polyproteins. Traffic, 7, 12, 1701–1723.

Sanderfoot, A.A. (2007). Increases in the number of SNARE genes parallels the rise of multicellularity among the green plants. Plant Physiol, 144, 6-17.

Sanderfoot, A.A., Kovaleva, V., Bassham, D.C. and Raikhel, N.V. (2001). Interactions between syntaxins identify at least five SNARE complexes within the Golgi/prevacuolar system of the *Arabidopsis* cell. Mol. Biol. Cell, 12, 3733–3743.

Sanmartín, M., Ordóñez, A., Sohn, E.J., Robert, S., Sánchez-Serrano, J.J., Surpin, M.A., Raikhel, N.V. and Rojo, E. (2007). Divergent functions of VTI12 and VTI11 in trafficking to storage and lytic vacuoles in Arabidopsis. Proc. Natl. Acad. Sci USA, 104, 3645–3650.

Sauer, M. (2014). MTV1 Pull-down Assay in *Arabidopsis*. Bio-protocol 4, 12, 1152.

Sauer, M., Delgadillo, M.O., Zouhar, J., Reynolds, G.D., Pennington, J.G., Jiang, L., Liljegren, S.J., Stierhof, Y.D., Jaeger, G.D., Otegui, M.S., Bednarek, S.Y. and Rojo, E. (2013). MTV1 and MTV4 Encode Plant-Specific ENTH and ARF GAP Proteins That Mediate Clathrin-Dependent Trafficking of Vacuolar Cargo from the Trans-Golgi Network. Plant Cell, 25, 2217–2235.

Sauter, M., Seagull, R.W. and Kende, H. (1993) Internodal elongation and orientation of cellulose microfibrils and microtubules in deepwater rice. Planta, 190, 354–362.

Scheuring, D., Schöller, M., Kleine-Vehn, J., & Löfke, C. (2015). Vacuolar staining methods in plant cells. Methods Mol Biol., 1242, 83–92.

Schumacher, K., Vafeados, D.,McCarthy, M., Sze, H., Wilkins, T. and Chory, J. (1999). The Arabidopsis det3 mutant reveals a central role for the vacuolar H+–ATPase in plant growth and development. Genes. Dev., 13, 3259–3327.

Schwarz, D.S. and Blower, M.D. (2016). The endoplasmic reticulum: structure, function and response to cellular signaling. Cell. Mol. Life Sci., 73, 79–94.

Seki, N., Muramatsu, M., Sugano, S., Suzuki, Y., Nakagawara, A., Ohhira, M., Hayashi, A., Hori, T. and Saito, T. (1998). Cloning, expression analysis, and chromosomal localization of HIP1R, an isolog of huntingtin interacting protein (HIP1). J. Hum. Genet., 43, 4, 268–271.

Serafini, T., Stenbeck, G., Brecht, A., Lottspeich, F., Orel, L., Rothman, J.E. and Wieland, F.T. (1991). A coat subunit of Golgi-derived non-clathrin-coated vesicles with homology to the clathrin-coated vesicle coat protein β-adaptin. Nature, 349, 215–220.

Sessions, A., Burke, E., Presting, G., Aux, G., McElver, J., Patton, D., Dietrich, B., Ho, P., Bacwaden, J., Ko, C., Clarke, J.D., Cotton, D., Bullis, D., Snell, J., Miguel, T., Hutchison, D., Kimmerly, B., Mitzel, T., Katagiri, F., Glazebrook, J., Law, M. and Goff, S.A. (2002). A High-Throughput Arabidopsis Reverse Genetics System. Plant Cell, 14, 12, 2985-2994.

Sever, S., Damke, H. and Schmid, S.L. (2002). Garrotes, Springs, Ratchets, and Whips: Putting Dynamin Models to the Test. Traffic, 1, 385–392.

Shimada, T., Fuji, K., Tamura, K., Kondo, M., Nishimura, M. and Hara-Nishimura, I. (2003). Vacuolar sorting receptor for seed storage proteins in Arabidopsis thaliana. Proc. Natl. Acad. Sci USA, 100, 16095–16100.

Shimada, T., Kunieda, T., Sumi, S., Koumoto, Y., Tamura, K., Hatano, K., Ueda, H., and Hara-Nishimura, I. (2018). The AP-1 Complex is Required for Proper Mucilage Formation in Arabidopsis Seeds. Plant & cell physiology, 59, 11, 2331–2338.

Shirakawa, M., Ueda, H., Koumoto, Y., Fuji, K., Nishiyama, C., Kohchi, T., Hara-Nishimura, I. and Shimada, T. (2014). CONTINUOUS VASCULAR RING (COV1) is a trans-Golgi network-localized membrane protein required for Golgi morphology and vacuolar protein sorting. Plant Cell Physiol., 55, 4, 764–772.

Simpson, F., Bright, N.A., West, M.A., Newman, L.S., Darnell, R.B. and Robinson, M.S. (1996). A novel adaptor-related protein complex. J. Cell Biol., 133, 749–760.

Sinclair, R., Rosquete, M. R. and Drakakaki, G. (2018). Post-Golgi Trafficking and Transport of Cell Wall Components. Frontiers in plant sci., 9, 1784.

Skruzny, M., Brach, T., Ciuffa, R., Rybina, S., Wachsmuth, M. and Kaksonen, M. (2012). Molecular basis for coupling the plasma membrane to the actin cytoskeleton during clathrin-mediated endocytosis. Proc. Natl. Acad. Sci USA, 109, 38, E2533-42.

Song, J., Lee, M. H., Lee, G. J., Yoo, C. M., & Hwang, I. (2006). Arabidopsis EPSIN1 plays an important role in vacuolar trafficking of soluble cargo proteins in plant cells via interactions with clathrin, AP-1, VTI11, and VSR1. Plant cell, 18, 9, 2258–2274.

Stahelin, R.V., Long, F., Peter, B.J., Murray, D., Camilli, P.D., McMahon, H.T. and Cho, W. (2003). Contrasting Membrane Interaction Mechanisms of AP180 N-terminal Homology (ANTH) and Epsin N-terminal Homology (ENTH) Domains. J. Biol. Chem. 278, 28993–28999.

Stepp, J.D., Huang, K. and Lemmon, S.K. (1997). The Yeast Adaptor Protein Complex, AP-3, Is Essential for the Efficient Delivery of Alkaline Phosphatase by the Alternate Pathway to the Vacuole. J. Cell Biol. 139, 1761–1774.

Tan, J. and Gleeson, P.A. (2019). Cargo Sorting at the *trans*-Golgi Network for Shunting into Specific Transport Routes: Role of Arf Small G Proteins and Adaptor Complexes. Cells, 8, 6, 531.

Taylor, M.J., Perrais, D. and Merrifield, C.J. (2011). A High Precision Survey of the Molecular Dynamics of Mammalian Clathrin-Mediated Endocytosis. PLOS Biology 9, e1000604.

Teh, O. K., Shimono, Y., Shirakawa, M., Fukao, Y., Tamura, K., Shimada, T., and Hara-Nishimura, I. (2013). The AP-1 μ adaptin is required for KNOLLE localization at the cell plate to mediate cytokinesis in Arabidopsis. Plant Cell Physiol., 54, 6, 838–847.

Traub, L. M., Downs, M. A., Westrich, J. L., and Fremont, D. H. (1999). Crystal structure of the alpha appendage of AP-2 reveals a recruitment platform for clathrin-coat assembly. Proc. Natl. Acad. Sci USA, 96, 16, 8907–8912.

Uemura, T. (2016). Physiological Roles of Plant Post-Golgi Transport Pathways in Membrane Trafficking, Plant Cell Physiol., 57, 10, 2013–2019.

Uemura, T., Kim, H., Saito, C., Ebine, K., Ueda, T., Schulze-Lefert, P. and Nakano, A. (2012). Qa-SNAREs localized to the trans-Golgi network regulate multiple transport pathways and extracellular disease resistance in plants. Proc. Natl. Acad. Sci USA, 109, 5, 1784–1789.

Uemura, T., Suda, Y., Ueda, T. and Nakano, A. (2014). Dynamic Behavior of the *trans*-Golgi Network in Root Tissues of Arabidopsis Revealed by Super-Resolution Live Imaging. Plant Cell Physiol., 55, 4, 694–703.

Uemura, T., Ueda, T., Ohniwa, R.L., Nakano, A., Takeyasu, K. and Sato, M.H. (2004). Systematic Analysis of SNARE Molecules in Arabidopsis: Dissection of the post-Golgi Network in Plant Cells. Cell Struct. Funct., 29, 2, 49-65.

Ungewickell, E. and Branton, D. (1981). Assembly units of clathrin coats. Nature, 289, 420–422.

Ursache, R., Andersen, T.G., Marhavý, P. and Geldner, N. (2018). A protocol for combining fluorescent proteins with histological stains for diverse cell wall components. Plant J., 93, 2, 399-412.

Van Damme, D., Coutuer, S., De Rycke, R., Bouget, F. Y., Inzé, D. and Geelen, D. (2006). Somatic cytokinesis and pollen maturation in Arabidopsis depend on TPLATE, which has domains similar to coat proteins. Plant cell, 18, 12, 3502–3518.

Van Damme, D., Gadeyne, A., Vanstraelen, M., Inzé, D., Van Montagu, M. C., De Jaeger, G., Russinova, E. and Geelen, D. (2011). Adaptin-like protein TPLATE and clathrin recruitment during plant somatic cytokinesis occurs via two distinct pathways. Proc. Natl. Acad. Sci USA, 108, 2, 615–620.

Verkerk, A.J.M.H., Schot, R., Dumee, B., Schellekens, K., Swagemakers, S., Bertoli-Avella, A.M., Lequin, M.H., Dudink, J., Govaert, P., van Zwol, A.L., Hirst, J., Wessels, M.W., Catsman-Berrevoets, C., Verheijen, F.W., de Graaff, E., de Coo, I.F., Kros, J.M., Willemsen, R., Willems, P.J., van der Spek, P.J. and Mancini, G.M. (2009). Mutation in the AP4M1 Gene Provides a Model for Neuroaxonal Injury in Cerebral Palsy. Am. J. Hum. Genet., 85, 40–52.

Vicinanza, M., D'Angelo, G., Di Campli, A. and De Matteis, M.A. (2008). Function and dysfunction of the PI system in membrane trafficking. The EMBO journal, 27, 19, 2457–2470.

Viotti, C., Bubeck, J., Stierhof, Y.D., Krebs, M., Langhans, M., van den Berg, W., van Dongen, W., Richter, S., Geldner, N., Takano, J., Jürgens, G., de Vries, S.C., Robinson, D.G. and Schumacher, K. (2010). Endocytic and secretory traffic in Arabidopsis merge in the trans-Golgi network/early endosome, an independent and highly dynamic organelle. Plant Cell, 22, 4, 1344-57.

Voiniciuc, C., Pauly, M. and Usadel, B. (2018). Monitoring Polysaccharide Dynamics in the Plant Cell Wall. Plant Physiol., 176,4, 2590-2600.

Waelter, S., Scherzinger, E., Hasenbank, R., Nordhoff, E., Lurz, R., Goehler, H., Gauss, C., Sathasivam, K., Bates, G. P., Lehrach, H. and Wanker, E.E. (2001). The huntingtin interacting protein HIP1 is a clathrin and alpha-adaptin-binding protein involved in receptor-mediated endocytosis. Hum. Mol. Genet., 10, 17, 1807–1817.

Wang, C., Hu, T., Yan, X., Meng, T., Wang, Y., Wang, Q., Zhang, X., Gu, Y., Sánchez-Rodríguez, C., Gadeyne, A., Lin, J., Persson, S., Van Damme, D., Li, C., Bednarek, S. Y. and Pan, J. (2016). Differential Regulation of Clathrin and Its Adaptor Proteins during Membrane Recruitment for Endocytosis. Plant physiol., 171, 1, 215–229.

Wang, J., Gossing, M., Fang, P., Zimmermann, J., Li, X., Mollard, G.F. von, Niu, L. and Teng, M. (2011). Epsin N-terminal homology domains bind on opposite sides of two SNAREs. Proc. Natl. Acad. Sci. USA, 108, 12277–12282.

Wang, J.G., Feng, C., Liu, H.H., Feng, Q.N., Li, S. and Zhang, Y. (2017). AP1G mediates vacuolar acidification during synergid-controlled pollen tube reception. Proc. Natl. Acad. Sci. USA, 114, 24, 4877-4883.

Wang, J. G., Li, S., Zhao, X. Y., Zhou, L. Z., Huang, G. Q., Feng, C., and Zhang, Y. (2013). HAPLESS13, the Arabidopsis μ1 adaptin, is essential for protein sorting at the trans-Golgi network/early endosome. Plant Physiol., 162, 4, 1897–1910.

Wang, Y.J., Wang, J., Sun, H.Q., Martinez, M., Sun, Y.X., Macia, E., Kirchhausen, T., Albanesi, J.P., Roth, M.G. and Yin, H.L. (2003). Phosphatidylinositol 4 phosphate regulates targeting of clathrin adaptor AP-1 complexes to the Golgi. Cell, 114, 3, 299–310.

Wasiak, S., Legendre-Guillemin, V., Puertollano, R., Blondeau, F., Girard, M., de Heuvel, E., Boismenu, D., Bell, A.W., Bonifacino, J.S. and McPherson, P.S. (2002). Enthoprotin: a novel clathrin-associated protein identified through subcellular proteomics. J. Cell Biol., 158, 5, 855-862.

Waters, M.G., Serafini, T. and Rothman, J.E. (1991). “Coatomer”: a cytosolic protein complex containing subunits of non-clathrin-coated Golgi transport vesicles. Nature, 349, 248–251.

Wendland B. (2002). Epsins: Adaptors in endocytosis? Nat. Rev. Mol. Cell Biol., 3, 971–977.

Wendland, B., Steece, K.E. and Emr, S.D. (1999). Yeast epsins contain an essential N-terminal ENTH domain, bind clathrin and are required for endocytosis. EMBO J., 18, 16, 4383-4393.

Western, T.L., Burn, J., Tan, W.L., Skinner, D.J., Martin-McCaffrey, L., Moffatt, B.A. and Haughn, G.W. (2001). Isolation and characterization of mutants defective in seed coat mucilage secretory cell development in Arabidopsis. Plant Physiol., 127, 998–1011.

Western, T.L., Skinner, D.J. and Haughn, G.W. (2000). Differentiation of Mucilage Secretory Cells of the Arabidopsis Seed Coat. Plant Physiol., 122, 345–356.

Wilkop, T., Pattathil, S., Ren, G., Davis, D.J., Bao, W., Duan, D., Peralta, A.G., Domozych, D.S., Hahn, M.G. and Drakakaki, G. (2019). A Hybrid Approach Enabling Large-Scale Glycomic Analysis of Post-Golgi Vesicles Reveals a Transport Route for Polysaccharides. Plant Cell, 31, 3, 627-644.

Yamaoka, S., Shimono, Y., Shirakawa, M., Fukao, Y., Kawase, T., Hatsugai, N., Tamura, K., Shimada, T. and Hara-Nishimura, I. (2013). Identification and Dynamics of Arabidopsis Adaptor Protein-2 Complex and Its Involvement in Floral Organ Development. Plant Cell 25, 2958–2969.

Young, R.E., McFarlane, H.E., Hahn, M.G., Western, T.L., Haughn, G.W. and Samuels, A.L. (2008). Analysis of the Golgi apparatus in Arabidopsis seed coat cells during polarized secretion of pectin-rich mucilage. Plant Cell, 20, 6, 1623–1638.

Yperman, K., Wang, J., Eeckhout, D., Winkler, J., Vu, L. D., Vandorpe, M., Grones, P., Mylle, E., Kraus, M., Merceron, R., Nolf, J., Mor, E., De Bruyn, P., Loris, R., Potocký, M., Savvides, S. N., De Rybel, B., De Jaeger, G., Van Damme, D., and Pleskot, R. (2021). Molecular architecture of the endocytic TPLATE complex. Sci. adv., 7, 9, eabe7999.

Zhao, L., Rehmani, M. S. and Wang, H. (2020). Exocytosis and Endocytosis: Yin-Yang Crosstalk for Sculpting a Dynamic Growing Pollen Tube Tip. Front. plant sci., 11, 572848.

Zhen, Y. and Stenmark, H. (2015). Cellular functions of Rab GTPases at a glance. J. Cell Sci., 128, 17, 3171-3176.

Zheng, H., Fischer von Mollard, G., Kovaleva, V., Stevens, T.H. and Raikhel, N.V. (1999). The plant vesicle-associated SNARE AtVTI1a likely mediates vesicle transport from the trans-Golgi network to the prevacuolar compartment. Mol. Biol. Cell, 10, 2251–2264.

Zheng, J., Han, S. W., Rodriguez-Welsh, M. F. and Rojas-Pierce, M. (2014). Homotypic vacuole fusion requires VTI11 and is regulated by phosphoinositides. Mol. plant, 7, 6, 1026–1040.

Zhu, J., Gong, Z., Zhang, C., Song, C.P., Damsz, B., Inan, G., Koiwa, H., Zhu, J.K., Hasegawa, P.M., Bressan, R.A. (2002). OSM1/SYP61: a syntaxin protein in Arabidopsis controls abscisic acid-mediated and non-abscisic acid-mediated responses to abiotic stress. Plant Cell, 14, 12, 3009-3028.

Zizioli, D., Meyer, C., Guhde, G., Saftig, P., Figura, K. von and Schu, P. (1999). Early Embryonic Death of Mice Deficient in γ-Adaptin. J. Biol. Chem. 274, 5385–5390.

Zonia, L. and Munnik, T. (2008). Vesicle trafficking dynamics and visualization of zones of exocytosis and endocytosis in tobacco pollen tubes. J. Exp. Bot., 59, 861–873.

Zonia, L. and Munnik, T. (2009). Uncovering hidden treasures in pollen tube growth mechanics. Trends Plan. Sci., 14, 318–327.

Zouhar, J. and Sauer, M. (2014). Helping Hands for Budding Prospects: ENTH/ANTH/VHS Accessory Proteins in Endocytosis, Vacuolar Transport, and Secretion. Plant Cell 26, 4232–4244.

Zwiewka, M., Feraru, E., Möller, B., Hwang, I., Feraru, M.I., Kleine-Vehn, J., Weijers, D., Friml, J. (2011). The AP-3 adaptor complex is required for vacuolar function in Arabidopsis. Cell Res. 21, 12, 1711-1722.

7. Appendix

7.1. Supplementary figures

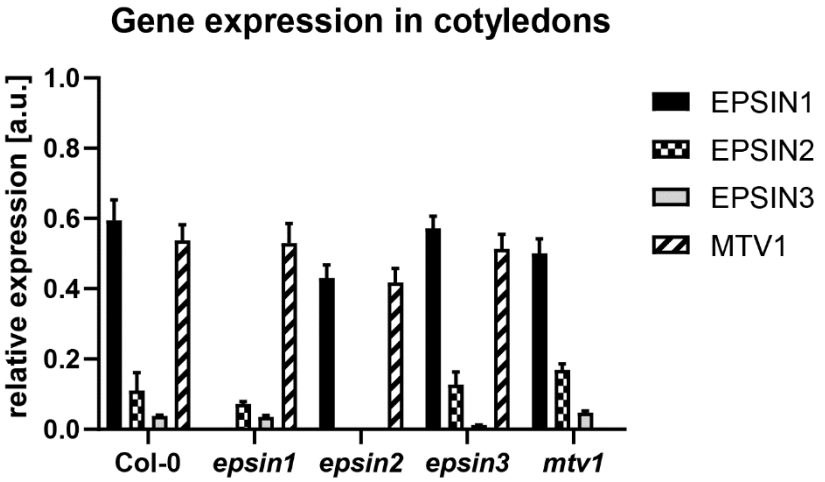

Supplementary figure 1: Gene expression in cotyledons.
A: Gene expression of *EPSIN1, 2* and *3* as well as *MTV1* detected in Col-0 and respective single mutant cotyledons by qPCR, normalized to three reference genes AT4G26410, AT5G60390 and AT5G12250. Arbitrary units (a.u.).

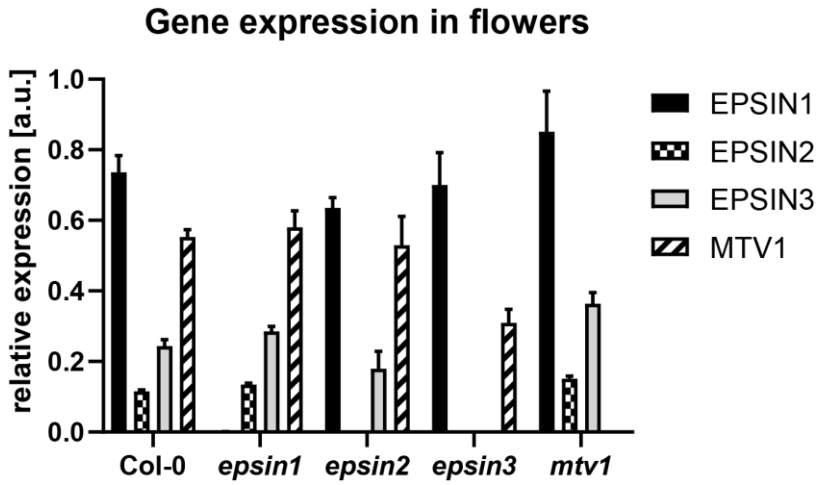

Supplementary figure 2: Gene expression in flowers.
Gene expression of *EPSIN1, 2* and *3* as well as *MTV1* detected in Col-0 and respective single mutant flowers by qPCR, normalized to three reference genes AT4G26410, AT5G60390 and AT5G12250. Arbitrary units (a.u.).

Supplementary figure 3: Growth phenotype of 36-day-old single and higher order mutant plants.
Plants were grown under long day conditions side by side. Scale bar 5 cm.

7.2 Supplementary tables

The following tables summarize all used materials with the respective manufacture.

Supplementary table 1: Equipment.

Equipment	Manufacture
1.5 ml tubes, 2.0 ml tubes, 13 ml culture tubes	SARSTEDT AG & Co. KG, Nümbrecht, Germany
15 ml and 50 ml polypropylene tubes	VWR International, Radnor, Pennsylvania, USA
8-channel pipette	BRAND GMBH + CO KG, Wertheim, Germany
8-tube PCR strip	BRAND GMBH + CO KG, Wertheim, Germany
96-well PCR plates	BRAND GMBH + CO KG, Wertheim, Germany
Amersham Protran 0.45 nitrocellulose Western blotting membranes	GE Healthcare Europe GmbH, Freiburg, Germany
Cellulosic cellophane membrane	325P Cellulose; AA Packaging Limited, Preston, UK; www.aapackaging.co.uk
Circle Writer Liquid Blocker Pen	Science Services GmbH, München, Germany
Culture plates (6-well and 12-well)	VWR International, Radnor, Pennsylvania, USA
Electroporation cuvette 2 mm gap	VWR International, Radnor, Pennsylvania, USA
MicroPulser Electroporator	Bio-Rad Laboratories GmbH, München, Germany
GelDoc XR+ system	Bio-Rad Laboratories GmbH, München, Germany
GFL Orbital shaker 3005	GFL Gesellschaft für Labortechnik mbH, Burgwedel / Deutschland
Gosselin™ Square Petri Dish, 120x120mm, Corning®	VWR International, Radnor, Pennsylvania, USA
High Precision cover glasses (24x50 mm or 50x50 mm)	Paul Marienfeld GmbH & Co. KG, Lauda-Königshofen, Germany
HP Scanjet G4050	HP Inc, Palo Alto, California, USA
Incubator (37°C and 30°C)	BINDER GmbH, Tuttlingen, Germany
Microscope slide	VWR International, Radnor, Pennsylvania, USA
Microtiter cluster tubes (8-well)	Simport Scientific, Saint-Mathieu-de-Beloeil,
Mikro 200 Hettich Zentrifuge	Sigma-Aldrich, St. Louis, Missouri, USA
Mini Trans-Blot Electrophoretic Transfer Cell	Bio-Rad Laboratories GmbH, München, Germany
Mini Trans-Blot® cell	Bio-Rad Laboratories GmbH, München, Germany
Mini-PROTEAN® Tetra Systems	Bio-Rad Laboratories GmbH, München, Germany
Mini-PROTEAN® Tetra Vertical Electrophoresis Cell	Bio-Rad Laboratories GmbH, München, Germany
Molecular Imager® Gel DocTM XR+ System with Image Lab™ Software	Bio-Rad Laboratories GmbH, München, Germany
Multipot Propagation Tray M50	Hermann Meyer KG, Rellingen, Germany
Nanodrop 2000	Thermo Fisher Scientific, Waltham, Massachusetts, USA
Parafilm M	Bemis, Neenah, Wisconsin, USA
Percival, Model CU-22L	CLF Plant Climatics, Wertingen, Germany
Percival, Model SE59-L2.3	CLF Plant Climatics, Wertingen, Germany
Petri dish	SARSTEDT AG & Co. KG, Nümbrecht, Germany
Photometer, GeneQuant 100	GE Healthcare Europe GmbH, Freiburg, Germany
Pipette (10 µl/200 µl/1000 µl)	BRAND GMBH + CO KG, Wertheim, Germany
Pipette (5 ml)	Eppendorf Vertrieb Deutschland GmbH, Wesseling-Berzdorf, Germany
Pipette tips (10 µl/200 µl/1000 µl)	SARSTEDT AG & Co. KG, Nümbrecht, Germany
ProFlex PCR System	Life Technologies, Carlsbad, California, USA
Revolver Rotator D-6050	neoLab Migge GmbH, Heidelberg, Germany
SIGMA 3K30 Lab Centrifuge	Sigma-Aldrich, St. Louis, Missouri, USA

SimpliAmp Thermal cycler	Life Technologies, Carlsbad, California, USA
Slide-A-Lyzer™ Dialysis Cassettes	Thermo Fisher Scientific, Waltham, Massachusetts, USA
Stemi 2000-C stereomicroscope	Zeiss, Hintertupfing, Strangeland
The Pierce™ Disposable Columns	Thermo Fisher Scientific, Waltham, Massachusetts, USA
Thermomixer compact	Eppendorf Vertrieb Deutschland GmbH, Wesseling-Berzdorf, Germany
TissueLyser II	QIAGEN, Hilden, Germany
Ultramat 2, High speed multi-use triturator	SDI Germany GmbH, Cologne Germany
Whatmann Cellulose Filter Paper	Sigma-Aldrich, St. Louis, Missouri, USA
Zeiss LSM 880 Airyscan Fast	Zeiss, Hintertupfing, Strangeland

Supplementary table 2: Chemicals.

Chemical	**Manufacture**
1,4-Dithioerythritol (DTE)	Carl Roth GmbH + Co. KG, Karlsruhe, Germany
2-(N-morpholino)ethanesulfonic acid (MES)	Carl Roth GmbH + Co. KG, Karlsruhe, Germany
2-propanol	Carl Roth GmbH & Co. KG, Karlsruhe, Germany
Acetic acid	Carl Roth GmbH + Co. KG, Karlsruhe, Germany
Acetosyringone (AS)	Sigma-Aldrich Corporation, St. Louis, MO, USA
Agar-agar	Carl Roth GmbH + Co. KG, Karlsruhe, Germany
Ammonium ferric citrate	Sigma-Aldrich Corporation, St. Louis, MO, USA
Ammonium persulfate (APS)	Carl Roth GmbH + Co. KG, Karlsruhe, Germany
Boric acid	Carl Roth GmbH + Co. KG, Karlsruhe, Germany
Bradford assay	Sigma-Aldrich Corporation, St. Louis, MO, USA
Bromphenol blue	SERVA Electrophoresis GmbH, Heidelberg, Germany
Calcium nitrate	Carl Roth GmbH + Co. KG, Karlsruhe, Germany
Calcium chloride	Carl Roth GmbH + Co. KG, Karlsruhe, Germany
Casein hydrolysate	Duchefa Biochemie B.V., Haarlem, Netherlands
Chloral hydrate	Carl Roth GmbH + Co. KG, Karlsruhe, Germany
Coatosil 77	Momentive Performance Materials GmbH & Co. KG, Leverkusen, Germany
Coomassie Brilliant Blue R	Sigma-Aldrich Corporation, St. Louis, MO, USA
Difco™ Beef extract	Becton, Dickinson & Company, Franklin Lakes, NJ, USA
Dimethyl sulfoxide (DMSO)	Carl Roth GmbH + Co. KG, Karlsruhe, Germany
Ethanol absolute	VWR International GmbH, Darmstadt, Germany
Ethidium bromide solution 1%	Carl Roth GmbH + Co. KG, Karlsruhe, Germany
Ethylenediaminetetraacetic acid (EDTA)	Carl Roth GmbH & Co. KG, Karlsruhe, Germany
GeneRuler DNA Ladder Mix	Thermo Fisher Scientific, Waltham, MA, USA
GeneRuler™ 1 kb DNA Ladder	Thermo Fisher Scientific, Waltham, MA, USA
Glutathione sepharose 4B	GE Healthcare Europe GmbH, Freiburg, Germany
Glycerol	Carl Roth GmbH & Co. KG, Karlsruhe, Germany
Glycine	Carl Roth GmbH & Co. KG, Karlsruhe, Germany
Isopropyl-β-D-thiogalactopyranoside (IPTG)	Carl Roth GmbH & Co. KG, Karlsruhe, Germany
Low melt agarose	Sigma-Aldrich Corporation, St. Louis, MO, USA
Methanol (MeOH)	Sigma-Aldrich Corporation, St. Louis, MO, USA
Magnesium sulfate ($MgSO_4$ x 7 H_2O)	Sigma-Aldrich Corporation, St. Louis, MO, USA
Murashige & Skoog medium incl. vitamins (MS)	Duchefa Biochemie B.V., Haarlem, Netherlands
Myo-Inositol	Duchefa Biochemie B.V., Haarlem, Netherlands

Orange G	Sigma-Aldrich Corporation, St. Louis, MO, USA
Plant agar	Duchefa Biochemie B.V., Haarlem, Netherlands
Ponceau S	Sigma-Aldrich Corporation, St. Louis, MO, USA
Potassium chloride (KCl)	Carl Roth GmbH & Co. KG, Karlsruhe, Germany
Powdered milk	Carl Roth GmbH & Co. KG, Karlsruhe, Germany
Protease-Inhibitor Mix P	SERVA Electrophoresis GmbH, Heidelberg, Germany
Protein Marker VI (10 –245) prestained	AppliChem GmbH, Darmstadt, Germany
Rotiphorese® Gel 30 (37.5:1)	Carl Roth GmbH & Co. KG, Karlsruhe, Germany
SDS Pellets	Carl Roth GmbH & Co. KG, Karlsruhe, Germany
Sodium chloride (NaCl)	Carl Roth GmbH & Co. KG, Karlsruhe, Germany
Spermidin	Sigma-Aldrich Corporation, St. Louis, MO, USA
Sucrose	Fisher Scientific, Loughborough, U. K.
Tetramethylethylenediamine (TEMED)	Sigma-Aldrich Corporation, St. Louis, MO, USA
Tris(hydroxymethyl)-aminomethane (Tris)	Carl Roth GmbH & Co. KG, Karlsruhe, Germany
Triton™ X-100	Sigma-Aldrich Corporation, St. Louis, MO, USA
Tryptone/Peptone ex casein	Carl Roth GmbH + Co. KG, Karlsruhe, Germany
TWEEN® 20	Sigma-Aldrich Corporation, St. Louis, MO, USA
Yeast extract	Carl Roth GmbH + Co. KG, Karlsruhe, Germany
γ-aminobutyric acid (GABA)	Sigma-Aldrich Corporation, St. Louis, MO, USA

Supplementary table 3: Antibiotics with their final concentration.

Antibiotic	**Final concentration [µg/ml]**	**Manufacture**
Ampicillin	100	Carl Roth GmbH & Co. KG, Karlsruhe, Germany
Carbenicillin Disodium	100	Formedium Ltd., Hunstanton, U.K.
Hygromycin B	50	Sigma-Aldrich, St. Louis, Missouri, USA
Kanamycin	50	Carl Roth GmbH & Co. KG, Karlsruhe, Germany
Rifampicin	100	Sigma-Aldrich, St. Louis, Missouri, USA
Spectinomycin	50	Sigma-Aldrich, St. Louis, Missouri, USA

Supplementary table 4: Reaction kits.

Name	**Manufacture**	**Application**
5X FIREPol® Master Mix, 12.5 mM $MgCl_2$	Solis BioDyne, Tartu, Estonia	Genotyping PCR
GoTaq qPCR Master	Promega GmbH, Walldorf, Germany	qPCR
RevertAid H Minus First Strand cDNA Synthesis Kit	Thermo Fisher Scientific, Waltham, MA, USA	cDNA synthesis
RNeasy Plant Mini Kit	QIAGEN, Hilden, Germany	RNA extraction
SERVALight Polaris CL HRP WB Substrate Kit	SERVA Electrophoresis GmbH, Heidelberg, Germany	Detection of secondary antibodies used in western blot experiment

Supplementary table 5: Software used for analysis and image processing.

Name	**Manufacture**
Adobe Illustrator, Creative Suite 6 (CS6)	Adobe Systems Inc., San Jose, USA
Adobe Photoshop, Creative Suite 6 (CS6)	Adobe Systems Inc., San Jose, USA
GraphPad Prism 7.0	GraphPad Software, Inc., La Jolla, USA
ImageJ (with Plugin ObjectJ)	US National Institute of Health, Bathesda, Maryland, USA

SnapGene 4.3	GSL Biotech LLC, Chicago, USA
ZEN (blue) and (black)	ZEISS Efficient Navigation Carl Zeiss AG, Oberkochen, Germany

Supplementary table 6: Oligonucleotides used for PCR and qPCR.

Name	**Sequence**	**Application**
AT4G26410_fw	GAGCTGAAGTGGCTTCAATGAC	qPCR
AT4G26410_rev	GGTCCGACATACCCATGATCC	qPCR
AT5G60390_fw	TGAGCACGCTCTTCTTGCTTTCA	qPCR
AT5G60390_rev	GGTGGTGGCATCCATCTTGTTA	qPCR
ECH_LP	AAACGGAAAGGGAAACACAAC	genotyping *echidna*
ECH_RP	AGAGAAGAGTTATCGGGCTCG	genotyping *echidna*
eps1-2 fw1	CGAATGGATCAGAACGAGCG	qPCR
eps1-2 rev3	GCGACTATGTTTTCCGCCTT	qPCR
eps2-2 rev4	GTGTCGCTAAGGCGTTTCCA	qPCR
eps3-3 fw1	TGCTGCTCCACCTAGTTATGA	qPCR
eps3-3 rev3	AGCAAGAGGAGAAGCAGCAG	qPCR
EPSIN2-F-1	ATGAAGAAAGTCTTCGGACAAACTG	qPCR
mtv1-fw1-new	CAAAAGCCCCATTGTTAAGCAG	qPCR
mtv1-rev1-new	GGAGCAGCTGGTTTAGTACCAT	qPCR
Sail garlic LB3	TAGCATCTGAATTTCATAACCAATCTCGAT ACAC	left border primer for genotyping the insert of sail lines
SAIL_172_B07-L	TTCCTTGTCATTCACCAAAGC	genotyping *epsin2*
SAIL_172_B07-R	GACGGGATGCTTCATTTTATG	genotyping *epsin2*
SAIL_394_G02 L	TTGATGAGAGGCCAACATACC	genotyping *epsin1*
SAIL_394_G02 R	GGCAAAATGATCGAAAACTTTC	genotyping *epsin1*
SAIL_781_H01-fw	TCCGGCTCTTTGATTGGACTA	genotyping *ap4b2*
SAIL_781_H01-rev	ACACGGTCTTTGATTTCACTG	genotyping *ap4b2*
SAIL_796_A10-fw	GTGGTATTTACCATTGTGGTG	genotyping *ap4b1*
SAIL_796_A10-rev	GCTCCATTGTGGATACTTCC	genotyping *ap4b1*
SALK_014326-fw	CGATTTGGTTGGATCCAATACA	genotyping *ap4m1*
SALK_014326-rev	GCCATCAATCTCAGAAGTCAG	genotyping *ap4m1*
SALK_060899 L	TTTTGTTTTTCTCATGCAGCC	genotyping *epsin3*
SALK_060899 R	CGGTCCAATTTAAAGAGGGAG	genotyping *epsin3*
SALK_061811-L	CAATTTCTCCGTTCTCTGCTG	genotyping *mtv1*
SALK_061811-R	CTGCTGCCATTCTCATTCTTC	genotyping *mtv1*
SALK_079928-L2	ACAACAACCACTCCAAAGTGG	genotyping *mtv4*
SALK_079928-R2	AATGAAAATCCCTATGGGACG	genotyping *mtv4*
Salk-LBb1.3	ATTTTGCCGATTTCGGAAC	left border primer for genotyping the insert of salk lines
TUB6b-F	ACTCTTCCCTGATCTTAGATATGAGC	qPCR
TUB6b-R	GTCTTCAAGGTTTCCAAGTATGTCA	qPCR

7.3 List of figures

7.4 List of tables

7.5 Declaration/Selbstständigkeitserklärung

I (Laura Heinze) hereby confirm, that the present dissertation was prepared by me independently and only with the sources indicated. In addition, this work has not yet been submitted to any other university.

……

Laura Heinze

Hiermit bestätige ich, Laura Heinze, dass die vorliegende Dissertation von mir selbstständig und nur mit den angegebenen Quellen angefertigt wurde. Außerdem wurde diese Arbeit bisher an keiner anderen Hochschule eingereicht.

……

Laura Heinze